ESA CONTRACT REPORT

Contract Report to the European Space Agency

Global Validation of ENVISAT Wind, Wave and Water Vapour Products from RA-2, MWR, ASAR and MERIS

December 2005

Author: Saleh Abdalla

Final report for ESA contract 17585

Series: ECMWF - ESA Contract Report

A full list of ECMWF Publications can be found on our web site under:
http://www.ecmwf.int/publications/

Contract Report to the European Space Agency

Global Validation of ENVISAT Wind, Wave and Water Vapour Products from RA-2, MWR, ASAR and MERIS

Author: Saleh Abdalla

Final report for ESA contract 17585

European Centre for Medium-Range Weather Forecasts

Shinfield Park, Reading, Berkshire, UK

December 2005

(revised: March 2006)

	Name	Company	Date	Visa
Prepared by	S. Abdalla	ECMWF	Dec 22, 2005	
Quality visa:	P. Bougeault	ECMWF	Mar 3, 2006	
Application Authorized by	P. Féménias	ESA/ESRIN		

Distribution list:

ESA/ESRIN: EOP-GOQ Sensor Performance, Product and Algorithm Section

Pierre Féménias
Philippe Goryl
Pascal Lecomte
Betlem Rosich

ECMWF

HR
Division Section Heads
Ocean Wave Group

TABLE OF CONTENTS

ABSTRACT

On the 1st. of March 2002, the European Space Agency (ESA) launched the ENVISAT satel-lite that carries onboard 9 instruments (for detailed description see ESA (2002, 2004)), two of which are relevant for understanding of ocean waves, namely the Radar Altimeter-2 (RA-2) and the Advanced Synthetic Aperture Radar (ASAR). The other two related instruments are the Microwave Radiometer (MWR) and the Medium Resolution Imaging Spectrometer (MERIS).

ENVISAT near real time (NRT) surface wind speed and significant wave height (SWH) products from RA-2 instrument (both Ku and S-Band), wet tropospheric correction (WTC) and total column water vapour (TCWV) products from the MWR instrument, wave mode spectra (both Level 1b and Level 2) from the ASAR instrument and TCWV product from the MERIS instrument have been monitored and validated against corresponding parameters from ECMWF atmospheric and wave models (both first-guess, FG, and analysis, AN), in-situ buoy and platform instruments and other satellites (ERS-2 and Jason).

In general, RA-2 products are of good quality. However, NRT wind product needs some ad-justment at low and high wind speed regimes. This was partially done recently (24 October 2005). Although Ku-Band SWH product is slightly high, it is of high quality. The S-Band SWH product is generally of acceptable quality except for a number of clearly wrong outliers during what is known as RA-2 S-Band Anomaly. The ratio of the global mean of Ku-Band SWH to that of S-Band shows seasonal variation with minima during July-August. Compared to the model, the MWR products are in general of good quality since 26 November 2003 apart from few outliers near the ice edges.

NRT ASAR Wave Mode Level 1b (ASA_WVS_1P) product as inverted using the Max-Planck Institut für Meteorologie (MPIM) scheme agrees well with the wave model counterpart in terms of all integrated parameters used for the comparison. On the other hand, Wave Mode Level 2 (ASA_WVW_2P) product agrees well with wave model in terms of swell significant wave height and mean period. The agreement is not so good for spectral peakedness factor and the directional spread. The PF-ASAR Version 3.07 has positive impact on the quality of the inverted spectra and no impact on Level 2 product. The impact of wave model changes on 9 March 2004 (unresolved bathymetry) and 5 April 2005 (improved dissipation term) is positive except for Level 1b wave height and peakedness factor (due to new model sensitivity). ASAR Wave Mode Level 1b is planned to be assimilated operationally at ECMWF on the 1 February 2006.

Although not optimal, the MERIS TCWV product proves to have an important potential. The product is, in general, much dryer and much noisier than the model or even the MWR instruments. There are several spots around the world when MERIS is too dry (e.g. Gulf of Panama) or too wet (e.g. Amazon Delta). The product however needs some adjustment.

ABBREVIATIONS

AN	Analysis
ASAR	Advanced Synthetic Aperture Radar
BUFR	Binary Universal Form for the Representation of meteorological data
ECMWF	European Centre for Medium-Range Weather Forecasts
ECWAM	ECMWF wave model
ENVISAT	Environmental Satellite
ERS	European Remote Sensing satellite
FD	Fast Delivery product
FDGDR	Fast Delivery Geophysical Data Record
FDMAR	Fast Delivery Marine Abridged Records Product
FG	First guess
GTS	Global Telecommunication System
IPF	Instrument Processing Facility
MERIS	MEdium Resolution Imaging Spectrometer
MPIM	Max-Planck Institut für Meteorologie
MWD	Mean wave direction
MWP	Mean wave period
MWR	MicroWave Radiometer
NH	Northern Hemisphere extra-tropics (north of latitude 20□N)
NRT	Near real time
NWP	Numerical weather prediction
PF-ASAR	ASAR Processing Facility
QC	Quality control
QWG	Quality Working Group
RA	ERS Radar Altimeter
RA-2	ENVISAT Radar Altimeter-2
SH	Southern Hemisphere extra-tropics (south of latitude 20□S)
SI	Scatter Index
SWH	Significant wave height
TCWV	Total column water vapour

UTC	Coordinated Universal Time
WAM	Wave model
WDS	Wave directional spread
WPF	Wave spectral peakedness factor of Goda
WTC	Wet tropospheric correction

PART I

RADAR ALTIMETER - 2 (RA-2)
AND
MICROWAVE RADIOMETER (MWR)

I.1. Introduction

RA-2 is a dual-frequency altimeter operating on both Ku- and S-Band. It was derived from the RA of the ERS satellite series, providing improved measurement performance and new capabilities. The main objectives of the RA-2 are the high-precision measurements of the time delay, the power and the shape of the reflected radar pulses for the determination of the satellite height and the Earth surface characteristics. RA-2 transmits radio frequency pulses that propagate at approximately the speed of light. The time elapsed from the transmission of a pulse to the reception of its echo, reflected from the surface of the Earth, is proportional to the altitude of the satellite. The magnitude and shape of the echoes contain information on the characteristics of the surface that caused the reflection. Operating over oceans, these measurements are used to determine the ocean surface topography, thus supporting studies of ocean waves, marine surface winds, circulation, bathymetry, gravity anomalies and marine geoid characteristics. Furthermore, the RA-2 is able to map and monitor sea ice and polar ice sheets. The product to be validated here is the Fast Delivery Marine Abridged Records Product (FDMAR). Specifically, the backscatter coefficient, surface wind speed, Ku-Band significant wave height (SWH) and S-Band SWH are validated.

MWR is a dual-channel nadir-pointing radiometer, operating at frequencies of 23.8 GHz and 36.5 GHz. The main objective of the MWR is the measurement of the integrated atmospheric water vapour column and cloud liquid water content, as correction terms for the radar altimeter signal. In addition, MWR measurement data are useful for the determination of surface emissivity and soil moisture over land, for surface energy budget investigations to support atmospheric studies, and for ice characterization. To measure the strength of the weak water-vapour emission-line at 22 GHz, the frequencies 23.8 GHz and 36.5 GHz are optimally selected in order to eliminate the microwave radiation emitted by the Earth surface. The two products to be verified are the total column water vapour (TCWV) and the wet tropospheric correction (WTC) available in FDMAR product.

The European Centre for Medium-Range Weather Forecasts (ECMWF) monitors routinely the quality of the wind and wave products from RA-2 since an early stage of commissioning phase data dissemination on 18 July 2002. The monitoring is based on the data processed in near real time (NRT) provided by ESA. Radar backscatter coefficient (σ°), surface wind speed and Ku- and S-Band SWH products from the RA-2 instrument and WTC and TCWV products from the MWR instrument are among the parameters monitored and validated against the ECMWF model products and, for wind and wave products, against the in-situ buoy and platform observations available through the Global Telecommunication System (GTS) as well as the ERS-2 RA products. When possible, a combination of all of the observation sources (multiple-collocation) is also used for validation. It must be stressed that the number of in-situ observing stations is very limited (few-several 10's) and most of them are located in the Northern Hemisphere (NH) around the North American and European coasts. The exceptions are few buoys in the Tropics, mainly around Hawaii, and off the South African coasts in the Southern Hemisphere (SH). Therefore, any validation against in-situ data mainly reflects the quality of the products in the NH.

The aim of the validation is to assess and monitor the quality of those products. The Ku-Band SWH product is of significant importance as it is assimilated in the operational forecasting system at ECMWF. For proper validation, the observations and the model results should be of comparable scales. The model scale is much larger than the scale of the altimeter observations. Therefore, an averaging process is used to form altimeter and MWR super-observations of comparable scales as the model. The super-observations are collocated with

the model and the in-situ (if applicable) data. The main results of the validation over the last 2-3 years are presented here. It should be noticed that there were at least five major changes/events during this period that would affect the interpretation of the results:

- The first was related to wave model data assimilation. The WAM wave model at ECMWF (c.f. Komen et al., 1994, Janssen, 2004), was assimilating ERS-2 radar altimeter (RA) SWH data. On 22 June 2003 there was a permanent failure in the tape recorders onboard ERS-2 resulting in loss of its global coverage. Consequently, the model use of data was limited to that coverage. On 21 October 2003, the assimilation of ERS-2 RA SWH was switched off and replaced by ENVISAT RA-2 Ku-Band SWH assimilation (Abdalla et al., 2004). Although the SWH validation against the model depends on the first-guess (FG) fields, one would expect some impact of altimeter data assimilated during previous analysis cycles.

- The second change is on the satellite side. On 26 November 2003, a new RA-2 and MWR Instrument Processing Chain (IPF Version 4.56) was introduced at the ESA ENVISAT PDS processing centres. This change is an implementation of the neural network algorithm for the evaluation of the MWR WTC, TCWV and liquid water content.

- The third change was the treatment of the unresolved bathymetry in the wave model. This change blocks the energy flux through small-scale land formations that are not resolved at the model scale. This change was implemented operationally on 9 March 2004.

- The fourth event was an update to the PDS format of the product (IPF Version 4.58) which caused the BUFR conversion software to introduce missing values in some of the crucial fields. This resulted in the rejection of most of those products by the quality control procedure as corrupt products. Therefore, there was very limited amount of SWH data for assimilation in the wave model. This event lasted from 9 August to 4 October 2004.

- Finally, there was a model change that uses an improved wave dissipation source term. This change was implemented on 5 April 2005.

Results of the routinely global monitoring and validation of ENVISAT RA-2 wind and wave products as well as MWR WTC and TCWV products are summarised in form of monthly reports. These reports are available online at: http://earth.esa.int/pcs/envisat/ra2/reports/ecmwf/

I.2. RA-2 and MWR data processing

The validation is based on FDMAR (Fast Delivery Marine Abridged Record) which is a sub-set of the Fast Delivery Geophysical Data Record (FDGDR) product produced in NRT. The data files are retrieved in BUFR (Binary Universal Form for the Representation of meteorological data) format from two ftp sites at Kiruna and ESRIN. The raw data product is collected for 6-hourly time windows centred at synoptic times (00, 06, 12 and 18 UTC). For proper validation, the observations and the model results should be of comparable scales. As the model scale (~ 80 km) is much larger than the scale of an individual 1 Hz altimeter observation (~ 7 km), the latter needs to be averaged. Therefore, the stream of altimeter data is split into short observation sequences each consisting of 11 individual (1-Hz) observations. A quality control

procedure is performed on each short sequence. Erratic and suspicious individual observations are removed and the remaining data in each sequence are averaged to form a representative super-observation, providing that the sequence has enough number of "good" individual observations (at least 7). The super-observations are collocated with the model and the in-situ (if applicable) data. The raw data pass the quality control and the collocated data are then investigated to derive the conclusions regarding the data quality. It is important to recall that the Ku-Band SWH product is of significant importance as it is assimilated in the operational forecasting system at ECMWF since 21 October 2003. The details of the method used for data processing is an extension to the method used for ERS-2 RA analysis and described in Abdalla and Hersbach (2004).

I.3. RA-2 Radar backscatter and surface wind speed

FD RA-2 Ku band backscatter coefficient (σ°) behaves as expected. A typical monthly distribution of the 1 Hz σ° values can be seen in Fig. (I.1) which is for September 2005. It is clear that the distribution after quality control is single-peaked. The monthly mean values of σ° are plotted in Fig. (I.2) over the period from May 2003 until October 2005. One can notice that the monthly mean Ku-Band σ° values vary within a narrow band between 10.96 and 11.24 dB.

Fig. (I.2) shows the monthly mean S-Band σ° values as well. Apart from the jump of about 0.6 dB between November and December 2003, the time series is rather stable. The jump coincides with the implementation of the IPF Version 4.56 processing chain on the 26 November 2003. For reference, Jason radar altimeter monthly mean σ° values are also plotted in Fig. (I.2). Although, Jason values are about 0.4 dB higher that those of ENVISAT Ku-Band values, the three lines are more or less parallel.

A bug fix (IPF Version 4.54 processing chain) was implemented on 7 April 2003 to remove a bug that was responsible for deteriorating the FD wind speed product since 24 October 2002. After the bug fix, surface wind speed product is of acceptable quality. Fig. (I.3) shows a typical distribution of RA-2 wind speed super-observations over a period of one year. The corresponding histogram of collocated ECMWF model winds is shown in Fig. (I.4). There is quite a good resemblance between the two histograms except for low wind speeds where RA-2 tends to accumulate more occurrences than the model. Also, one can notice that the altimeter wind speed has slightly higher variance.

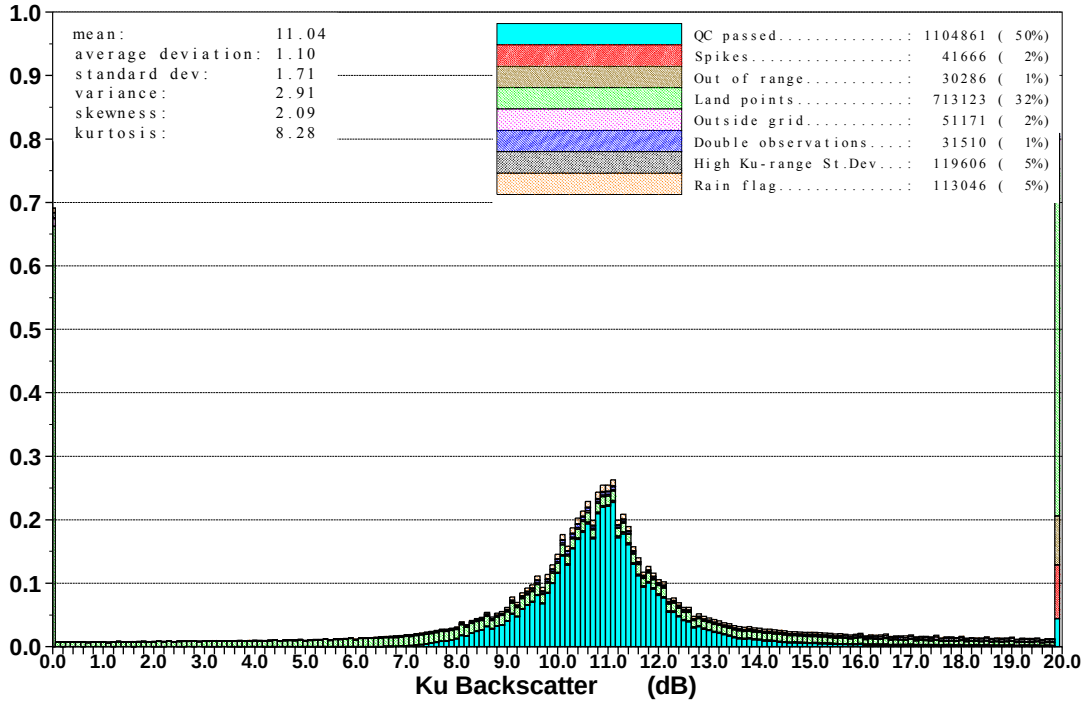

Fig. I.1. Distribution of the RA-2 Ku backscatter coefficient after QC for September 2005.

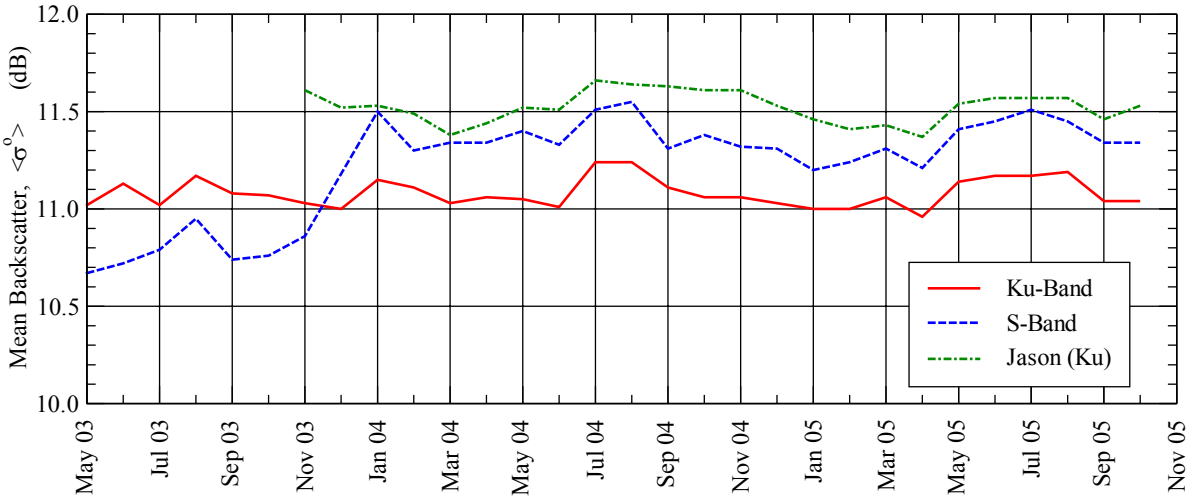

Fig. I.2. Monthly global mean backscatter coefficient of Ku- and S-Band altimeters after quality control. Jason Ku-Band mean backscatter is also shown for comparison.

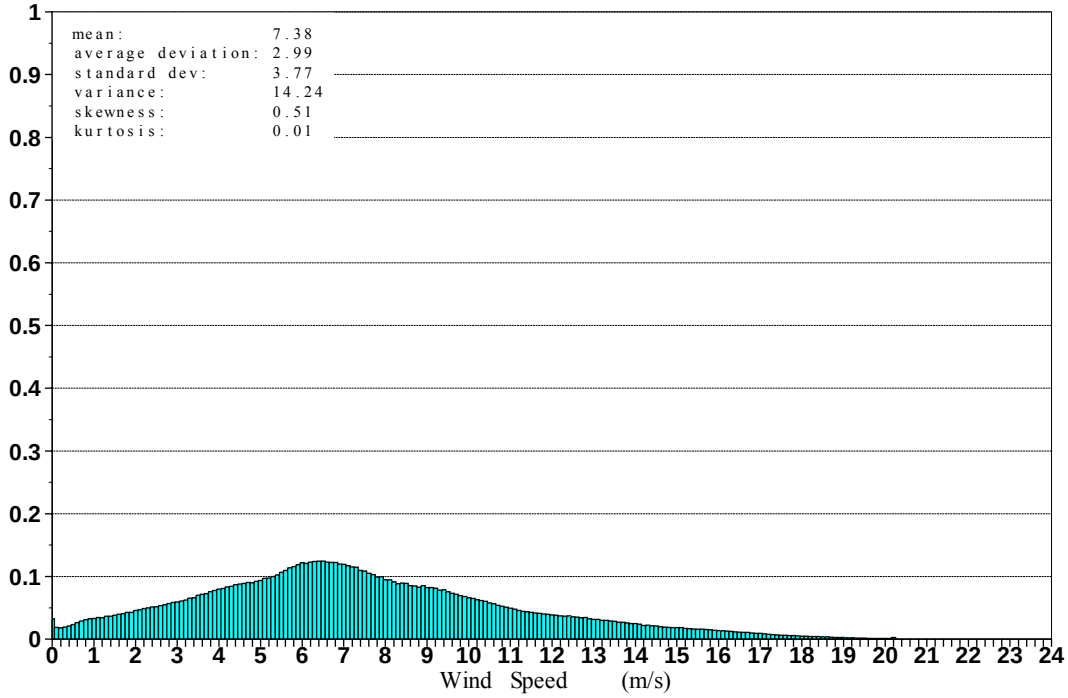

Fig. I.3. Distribution of the RA-2 wind speed after along-track averaging for the period from 1 June 2003 to 31 August 2005.

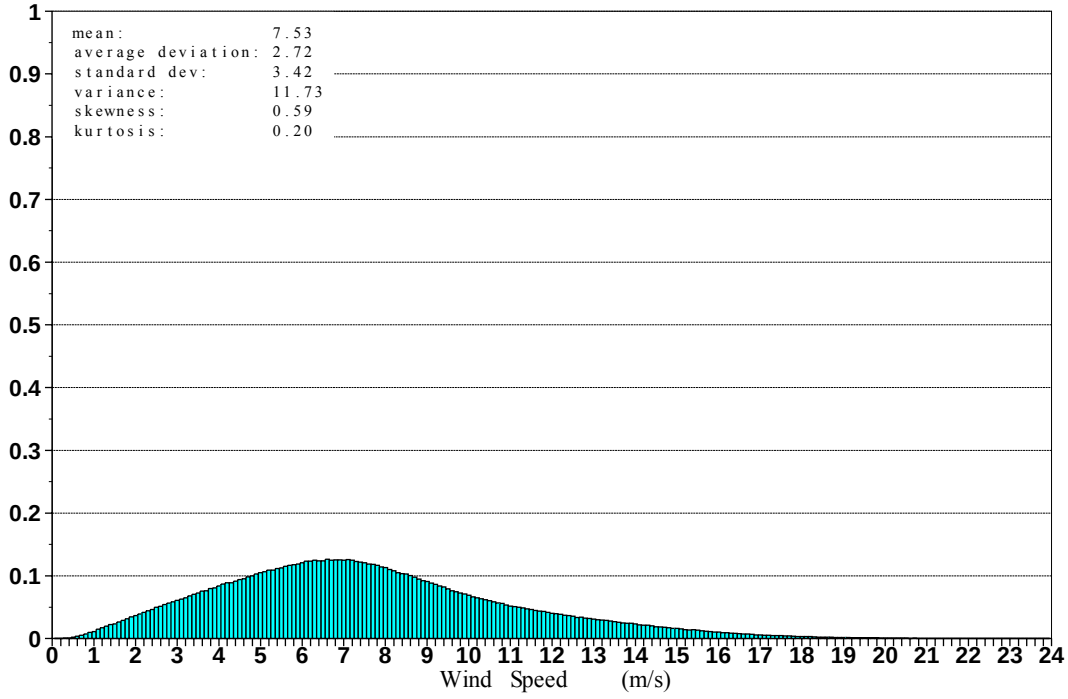

Fig. I.4. Distribution of the ECMWF model wind speed collocated with RA-2 observations for the period from 1 June 2003 to 31 August 2005.

Collocated pairs of RA-2 super-observation and the analysed (AN) ECMWF model wind speeds are plotted as a density scatter plot in Fig. (I.5) for the whole globe over a period of one year (from 1 September 2004 to 31 August 2005). Fig. (I.6) shows a similar plot comparing the altimeter winds against in-situ buoy data for a period of more than two years from 1 June 2003 to 31 August 2005. In general RA-2 wind speed data are in good agreement with the model and buoy data except for very low wind speeds (below ~ 4 m/s) and for high wind speeds (20 m/s and above). The wind speed algorithm needs some adjustments at those two regimes. The ceiling of 20 m/s seems to emerge from the strict application of Witter and Chelton (1991) algorithm implemented to convert backscatter into wind speed, which is limited to 20 m/s. On 24 October 2005, the NRT RA2/MWR Level 1b and Level 2 IPF Version 5.02 processing chain was operationally implemented (see EOO/EOX - Serco/Datamat, 2005). This processing chain introduces a new wind retrieval algorithm which proved to handle some of the mentioned concerns. The algorithm tries to adjust the altimeter low and high wind speed regimes to better fit ECMWF model and buoy wind speeds (Abdalla, 2006). The current implementation still restricts the wind speed but at slightly higher value (~21.5 m/s).

The wind speed bias (defined as the RA-2 minus the model or the buoy) and scatter index (SI, defined as the standard deviation of difference divided by the mean of the model or the buoy) for global, Northern Hemispheric extra-tropics (NH), Tropics and Southern Hemispheric extra-tropics (SH) are listed in Table (I.1). In general, before 24 October 2005 the RA-2 globally underestimates wind speeds by about 15 cm/s compared to the model and by about 65 cm/s compared to the buoys. The RA-2 wind speed scatter index is about 17% compared to the model and about 18% compared to the buoys. One need to keep in mind that most of the in-situ (buoy or platform) instruments are located around North America and Europe. Therefore, the comparison against in-situ observations mainly reflects the quality of the wind speed product in the NH (and to less extent in the Tropics).

The time series of weekly bias between RA-2 and model AN wind speeds over more than two years is shown in Fig. (I.7-a) and over the last year in Fig. (I.7-b) while similar plots for the scatter index are shown in Fig. (I.8-a) and Fig. (I.8-b). One can clearly see the seasonal variation of the bias in the NH. Before the recent IPF change, the bias is positive during the NH winter with a maximum value of about 40 cm/s and negative in the NH summer with a maximum value of about 80 cm/s (Fig. I.7-a). A less pronounced anti-phase seasonal cycle exists in the SH with values ranges between -20 and +20 cm/s. In the Tropics, the seasonal variation follows the NH cycle with a narrower range between -20 and -40 cm/s. Fig. (I.8-a) shows a seasonal variation in SI for NH with low values (~16%) in the summer and higher values (~20%) in the winter. On the other hand it is difficult to notice any seasonal SI variations in the Tropics and in the SH. On the other hand, the impact of the IPF Version 5.02 processing chain is clearly displayed in Fig. (I.7-b) and Fig. (I.8-b). The bias was flipped in all regions and the altimeter started to have higher wind speeds than the model with a global mean value of about 30 cm/s (about 60 cm/s in the NH and about 20 cm/s in the SH and the Tropics). This is in line with the comparison between the model and the buoys. Another desired feature of the new algorithm during the last two months is the collapse of the biases in the SH and the Tropics to almost the same value. Furthermore, Fig. (I.8-b) shows clear reduction in the global SI value by about one point. The SI reduction in the Tropics is relatively large (more than 2 points) while the trend is not so clear in the NH. The signals from the past two months of statistics indicate a good performance of the new algorithm. However, one still needs longer time series to fully assess the performance of the new algorithm.

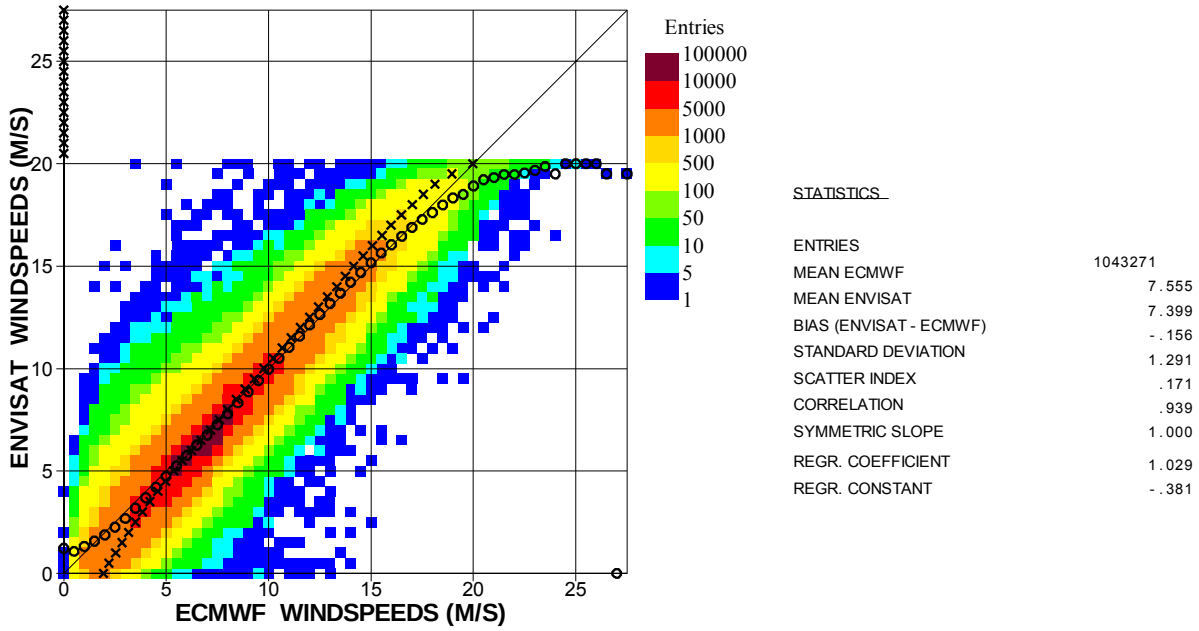

Fig. I.5. Global comparison between RA-2 and AN ECMWF model wind speed values during the period from 1 September 2004 to 31 August 2005.

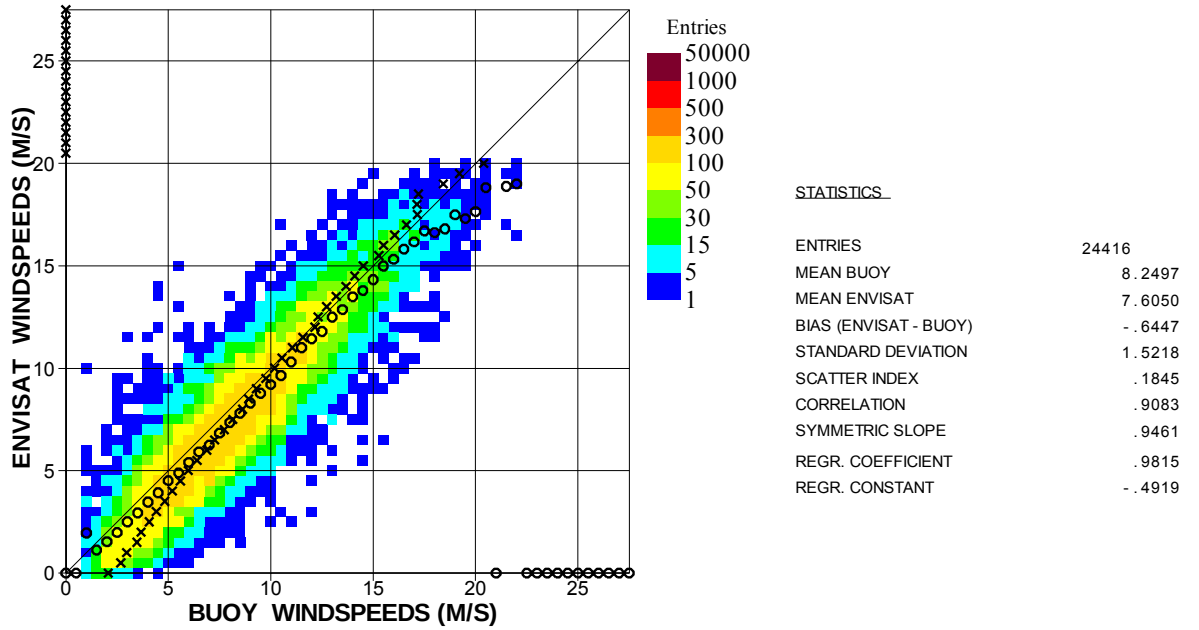

Fig. I.6. Global comparison between RA-2 and in-situ wind speed values during the period from 1 June 2003 to 31 August 2005 (mainly in the NH).

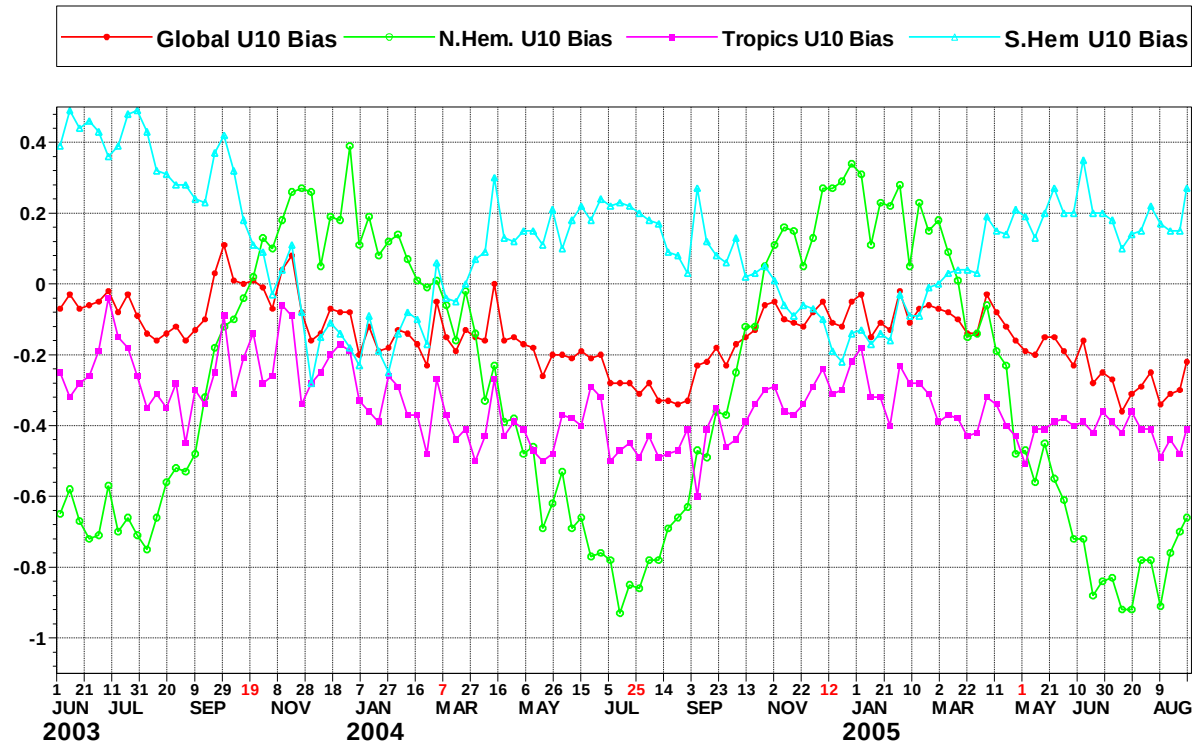

Fig. I.7-a. Time series of weekly wind speed bias (m/s) between RA-2 and ECMWF model AN.

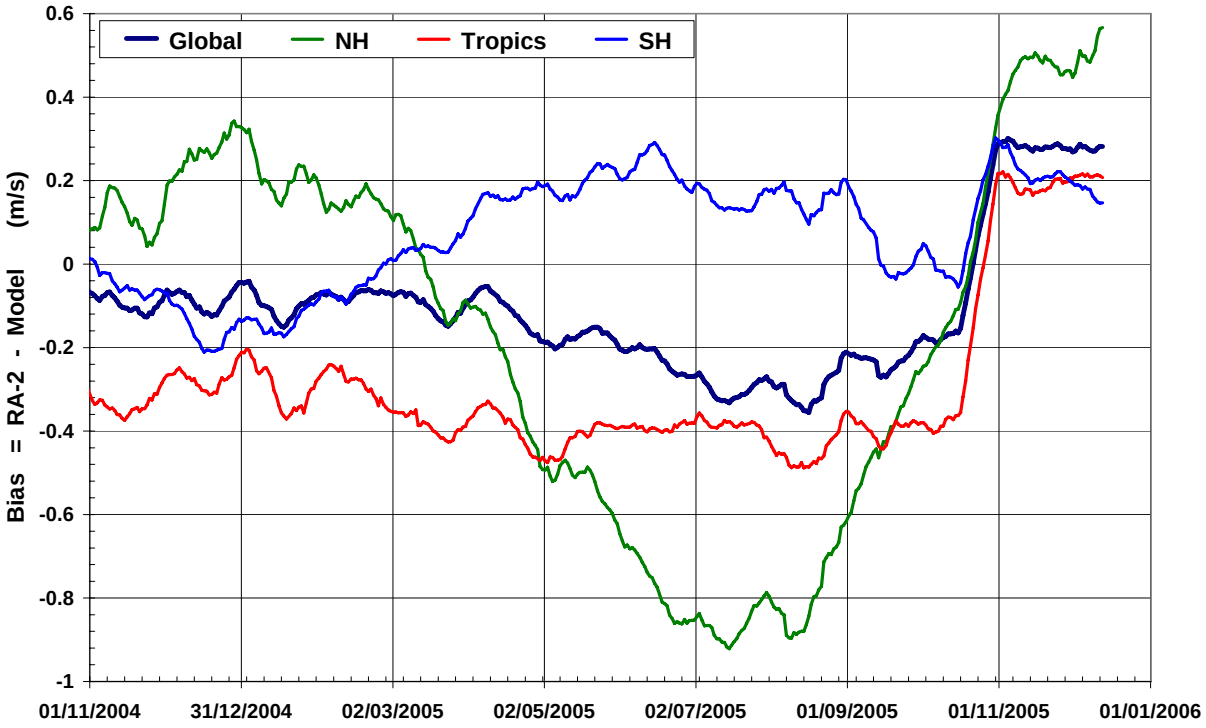

Fig. I.7-b. Time series of wind speed bias between RA-2 and ECMWF model AN over the last year.

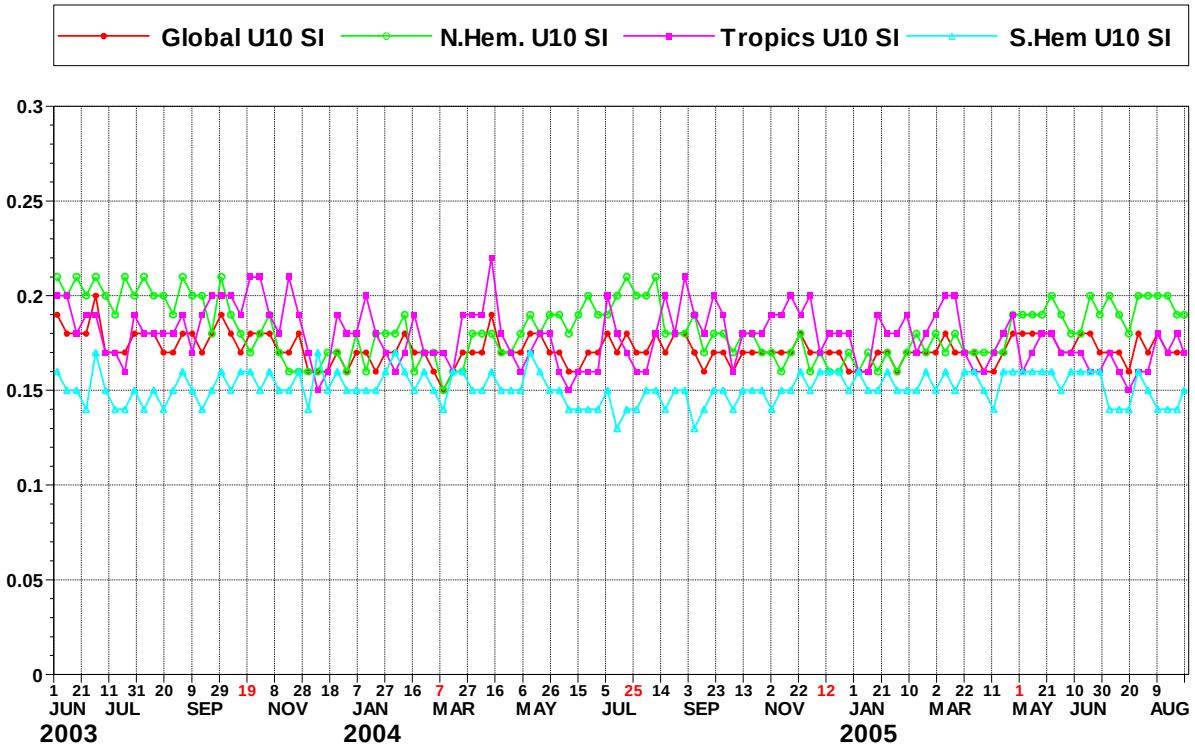

Fig. I.8-a. Time series of weekly wind speed SI between RA-2 and ECMWF model AN.

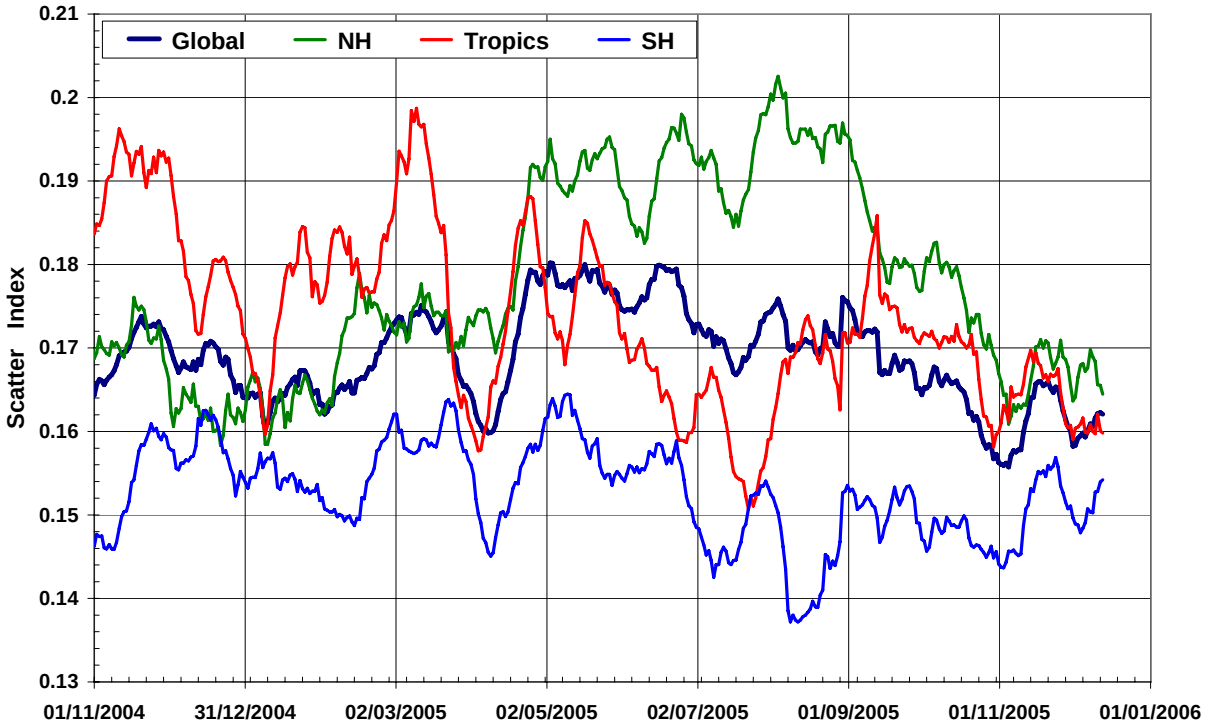

Fig. I.8-b. Time series of wind speed SI between RA-2 and ECMWF model AN over the last year.

	RA-2	Model AN		Buoys		
	1 September 2004 - 31 August 2005			1 June 2003 - 31 August 2005		
	Mean (m/s)	Bias (m/s)	SI (%)	Mean (m/s)	Bias (m/s)	SI (%)
Global	7.40	−0.16	17.1	8.25	−0.64	18.5
NH	7.17	−0.26	18.7	8.34	−0.61	18.9
Tropics	5.74	−0.37	17.7	7.64	−0.88	13.3
SH	8.71	+0.06	15.4	---	---	---

Table I.1: Comparison of Surface Wind Speed with ECMWF Model AN and Buoys for Different Regions

I.4. RA-2 KU-Band significant wave height

Ku-Band SWH product is characterised by stable performance and good quality since the start of the mission. Fig. (I.9) shows a typical distribution of RA-2 Ku-Band SWH super-observations over a period of more than two years (1 June 2003 to 31 August 2005). The corresponding histogram of collocated ECMWF wave model (WAM) for the same period is shown in Fig. (I.10). Apart from RA-2 histogram having slightly higher mean, the two histograms are in good agreement with each other. There are two other minor differences, however. The RA-2 histogram is truncated at about 40 cm and of slightly higher variance.

Collocated SWH pairs of RA-2 super-observation and the first-guess (FG) WAM model are plotted as a density scatter plot in Fig. (I.11) for the whole globe over a period of one year (from 1 September 2004 to 31 August 2005). Fig. (I.12) shows a similar plot comparing the altimeter SWH against in-situ buoy data for a period of more than two years from 1 June 2003 to 31 August 2005. The agreement between the altimeter SWH and both the model and the buoy values is in general very good. However, the altimeter overestimates wave heights by about 5% compared to the model FG and by about 2% compared to the buoy observations.

The SWH bias (RA-2 minus WAM or buoy) and SI for the whole globe, NH, Tropics and SH are listed in Table (I.2). In general, RA-2 globally overestimates SWH by about 11 cm and 9 cm compared to the model the buoys, respectively. The RA-2 SWH scatter index is about 12% compared to the model and about 16% compared to the buoys. Again, one needs to keep in mind that the comparison against buoys mainly reflects the quality of the SWH product in the NH (and to less extent in the Tropics).

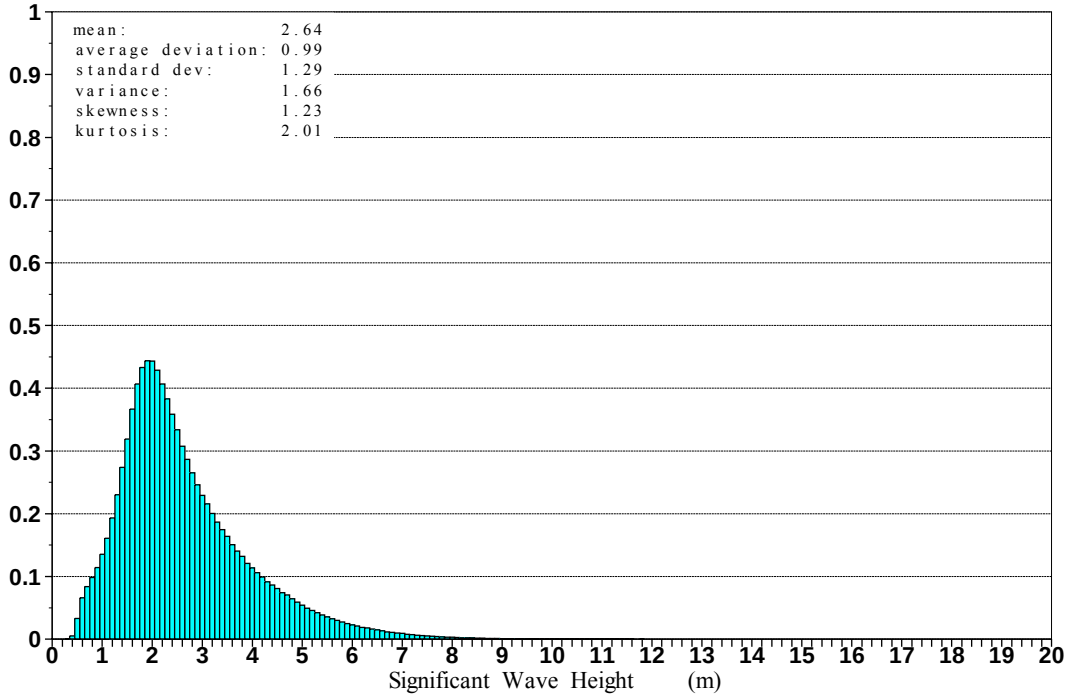

Fig. I.9. Distribution of the RA-2 SWH after along-track averaging for the period from 1 June 2003 to 31 August 2005.

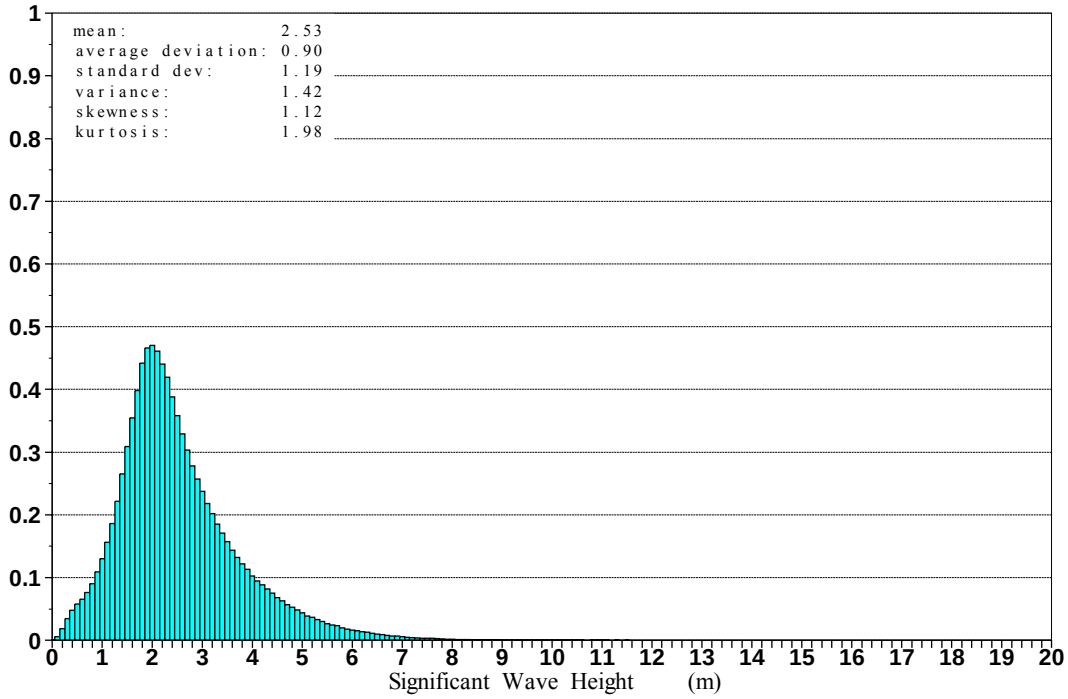

Fig. I.10. Distribution of the WAM model FG SWH collocated with RA-2 observations for the period from 1 June 2003 to 31 August 2005.

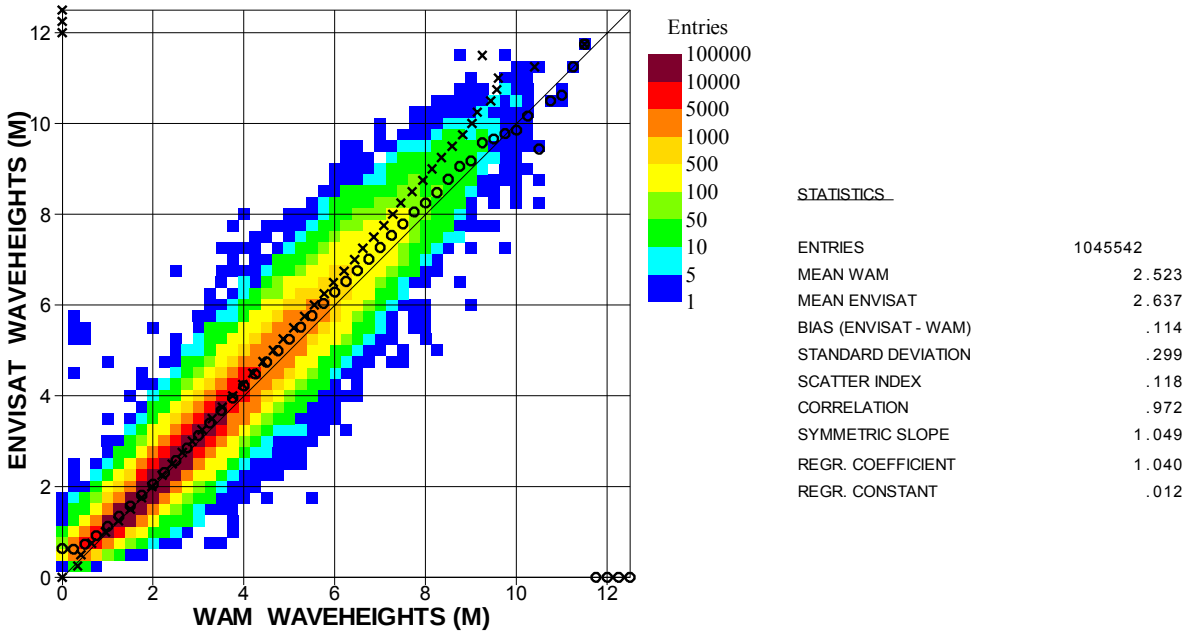

Fig. I.11. Global comparison between RA-2 Ku-Band and WAM wave model SWH FG values during the period from 1 September 2004 to 31 August 2005.

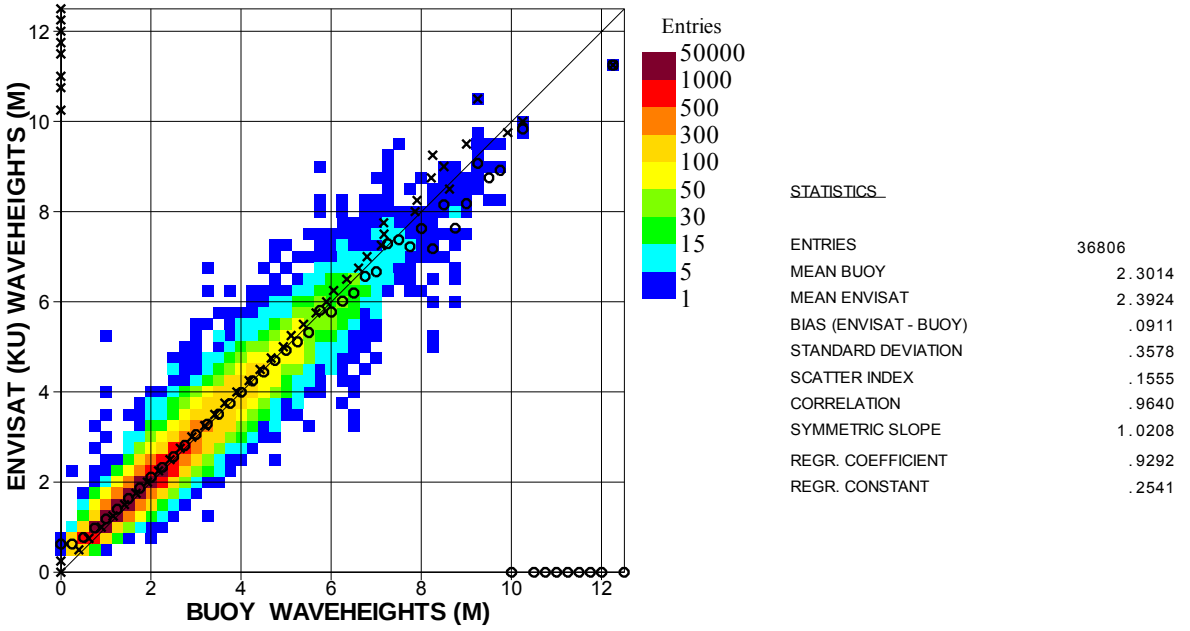

Fig. I.12. Global comparison between RA-2 Ku-Band and in-situ SWH values during the period from 1 June 2003 to 31 August 2005 (mainly in the NH).

	RA-2	Model FG		Buoys		
	1 September 2004 - 31 August 2005			1 June 2003 - 31 August 2005		
	Mean (m)	Bias (m)	SI (%)	Mean (m)	Bias (m)	SI (%)
Global	2.64	+0.11	11.8	2.30	+0.09	15.6
NH	2.40	+0.16	14.0	2.35	+0.09	15.8
Tropics	1.96	+0.05	11.0	1.99	+0.07	11.6
SH	3.26	+0.13	10.7	---	---	---

Table I.2: Comparison of Ku-Band SWH with WAM Model FG and Buoys for Different Regions

The time series of weekly bias between RA-2 and model FG SWH over more than two years is shown in Fig. (I.13) while a similar plot for the SI is shown in Fig. (I.14). Both figures also indicate the dates when significant model or RA-2 processing changes are introduced. Specifically; RA-2 SWH observations replaced ERS-2 RA (with reduced coverage) in wave data assimilation of WAM model on 22 October 2003, IPF Version 4.56 processing chain for RA-2 and MWR was implemented on 26 November 2003, parameterisation of unresolved bathymetry was introduced on 9 March 2004, most of RA-2 SWH observations were rejected by data assimilation after a PDS format change during the period from 9 August to 4 October 2004 and an improved wave dissipation source term was introduced to the wave model on 5 April 2005.

As can be seen in Fig. (I.13), seasonal cycles of the bias similar to the wind speed can be clearly seen for the NH and the SH. However, the bias is always positive in both NH and SH. The amplitudes of seasonal cycles change in time. During the summer 2003 and the following winter the maximum weekly bias exceeded 30 cm for both hemispheres. Several changes on the model side (data assimilation late October 2003 and unresolved bathymetry early March 2004) took the cycle peak to around 23 cm in summer 2004 for SH and the next winter for NH. Another model change in early April 2005 (new dissipation model) reduced the peak of following SH bias cycle to about 17 cm. On the other hand, the bias in the Tropics does not seem to follow any seasonal cycle. The bias in the Tropics was mainly negative before the model change in early March 2004 (unresolved bathymetry). Then it changed sign and settled to about 3 cm until the model change in April 2005 (new dissipation model) when it jumped to about 8 cm. Furthermore, the implementation of the new dissipation source term (April 2005) changed the bias in the different areas mainly in the proper direction. The time history of the SI (Fig. I.14) shows that there are higher SI values in NH during the summer while the SH and the Tropics do not show similar behaviour. The high SI values before 20 October 2003 and during August-September 2004 are due to the reduced (or total loss of) wave height observations for data assimilation.

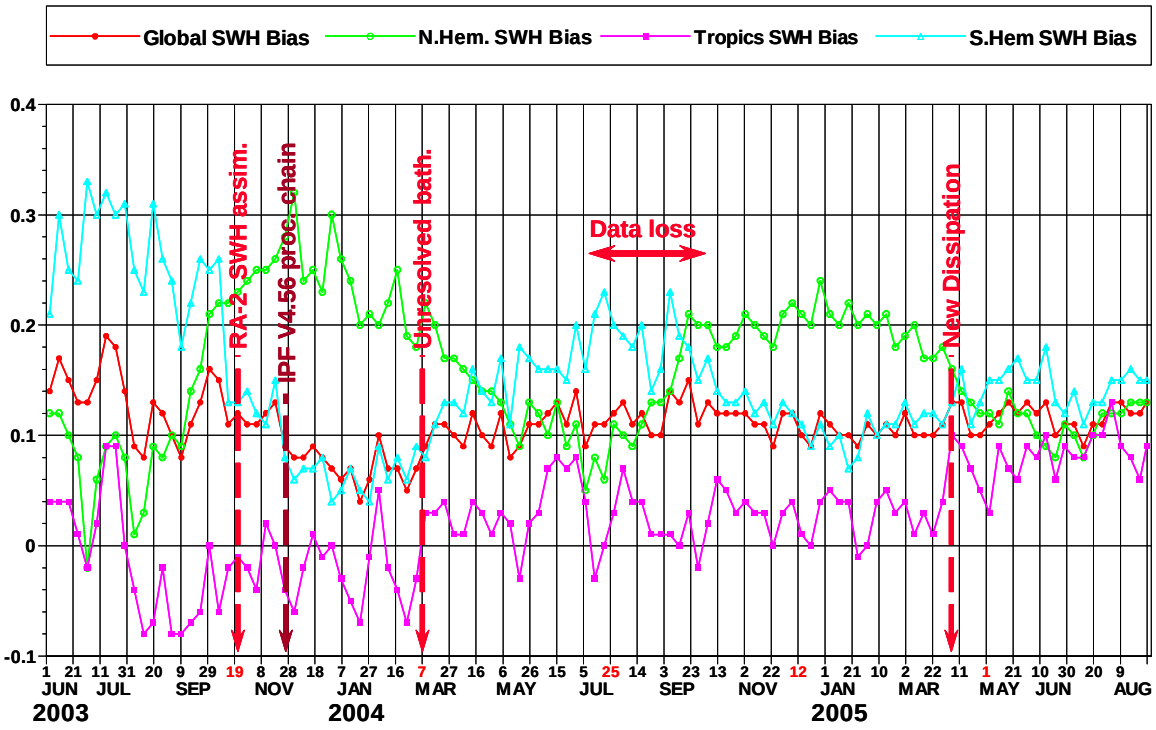

Fig. I.13. Time series of weekly SWH bias (metres) between RA-2 Ku-Band and WAM model FG.

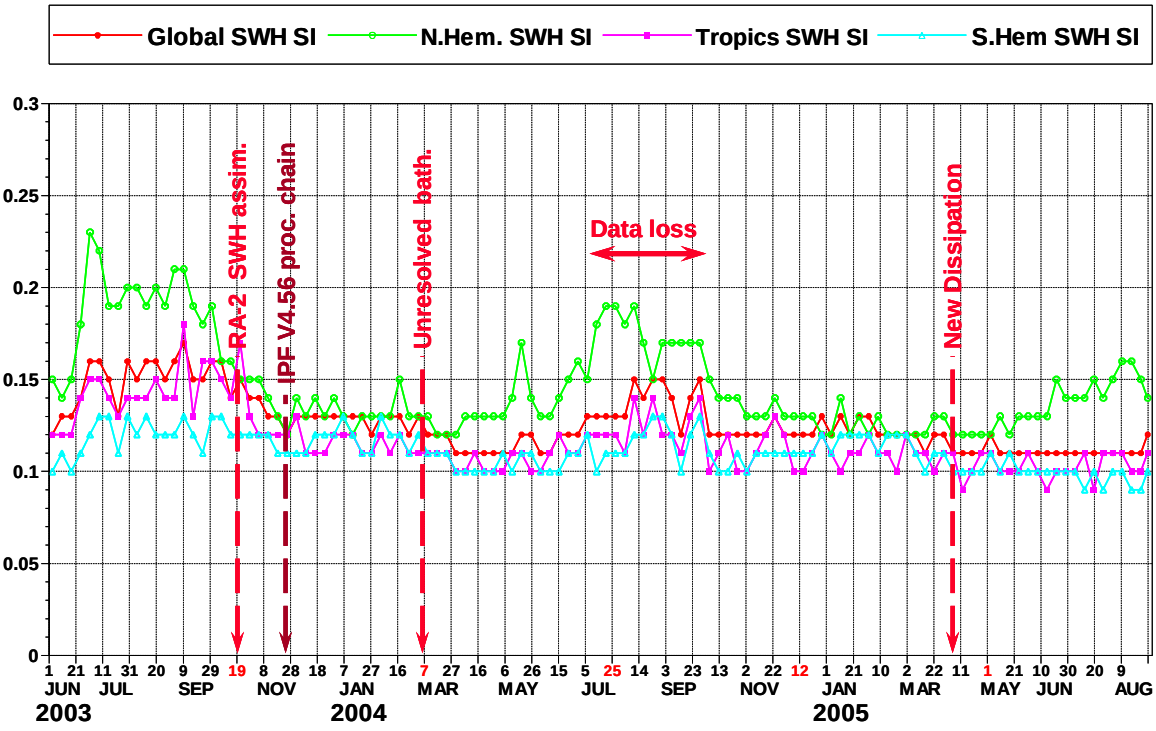

Fig. I.14. Time series of weekly SWH SI between RA-2 Ku-Band and WAM model FG.

Comparisons of pairs of observation products are usually not enough to estimate the error in each product. If enough data products are available, a multiple collocation analysis is needed to give some absolute error estimates of each product. Following Janssen et al. (2003), we have collocated SWH from ENVISAT RA-2 Ku-Band, ERS-2 RA, buoys, model FG and model analysis (AN) over the period from 18 July 2002 to 21 October 2003. To minimise the contribution of the dislocation, both in space and time, to the error estimates, the collocated quintuplets are rejected if the difference between the model estimates at the location of the RA-2 observation and the buoy location exceeds 5%. Furthermore, the fast delivery ERS-2 SWH used in the analysis suffer from a systematic error at low wave heights, as it is not able to detect any wave height below 60 cm. Therefore, we only considered collocations with wave heights in excess of 1 m. The total number of valid collocations used in the error estimation is 8312.

Each product is assumed to be a linear function of the truth multiplied by a calibration factor (slope) and an error. With several sources of data, there are several possibilities of triple collocation. Apparently, the model analysis and ERS-2 wave height are correlated as the latter is used in the assimilation process during the period considered. Assuming that the other data sets are independent, conflicting results for RA-2 wave height error estimate are obtained. Therefore, we concluded that RA-2 and ERS-2 errors are correlated. Hence, quintuple collocations were used to overcome the correlation problem. Fig. (I.15) shows the monthly scatter index (the absolute error divided by the mean) of SWH for each product. While interpreting the results in Fig. (I.15), one need to keep in mind that the results for July-September 2003 are not very conclusive due to the limited coverage of ERS-2 which caused the loss of an important part of the usual collocations during those months. For the whole period, the model analysis is, as expected, the one with the lowest overall error of about 5%. The RA-2 comes second with about 6%, followed by ERS-2 with about 7% and finally the buoy with about 8%. This result proves that the ENVISAT RA-2 Ku-Band SWH product is of high quality. If the buoy observations are selected as the reference, RA-2 SWH values turn out to be too high by about 2.0% (consistent with Fig. I.6), while ERS-2 and model analysis wave heights are too low by about 4.5% and 5.0%, respectively. The time series of the monthly slopes of each data source with respect to buoy SWH can be seen in Fig. (I.16). The overestimation of the RA-2 SWH product can be clearly seen at all months. Finally, the correlation between ENVISAT and ERS-2 altimeter wave heights is estimated to be 77%. This relatively high correlation may be due to the fact that both altimeters share the same principles of measurement.

Experiments with assimilation of Ku-Band SWH product proved to be very beneficial for the operational wave analysis (c.f. Abdalla et al., 2004). Therefore, this product started to be assimilated in the ECMWF wave model since 22 October 2003. It replaced the ERS-2 RA SWH product which had only limited coverage after the tape recorder failure on 22 June 2003.

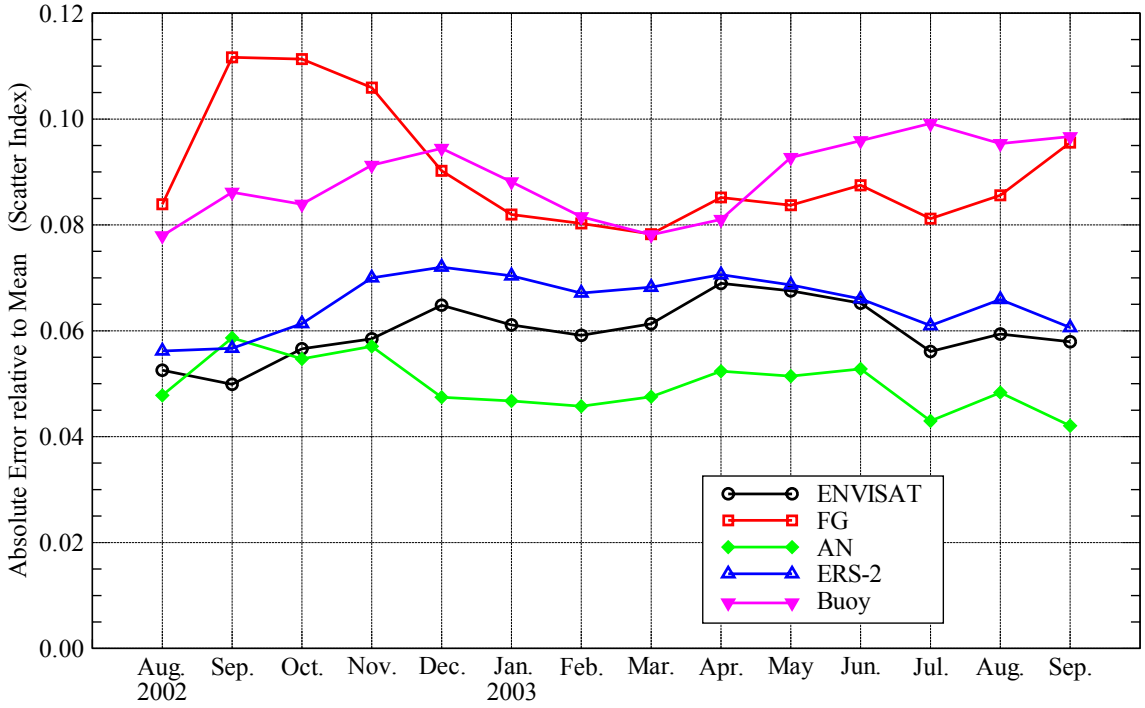

Fig. I.15. Monthly scatter index of ENVISAT RA-2, model FG, model AN, ERS-2 RA and buoy SWH (Maximum collocation difference is 5%, SWH > 1 m).

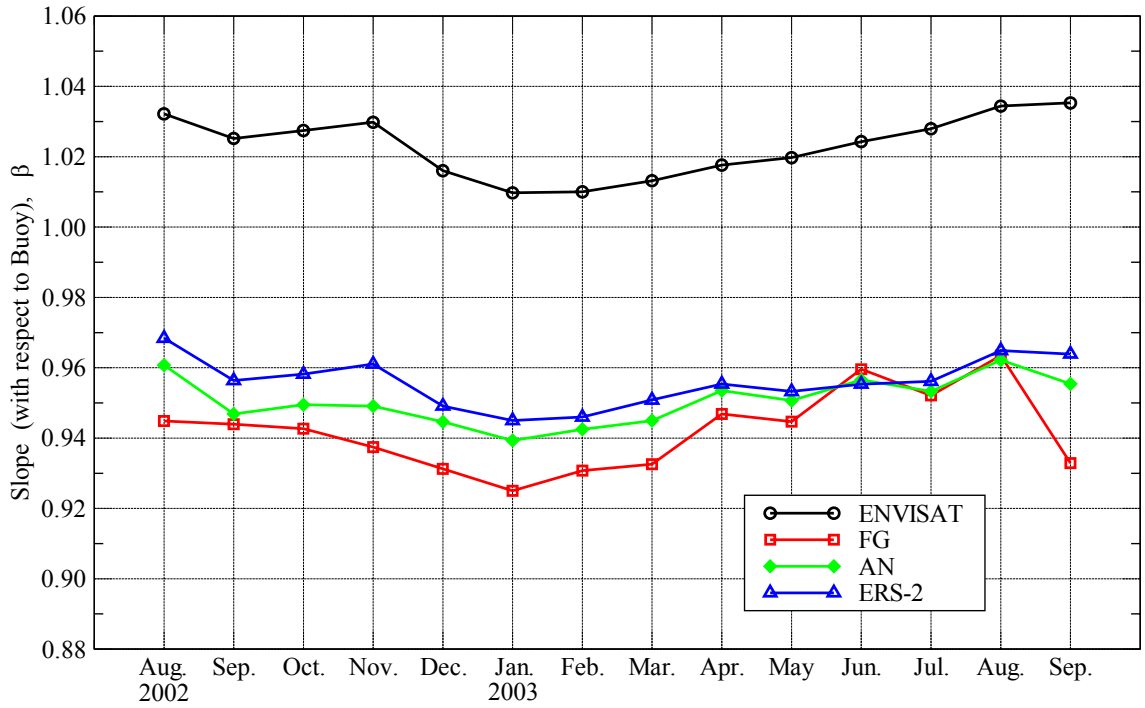

Fig. I.16. Monthly slopes of ENVISAT RA-2, model FG, model AN and ERS-2 RA SWH against buoy SWH (Maximum collocation difference is 5%, SWH > 1 m).

I.5. RA-2 S-Band significant wave height

The S-Band significant wave height product is of a lower quality than the Ku-Band product. Collocated SWH pairs of RA-2 S-Band super-observation and the first-guess (FG) WAM model are plotted as density scatter plot in Fig. (I.17) for the whole globe over a period of one year (from 1 September 2004 to 31 August 2005). Fig. (I.18) shows a similar plot comparing the altimeter SWH against in-situ buoy data for a period of more than two years from 1 June 2003 to 31 August 2005. Although the major part of the S-Band SWH observations agrees very well with the model and the buoys, there are a number of outliers (less than 1.0%). Most of the outliers are due to what is known as the RA-2 *S-Band Anomaly* caused by the accumulation of S-Band waveforms under some conditions. A typical S-Band anomaly event is clearly displayed in Fig. (I.19) which shows the global distribution of the difference (in metres) between S-Band and WAM FG SWH values on 10 January 2004. The tracks affected by the S-Band anomaly are surrounded by red ellipses. Stricter quality control (QC) criteria were used in an attempt to eliminate the S-Band anomaly and the scatter plot corresponding to Fig. (I.17) is shown in the Appendix as Fig. (A.1). Another obvious undesirable feature in the scatter plots of Figs (I.17), (I.18) and (A.1) is the S-Band overestimate at low wave heights (similar to the well-known feature of ERS FD RA SWH).

The S-Band SWH bias (RA-2 minus WAM or buoy) and SI for the whole globe, NH, Tropics and SH are listed in Table (I.3) for operational quality control and in Table (A.1) of the Appendix for stricter QC (only against model). Globally, RA-2 S-Band overestimates SWH by about 8 cm (6 cm for stricter QC) and 12 cm compared to the model and the buoys, respectively. The S-Band SWH SI is about 21% (about 14% for stricter QC) compared to the model and about 26% compared to the buoys. Again, one needs to keep in mind that the comparison against buoys is more or less a Northern Hemispheric. These SI values are much higher than the Ku-Band values.

	RA-2	**Model FG**		**Buoys**		
	1 September 2004 - 31 August 2005			1 June 2003 - 31 August 2005		
	Mean (m)	Bias (m)	SI (%)	Mean (m)	Bias (m)	SI (%)
Global	2.61	+0.08	20.9	2.30	+0.12	25.7
NH	2.43	+0.19	24.9	2.35	+0.12	25.6
Tropics	2.02	+0.11	28.6	1.99	+0.07	25.4
SH	3.14	+0.01	15.3	---	---	---

Table I.3: Comparison of S-Band SWH with WAM Model FG and Buoys for Different Regions

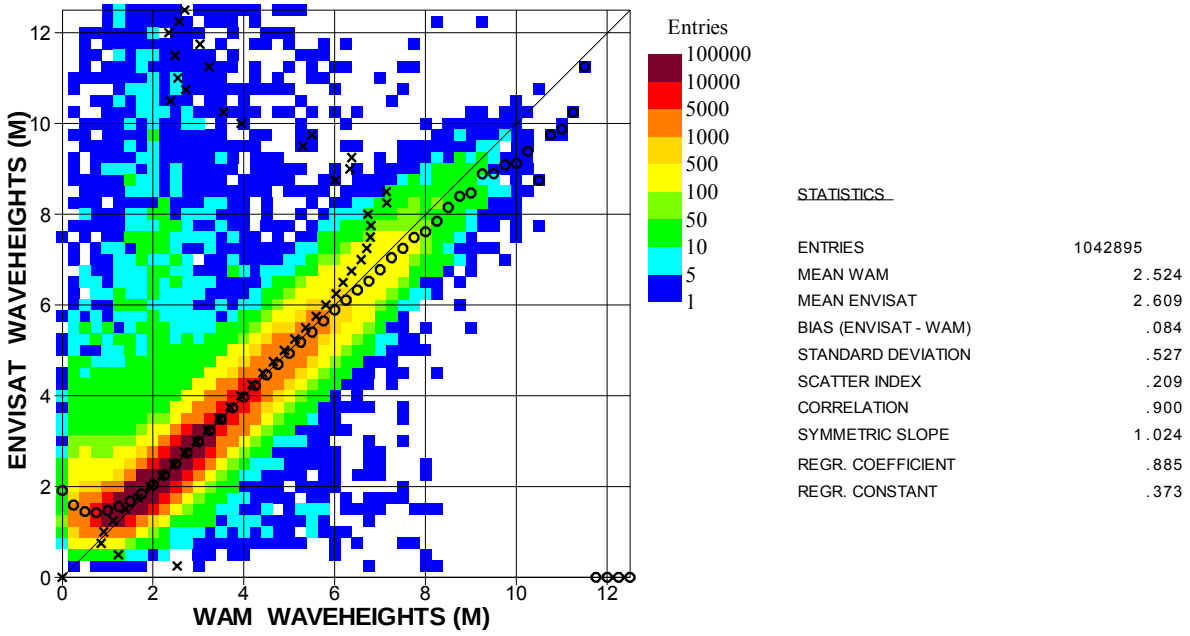

Fig. I.17. Global comparison between RA-2 S-Band and ECMWF wave model FG values during the period from 1 September 2004 to 31 August 2005.

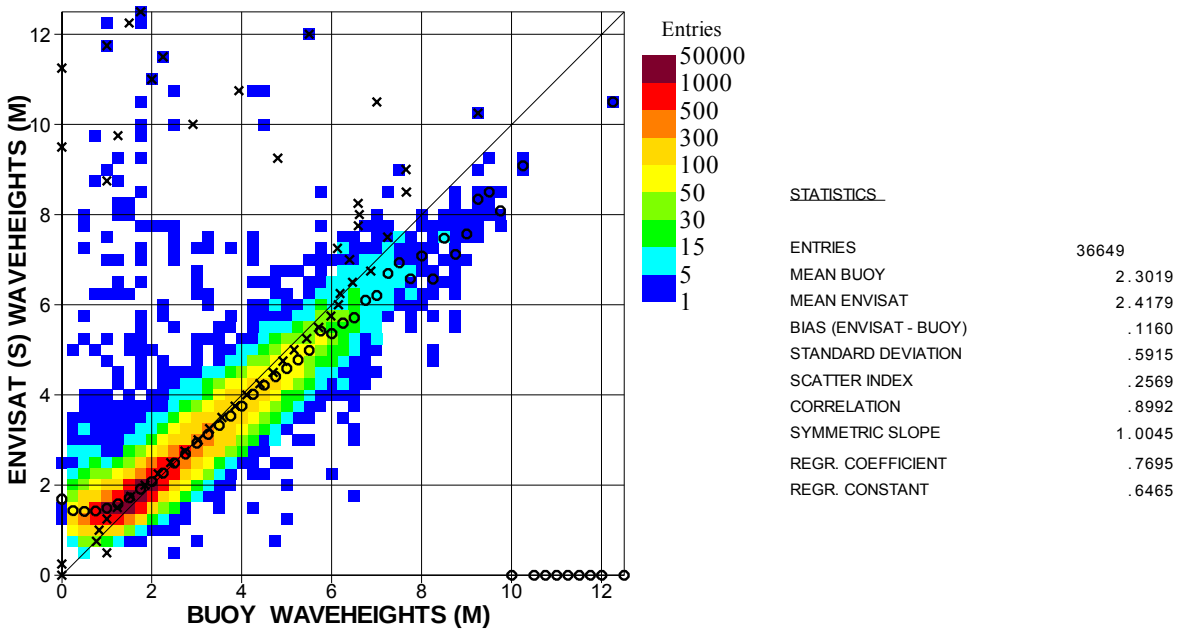

Fig. I.18. Global comparison between RA-2 S-Band and in-situ SWH values during the period from 1 June 2003 to 31 August 2005 (mainly in the NH).

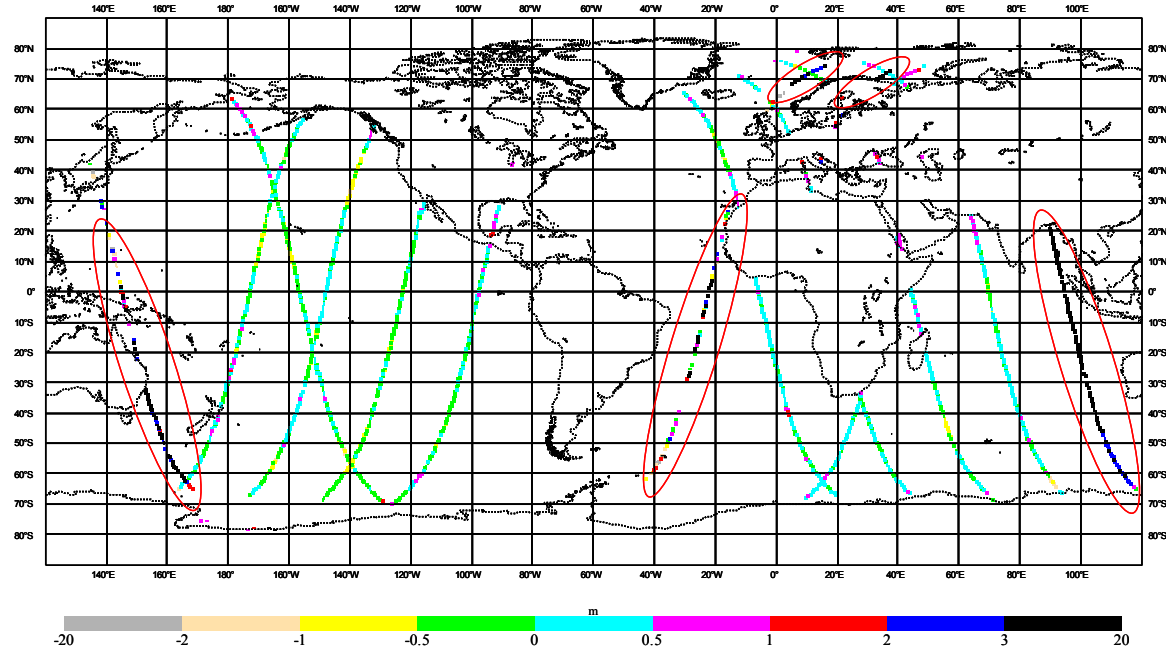

Fig. I.19. SWH difference (in metres) between RA-2 S-Band and WAM wave model FG values on 10 January 2004. The S-Band anomaly affected tracks are surrounded by red ellipses.

The time series of weekly bias between S-Band and model FG SWH over more than two years is shown in Fig. (I.20) while a similar plot for the SI is shown in Fig. (I.21). One can notice from Fig. (I.20) seasonal cycles of the bias which is well pronounced for the NH and to a less extent for the SH starting from late 2003 coinciding with the implementation of the IPF Version 4.56 instrument processing chain (26 November 2003). Interestingly, the seasonal cycles in the NH and the SH are out of phase with the corresponding cycles for the wind speed (Fig. I.7) and the Ku-Band SWH (Fig. I.13). Since 26 November 2003, the bias is in general positive for both the NH and the Tropics while in the SH the bias is fluctuating around zero. The time history of the SI (Fig. I.21) shows that the SI values in NH are too high during the summer while they do not change much in SH and the Tropics. This behaviour is similar to the Ku-Band SWH SI (Fig. I.14). The extremely high SI values are associated with S-Band anomaly events. Finally it is worth mentioning that most of the S-Band anomaly events coincide with highly active rain flagging according to the rain flag reported in the FDMAR product.

The time series of the ratio between the daily global mean Ku-Band SWH and the corresponding S-Band value is shown in Fig. (I.22). Apart from a number of dips, the ratio between Ku-Band and S-Band daily mean SWH changed between 0.92 and 1.02. The dips usually coincide with the extreme RA-2 S-Band anomaly events. It is important to notice the seasonal variation for this ratio with low values (~0.92-0.94) reached during the Northern hemispheric summer and high values (around 1.0) during the remaining part of the year.

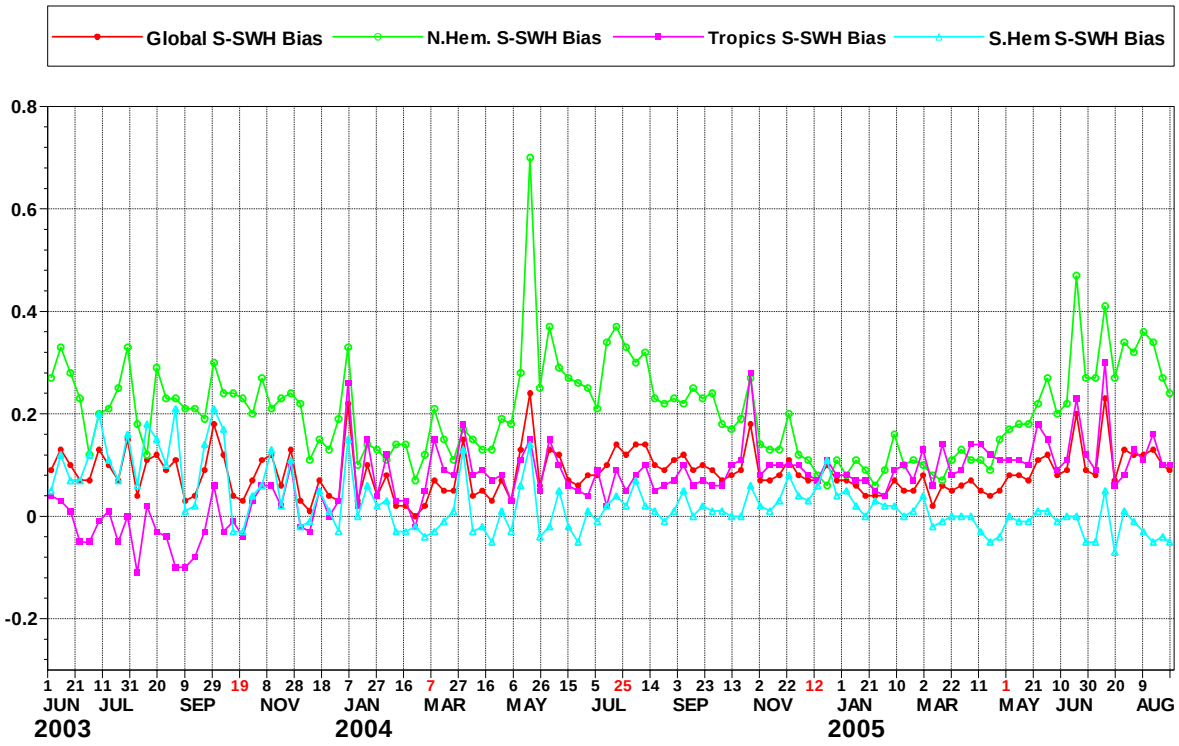

Fig. I.20. Time series of weekly SWH bias (metres) between RA-2 S-Band and WAM model FG.

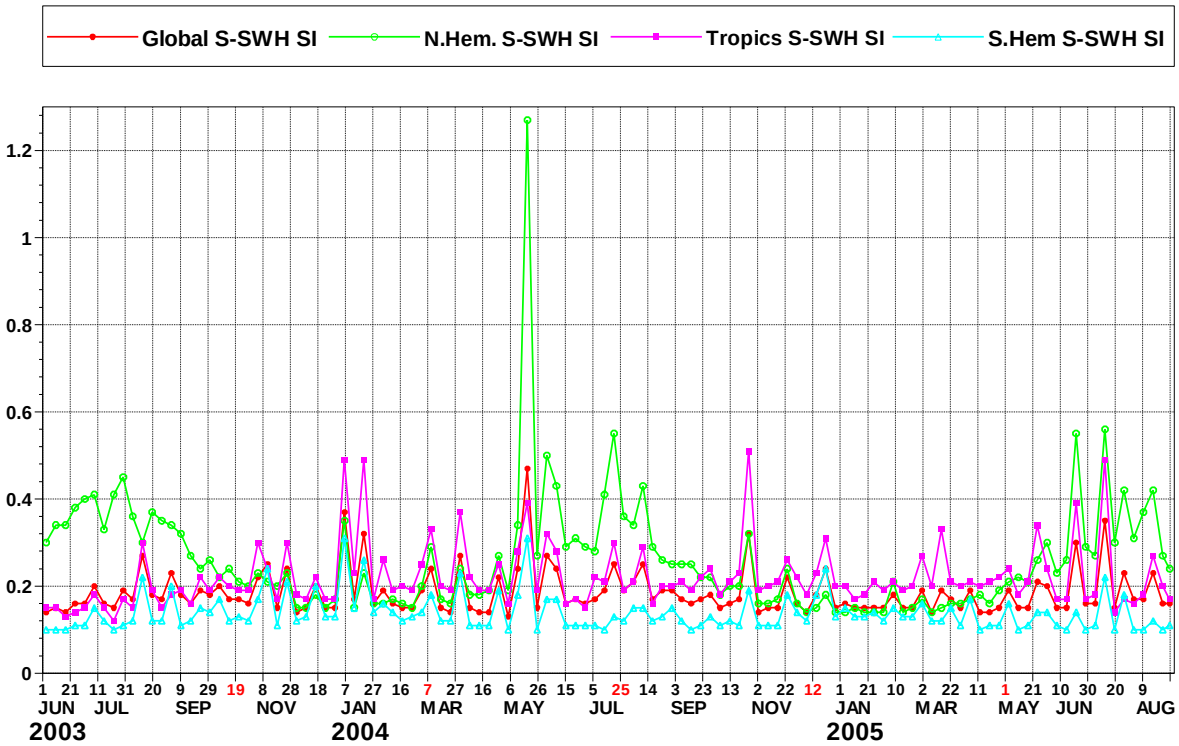

Fig. I.21. Time series of weekly SWH SI between RA-2 S-Band and WAM model FG.

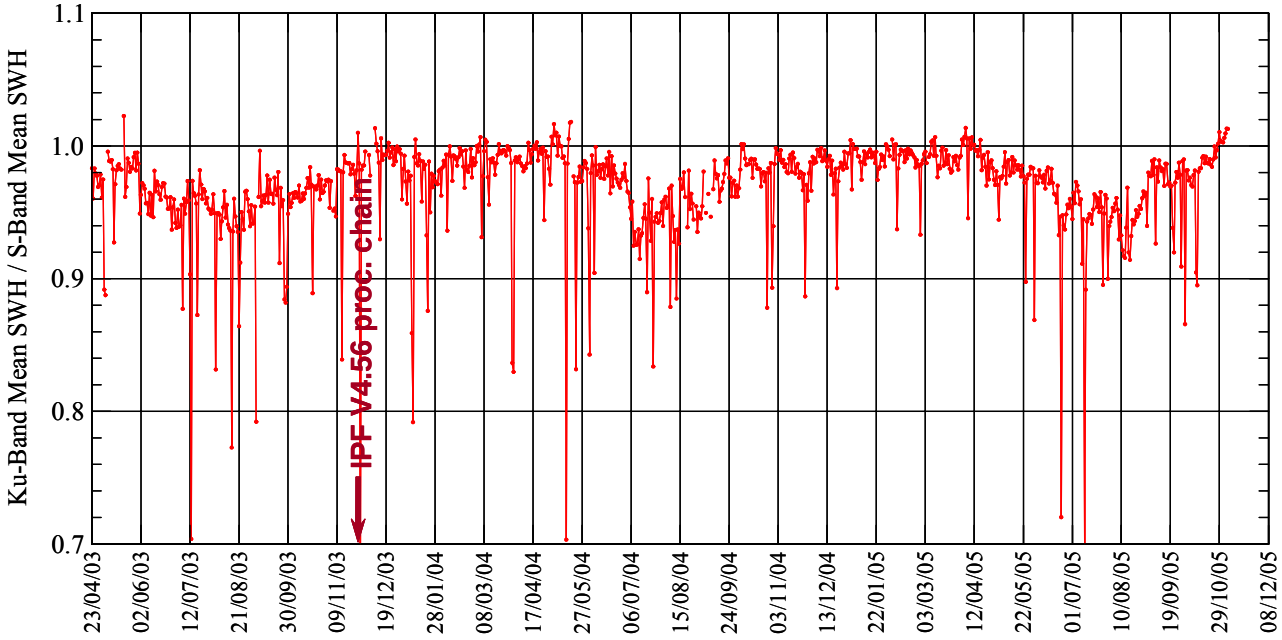

Fig. I.22. Time series of daily global ratio between mean Ku-Band to mean S-Band SWH.

I.6. MWR products

Two MWR products are monitored and validated: the total column water vapour (TCWV) and the wet tropospheric correction (WTC). Both parameters are functions of the 23.8-GHz (TB23) and 36.5-GHz (TB36) brightness temperatures and wind speed. ECMWF atmospheric model computes TCWV as one of its standard output products. Model WTC can be calculated from pressure, temperature and humidity fields. For the validation of the MWR products analysis (AN) model fields are used.

Collocated TCWV pairs of MWR super-observation and the ECMWF model AN are plotted as density scatter plot in Fig. (I.23) for the whole globe, and in Fig. (I.24) for the Tropics over a period of one year (from 1 September 2004 to 31 August 2005). Although the major part of the MWR TCWV observations agrees very well with the model, there are quite a number of outliers associated with model low values (less than ~15 kg/m^2). MWR reports extremely high values for some of them. It should be noted that such outliers do not exist in the Tropics (Fig. I.24). Examining the spatial distribution of difference between both products (not shown) suggests that a large portion of those outliers occurred near the poles. This means that it is very likely that those outliers are due to ice contamination. Stricter QC criteria, involving model sea ice information, were used in an attempt to eliminate those outliers and the scatter plot corresponding to Fig. (I.23) is shown in the Appendix as Fig. (A.2). It is clear that most of the outliers have disappeared. Another smaller part of the outliers happened very close to the coast, which suggests possible land contamination. On the other hand, one can notice a hump below the main cloud between model TCWV values of 15 and 20 kg/m2. This hump occurs at every region or sub-region. This hump, which is very clear for one year of data (Figs. I.23 and I.24), is barely seen in the monthly plots (and usually interpreted as outliers). At this stage, the reasons behind this type of outlier are not known.

The MWR TCWV bias (MWR minus model) and SI for the whole globe, NH, Tropics and SH are listed in Table (I.4) for operational QC and in Table (A.2) for stricter QC. It is clear that MWR observations are drier

than the model except for the Tropics. While the global value of the TCWV SI is about 16% (or 9% for stricter QC), that value is less than 7% in the Tropics.

The time series of weekly bias between MWR and ECMWF model TCWV over more than two years is shown in Fig. (I.25) while a similar plot for the SI is shown in Fig. (I.26). The impact of the IPF Version 4.56 instrument processing chain. (26 November 2003) is clearly evident. The large negative bias in the SH (~2.3 kg/m^2) reduced by about 1 kg/m^2. Also, the MWR TCWV levels increased by about 0.5 kg/m^2 in the Tropics. More important, the SI was reduced everywhere and the global SI reduced from ~23% to ~16%. While Fig. (I.25) does not give any indication for possible seasonal variation in TCWV bias; there is an apparent seasonal cycle in Fig. (I.26) for the SI in the extra-tropics. The SI in the NH has a peak during February-March while the peak for the SH occurs during August-September. The Tropics SI is more or less constant at about 6-7% after the implementation of the IPF V4.56 instrument processing chain.

	TCWV			WTC		
	MWR mean (kg/m^2)	Bias (kg/m^2)	SI (%)	MWR mean (mm)	Bias (mm)	SI (%)
Global	24.33	−0.52	15.9	149	−12	14.8
NH	19.80	−0.65	24.9	124	−11	24.6
Tropics	41.71	+0.59	6.6	252	−11	6.6
SH	14.64	−1.24	23.6	92	−14	20.3

Table I.4: Comparison of MWR Products with ECMWF Model AN for Different Regions (1 September 2004 - 31 August 2005)

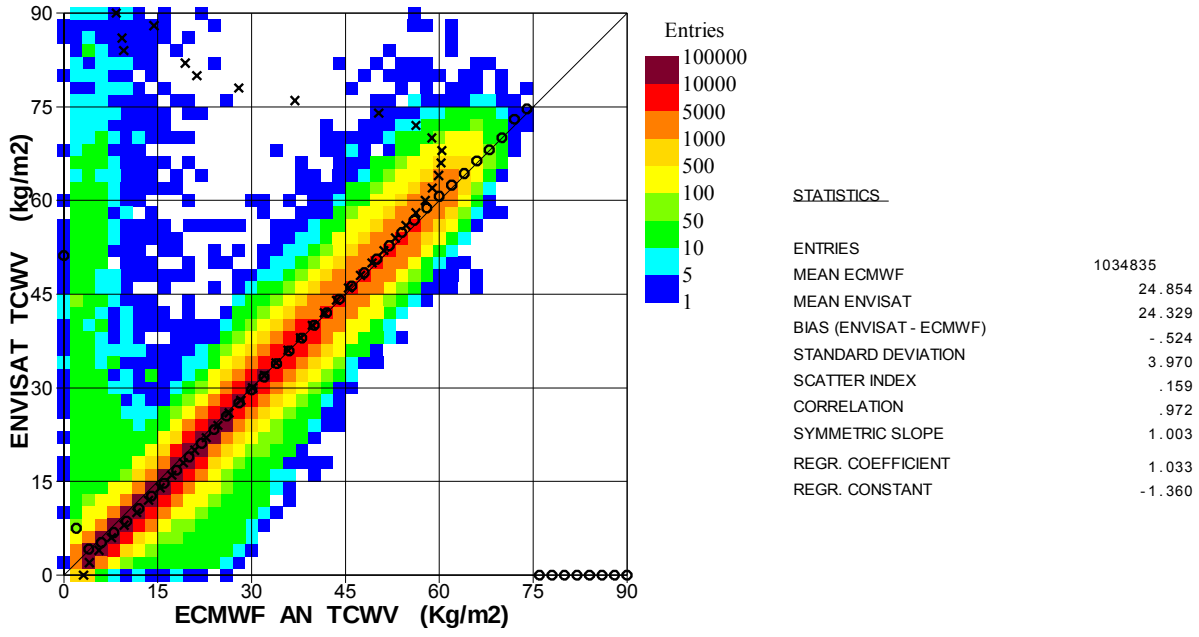

Fig. I.23. Global comparison between MWR and ECMWF model AN TCWV values during the period from 1 September 2004 to 31 August 2005.

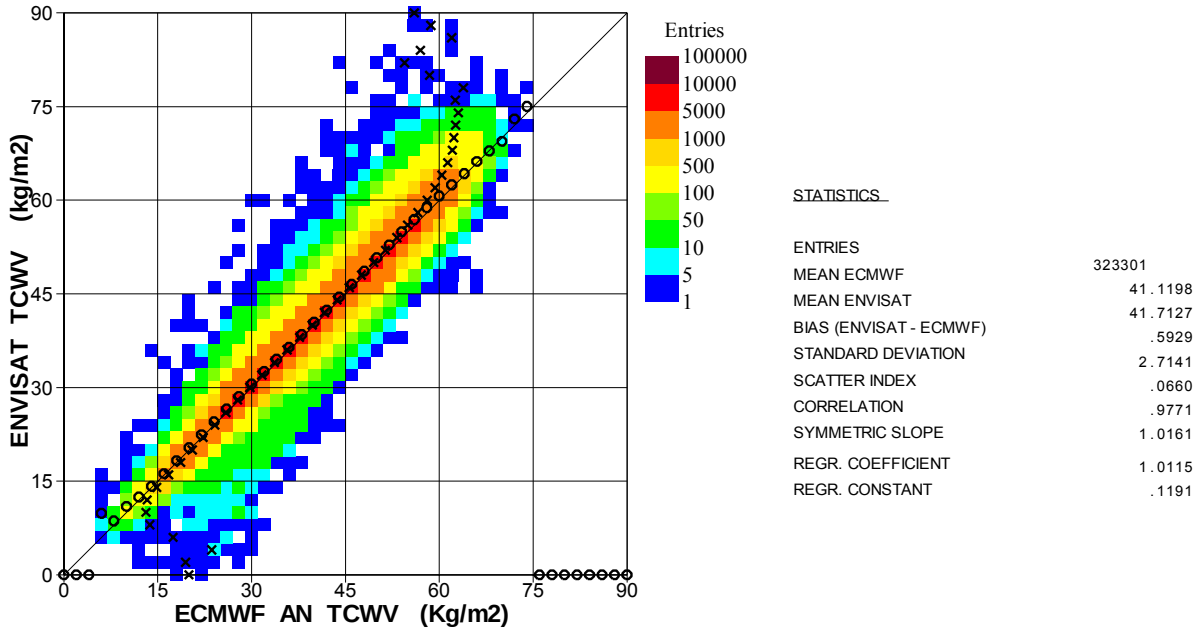

Fig. I.24. Tropical comparison between MWR and ECMWF model AN TCWV values during the period from 1 September 2004 to 31 August 2005.

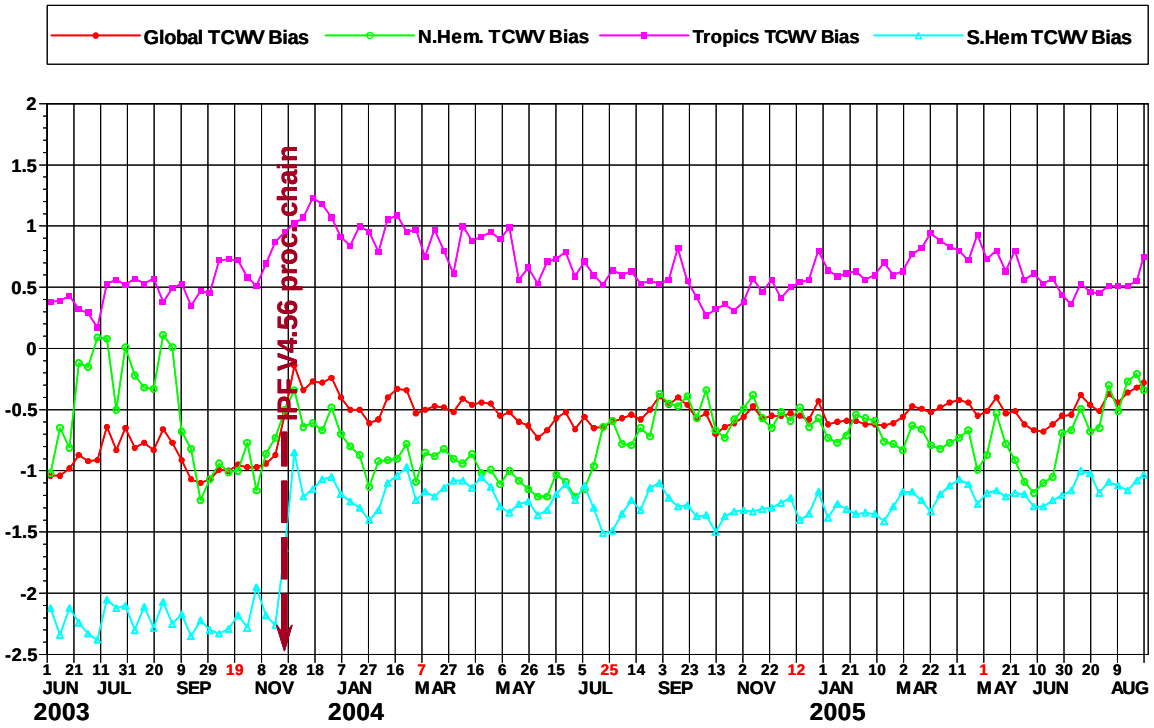

Fig. I.25. Time series of weekly TCWV bias (kg/m^2) between MWR and ECMWF model AN.

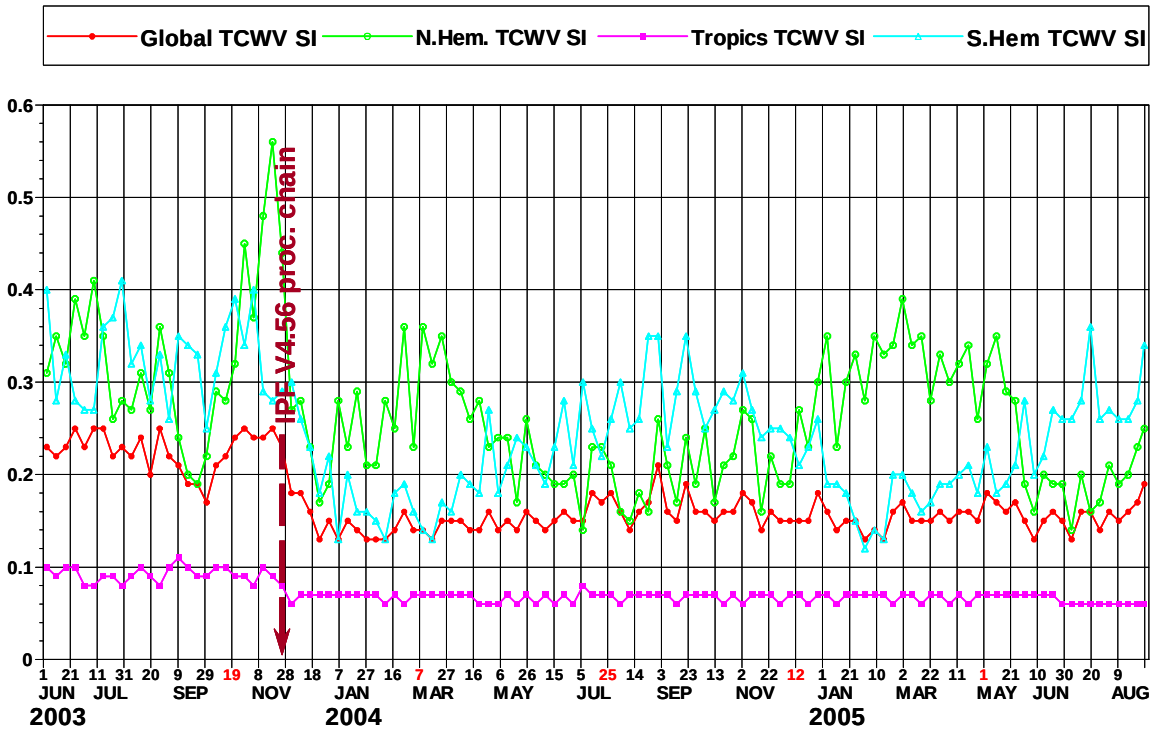

Fig. I.26. Time series of weekly TCWV SI between MWR and ECMWF model AN.

Collocated WTC pairs of MWR super-observation and the ECMWF model AN are plotted as density scatter plot in Fig. (I.27) for the whole globe and in Fig. (I.28) for the Tropics over a period of one year (from 1 September 2004 to 31 August 2005). Similar to the TCWV product, the major part of the MWR WTC observations agrees very well with the model counterpart. However, there are quite a number of outliers as well. The outliers are associated with model low values (less than ~10 cm). As for the TCWV, MWR reports extremely high WTC values. Similarly, those outliers, which can be attributed to ice contamination, do not exist in the Tropics (Fig. I.28). Stricter QC criteria, involving model sea ice information, were used in an attempt to eliminate those outliers and the scatter plot corresponding to Fig. (I.27) is shown in the Appendix as Fig. (A.3). It is clear that most of the outliers have disappeared. The hump appears in the TCWV plots (Figs. I.23 and I.24) does not exist for the WTC product.

The MWR WTC bias (MWR minus model) and SI for the whole globe, NH, Tropics and SH are listed in Table (I.4) for operational QC and in Table (A.2) for stricter QC. It is clear that MWR underestimates the WTC with respect to the model everywhere. One needs to recall that MWR overestimates the TCWV in the Tropics. The reason behind this conflict is not clear at the moment. The WTC bias varies between -11 and -14 mm irrespective of the mean value. Although slightly smaller, the WTC SI values are comparable with those of the TCWV.

The time series of weekly SI between MWR and ECMWF model WTC over more than two years is shown in Fig. (I.29). One can see that there is quite a good resemblance between this time series and the TCWV time series. Therefore, the same conclusions can be drawn for WTC regarding the impact of the IPF Version 4.56 instrument processing chain and the seasonal cycle.

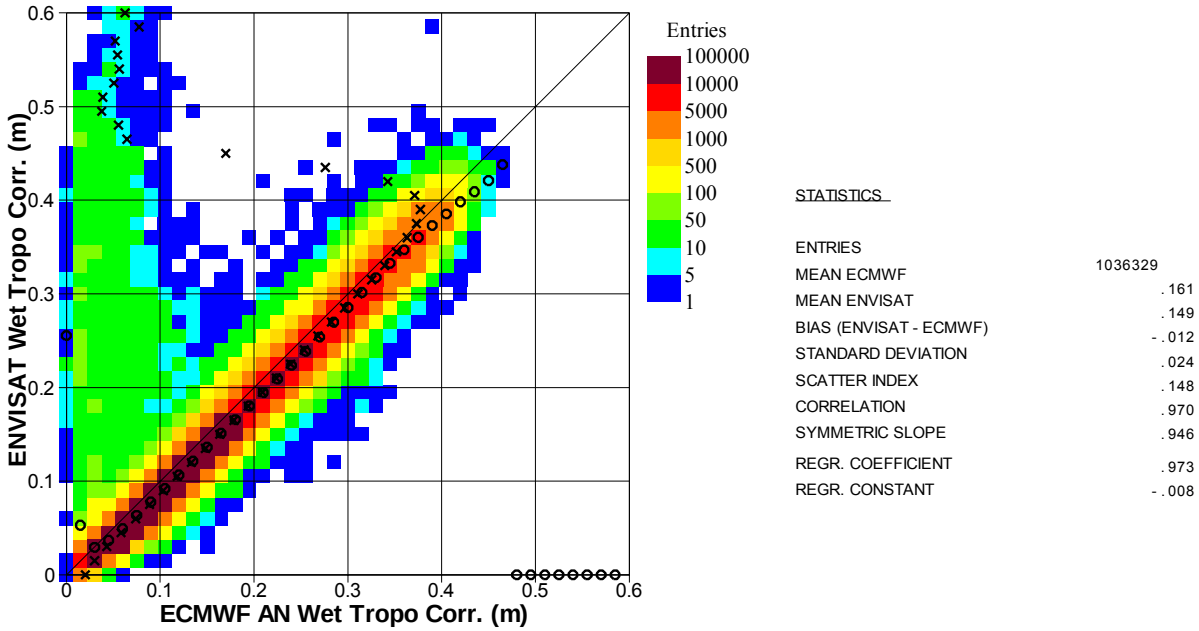

Fig. I.27. Global comparison between MWR and ECMWF model AN WTC values during the period from 1 September 2004 to 31 August 2005.

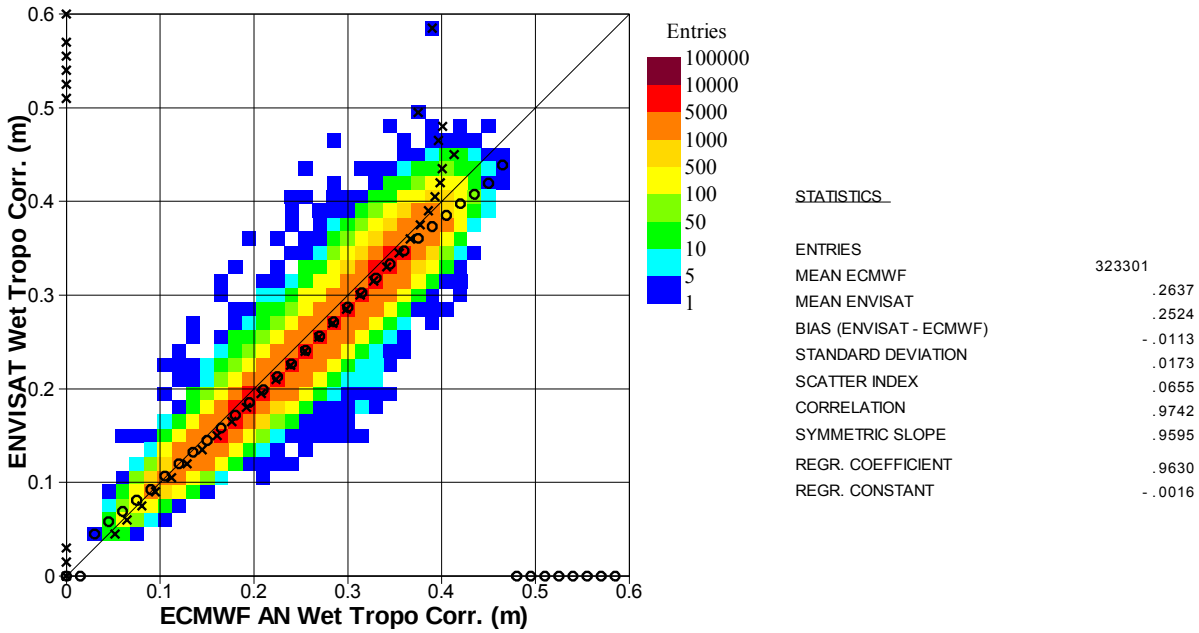

Fig. I.28. Tropical comparison between MWR and ECMWF model AN WTC values during the period from 1 September 2004 to 31 August 2005.

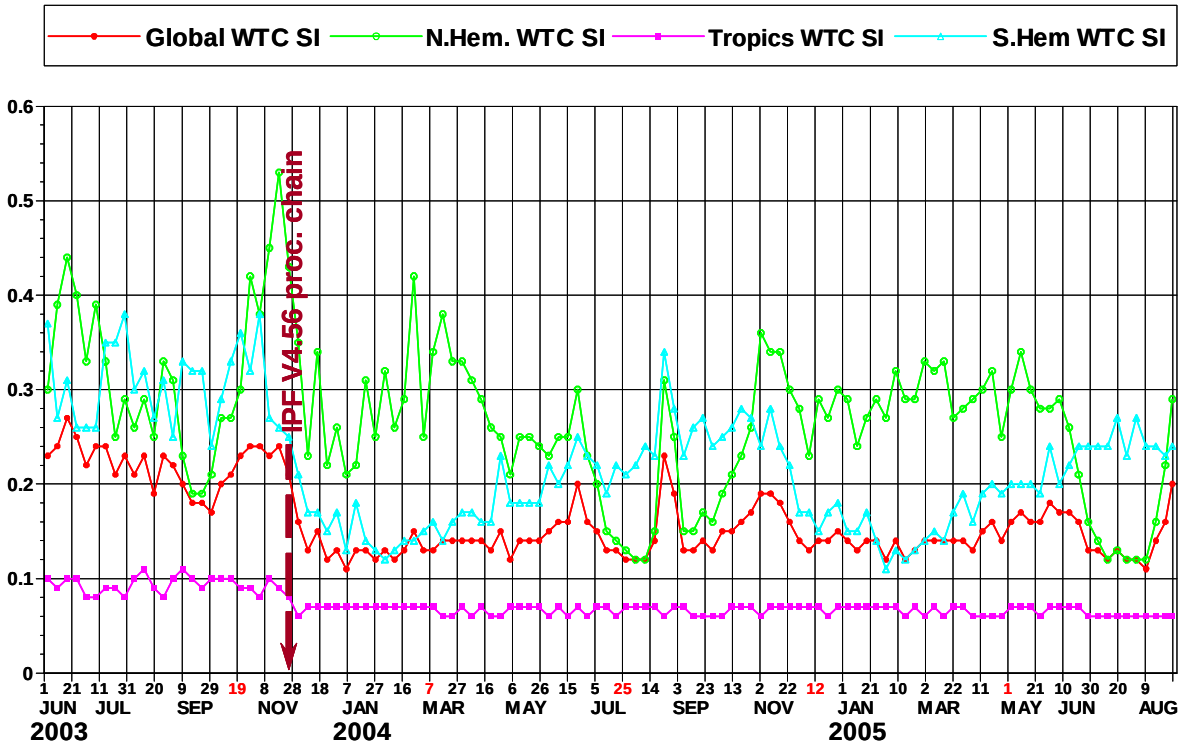

Fig. I.29. Time series of weekly WTC SI between MWR and ECMWF model AN.

I.7. Conclusions

Continuous monitoring and validation of the ENVISAT RA-2 wind and wave products together with the MWR water vapour products are carried out at ECMWF. Data from ECMWF atmospheric and wave models, from ERS-2 and from in-situ buoy and platform observations are used for this purpose.

The Ku-Band backscatter coefficient has a rather stable monthly mean value while S-Band had a jump of about 0.6 dB after the introduction of the IPF Version 4.56 processing chain on 26 November 2003. RA-2 wind speed data are in good agreement with the model and buoy data except for very low wind speeds (below ~4 m/s) and for high wind speeds (20 m/s and above). The wind speed algorithm needs some adjustments at those two regimes. This was done through the IPF Version 5.02 processing chain which has positive impact on the altimeter wind speed (at least the low wind speed problem).

Ku-Band SWH product is of high quality. The absolute error in Ku-Band SWH is about 6%. This is a low value compared to the other products used in the verification; namely: ERS-2 RA with an error of about 7% and the buoys with an error of about 8%. Compared to the wave buoys, Ku-Band SWH is higher by about 2.0% while ERS-2 RA is lower by 4.5%. There is a large correlation (about 77%) between RA-2 Ku-Band and ERS-2 RA wave height products. A possible reason for this correlation is that both instruments share the same measurement principle. Ku-Band SWH product is assimilated in the ECMWF wave model since 22 October 2003.

The quality of the S-Band wave height product is not as good as the Ku-Band. There are quite a number (less than 1.0%) of apparently erratic S-Band wave heights due to the RA-2 S-Band Anomaly. The bulk of the S-Band SWH data is in good agreement with the model analysis and the buoys. Compared to the Ku-Band

SWH, S-Band waves experienced several changes during the lifetime of the instrument. The ratio tends to have a seasonal cycle with a minimum in the NH summer.

The bias between the altimeter and the model follows a seasonal cycle for the surface wind speed, the Ku-Band SWH and the S-Band SWH. The wind speed and the Ku-Band SWH have similar seasonal cycles with peaks in October~February for the NH and in May~September for the SH. However, the S-Band SWH bias has an out of phase cycle.

The MWR products (TCWV and WTC) went through several phases of performance com-pared to the ECMWF model results. Since the introduction of the IPF V4.56 processing chain on 26 November 2003, MWR products compare well with the model except for a number of outliers at low model values. Most of the outliers can be attributed to ice and land contamination. Another group of outliers, with lower MWR values, appears in the TCWV comparison only. MWR products are slightly drier than the model except for the Tropical TCWV.

PART II

ADVANCED SYNTHETIC APERTURE RADAR (ASAR) WAVE MODE PRODUCTS

II.1. Introduction

ASAR consists of a coherent, active phased array SAR which is a distributed matrix of 320 transmitter/receiver elements operating at C-Band. The long axis of the SAR antenna is aligned in the direction of the satellite path (the azimuth direction). It images a strip of ground to the right side of the platform (range direction). The SAR produces two-dimensional representation of the scene reflectivity at high resolution. ASAR can operate in different modes with Wave Mode is the one of interest here. In the wave mode, ASAR senses the changes in the backscatter from the ocean surface due to the action of long ocean waves. As a result it produces small images (of ~ 5 km x 5km or larger) with 100 km spacing. This intermittent operation provides a low data rate so that the data can be stored on board the satellite and communicated whenever possible. The small images are then processed to produce the SAR cross-spectra (ASAR Wave Mode Level 1b, ASA_WVS_1P, product). Further processing produces the inverted ocean wave product (ASAR Wave Mode Level 2, ASA_WVW_2P, product). In fact this latter step can be done offline using several other inversion methods. One method, which is used at ECMWF for the verification of Level 1b product, is the MPIM scheme developed by Hasselmann et al. (1996). ASAR Wave Mode products represent a unique opportunity to provide ocean wave spectra with global coverage. However, there are several limitations. The most important is the inability of the instrument to resolve high frequency (short) ocean wave components. The shortest resolvable wavelength is called the azimuthal cut-off.

II.2. ASAR data processing

FD ASAR Wave Mode Level 1b (ASA_WVS_1P) and Level 2 (ASA_WVW_2P) products are validated. Level 1b product is the main product upon which basic quality control is done. Data processing is similar to the procedure used for ERS-2 SAR processing (see Abdalla and Hersbach, 2004). Here is a summary of this procedure:

The stream of ASAR product is split over 6-hour time windows centred at the main synoptic times to coincide with the model output times. The data contents of each time window is pre-processed to generate a list with output positions for the WAM model in order to produce a collocation file of wave spectra to be used for the SAR-inversion system. This includes basic pre-processing quality control checks to reject any spectrum with obvious anomalies and/or inconsistencies. The product parameters are checked and if any is found to be not logical, a quality control flag is set and the spectrum is rejected.

The nearest WAM wave spectra are extracted and used as the first guess (FG) to invert the ASAR product. The MPIM scheme (Hasselman et al., 1996) which is an iterative method based on the forward closed integral transformation, is used for the inversion. During and after the iterative inverting procedure further quality checks are done. The iterations stop when there is a convergence (within a given tolerance) or until the iteration procedure starts to be unstable. The value of the final cost function (the lower the cost function the better the inverted spectrum is) and the stability of the procedure are used to define the quality of the final inverted spectrum.

Any Level 2 product is accepted only if the corresponding Level 1b product passes the quality control. Further quality checks are performed over accepted Level 2 products to ensure their consistency. Each quality controlled product is then collocated with the closest wave model spectrum. It should be noted that most of the comparisons (scatter plots and time series derived from those plots) between Level 2 product and

the wave model are carried out within the spectral range resolvable by ASAR. Therefore, the part of the spectrum with wavelengths higher than the azimuthal cut-off length (as provided by the ASAR Level 2 product) is considered. This is different from the comparisons between ASAR Level 1b product and the wave model where the whole spectrum is considered. Therefore, one needs to be careful in drawing conclusions when intercomparing both products.

Validation of wave spectra with large number (100's) of degrees of freedom is not a straight-forward task. Therefore, the validation is usually done in terms of a limited number of integrated parameters. Significant wave height (SWH), mean wave period (MWP), wave spectral peakedness factor of Goda (WPF), wave directional spread (WDS) and mean wave direction (MWD) are among the most commonly used. These parameters can be defined as:

1. Significant wave height (SWH), H_s, is defined as:

   $$H_s = 4.0\sqrt{m_0}$$

   where m_0 is the "zeroth" moment of the wave spectrum. In general, the "n-th." moment of the spectrum, m_n, is defined as:

   $$m_n = \int \mathrm{d}\theta \int \mathrm{d}f \; f^n \, F(f,\theta)$$

   with F is the wave spectrum in frequency, f, - direction, θ, space. The first integration is done over all directions while the second is usually carried out from frequency 0 to ∞. However, for the verification of Level 2 product, the frequency integration is limited up to the frequency corresponding to the azimuthal cut-off wavelength.

2. The mean wave period (MWP) based on the "-1 th." moment (m_{-1}), T_{-1}, is defined as:

   $$T_{-1} = m_{-1} / m_0$$

   where m_0 and m_{-1} are the "zeroth" and the "-1 th" moments, respectively, of the wave spectrum with the "n-th." Moment, in general, is defined above.

3. The wave directional spread (MDS), σ, is defined as:

   $$\sigma = \sqrt{2[1 - r_1(f)]}$$
   $$r_1 = m_0^{-1} \int \mathrm{d}f \int \mathrm{d}\theta \, F(f,\theta) \cos[\theta - \varphi(f)]$$
   $$\varphi(f) = \mathrm{atan}\left\{ \left[\int \mathrm{d}\theta \, F(f,\theta) \sin(\theta) \right] \Big/ \left[\int \mathrm{d}\theta \, F(f,\theta) \cos(\theta) \right] \right\}$$

4. The mean wave propagation direction (MWD), φ, is defined as:

   $$\varphi = \mathrm{atan}\left\{ \left[\int \mathrm{d}f \int \mathrm{d}\theta \, F(f,\theta) \sin(\theta) \right] \Big/ \left[\int \mathrm{d}f \int \mathrm{d}\theta \, F(f,\theta) \cos(\theta) \right] \right\}$$

5. The wave spectral peakedness factor of Goda, (WPF), Qp, is defined as:

$$Q_p = 2\, m_0^{-2} \int \mathrm{d}\theta \int \mathrm{d}f\; f\, F^2(f,\theta)$$

Voorrips et al. (2001) suggested the use of the narrowband equivalent wave height, $H_{T1,T2}$, between wave periods T_1 and T_2 defined as:

Typically, the wave period interval [T_1, T_2] is selected as 2 seconds (2-s wave-period interval equivalent wave height). This enables a more detailed validation in terms of a rather limited number of parameters.

II.3. ASAR level 1B product

SWH is the most commonly used parameter for typical validation of ocean wave products. Fig. (II.1) shows a density scatter plot for globally collocated SWH pairs of inverted ASAR Wave Mode Level 1B and the analysis WAM wave model for the period from 11 April to 31 August 2005. There was a significant wave model change in early April 2005 affecting the details of the wave model spectra. This model change involves a new definition of the WAM dissipation source term. The choice of the period was done in order to eliminate the possible impact of using different model characteristics and to make use of the best possible model results. As can be seen in Fig. (II.1), the agreement between the ASAR and the model is quite good with ASAR slightly underestimating the wave heights. Table (II.1) lists the SWH bias (ASAR minus model) and SI for the whole globe, the NH, the Tropics and the SH. In general, the underestimation of ASAR for the SWH varies between 3 cm (in the Tropics) to 12 cm (in the SH) while the scatter index varies between 11% (in the Tropics) and 13.5% (in the SH).

The time series of bias between inverted ASAR Level 1b and WAM model SWH is shown in Fig. (II.2) while the scatter index time series is shown in Fig. (II.3). The reduction in SWH bias (especially in the SH) in early April 2005 can not be missed. However, this was associated with a slight increase in SI. Indeed, one of the expected side effects of the new model change is an increase of SWH variability that may be translated in slightly higher mismatch with the SWH observations. Another clear change in behaviour is the apparent convergence of the SI plots for the various regions since early May 2004. This coincides with the implementation of the PF-ASAR Version 3.07 on 4 May 2004. This version of PF-ASAR resolves a problem with the code that applies the elevation antenna pattern correction. Although this correction appears to increase the scatter index of various parameters (SWH in Fig. II.3, MWP in Fig. II.7, WPF in Fig. II.10 and WDS in Fig. II.13), it has a positive impact. The inversion process started to produce higher quality inverted spectra after the change as can be seen in the plot in Fig. (II.4). It is quite clear that the amount of excellent quality inversion (with cost < 0.1) started to dominate the inversion output. The SAR inversion method used at ECMWF (the MPIM scheme) returns a spectrum contaminated with the first-guess WAM spectrum if it is not able to proceed with the inversion (reached unstable iterations). As Fig. (II.4) shows, there used to be a great portion of unstable iterations forcing the comparison to be of model spectrum against itself (or a spectrum very close to the model) for those unstable iterations.

	Inverted Level 1b (whole spectral range)			Level 2 (wavelengths ≤ azimuthal cut-off)		
	ASAR mean (m)	Bias (m)	SI (%)	ASAR mean (m)	Bias (m)	SI (%)
Global	2.55	−0.08	13.5	0.60	−0.03	45.0
NH	1.83	−0.03	12.1	0.53	+0.09	64.8
Tropics	1.87	−0.12	11.1	0.59	−0.00	47.3
SH	3.49	−0.06	13.4	0.66	−0.11	34.3

Table II.1: Comparison of ASAR Wave Mode with WAM Wave Model SWH (11 April 2005 - 31 August 2005)

Fig. (II.5) shows a density scatter plot for globally collocated mean wave period (MWP) pairs of inverted ASAR Wave Mode Level 1B and the analysis WAM wave model for the period from 11 April to 31 August 2005. The agreement between the inverted ASAR and the model MWP is very good with virtually no bias and very small scatter index. Table (II.2) lists the MWP bias (inverted ASAR minus model) and SI for the whole globe, the NH, the Tropics and the SH. In general, the bias is less than about 0.1 s and the SI is about 6% everywhere.

The time series of bias between inverted ASAR Level 1b and WAM model MWP is shown in Fig. (II.6) while the scatter index time series is shown in Fig. (II.7). The impact of the PF-ASAR version 3.07 (4 May 2004) and the model change with new dissipation term (5 April 2005) can not be missed especially in the bias time series. The PF-ASAR version 3.07 increased the SI similar to the SWH case. One must recall from the discussion above that this is not a real increase of mismatch between ASAR and the model. On the other hand, the model change has a positive impact on both the bias and the SI. The motivation behind the new change in the wave model was the need to improve the model wave periods under mild storm conditions in the presence of swell. Figs. (II.6) and (II.7) prove that this new dissipation term is indeed doing a proper job.

	Inverted Level 1b (whole spectral range)			Level 2 (wavelengths ≤ azimuthal cut-off)		
	ASAR mean (s)	Bias (s)	SI (%)	ASAR mean (s)	Bias (s)	SI (%)
Global	9.12	+0.03	6.3	15.27	+0.46	6.3
NH	8.05	+0.08	6.2	14.59	+0.87	8.5
Tropics	8.50	−0.10	6.2	14.95	+0.59	7.5
SH	10.2	+0.11	6.2	15.89	+0.13	2.8

Table II.2: Comparison of ASAR Wave Mode with WAM Wave Model MWP (11 April 2005 - 31 August 2005)

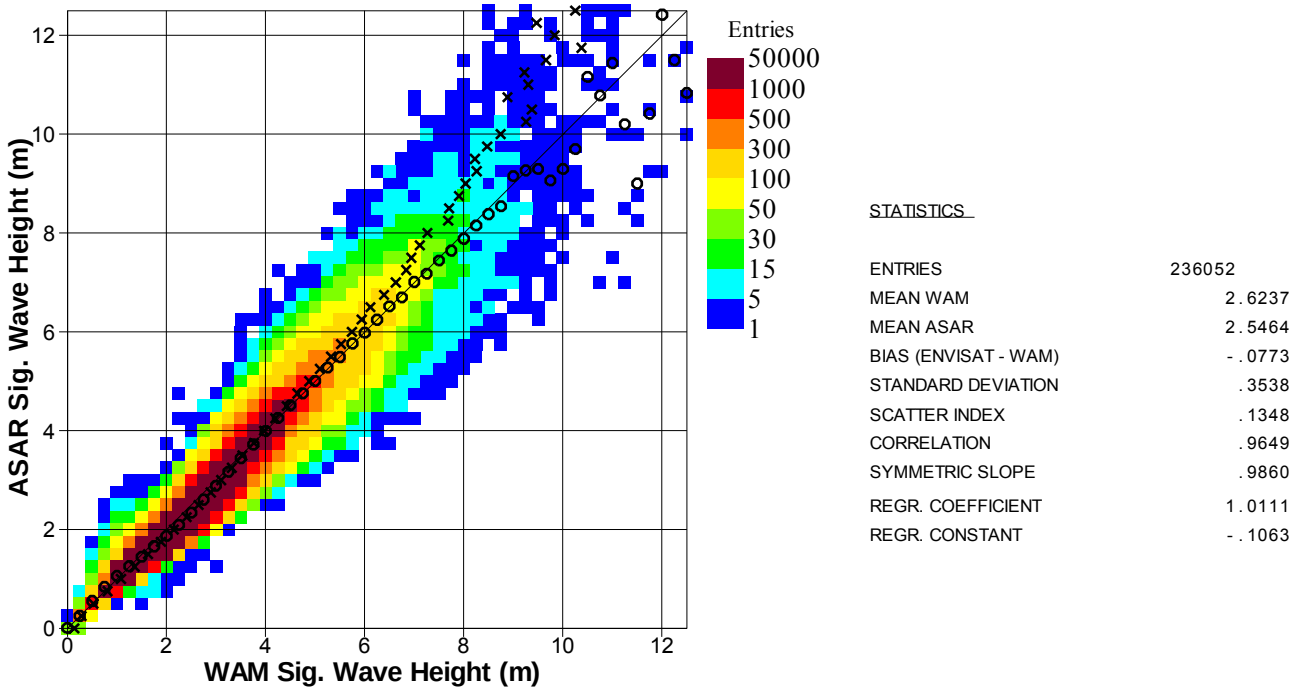

Fig. II.1. Global comparison between inverted ASAR level 1b and ECMWF model SWH during the period from 11 April to 31 August 2005.

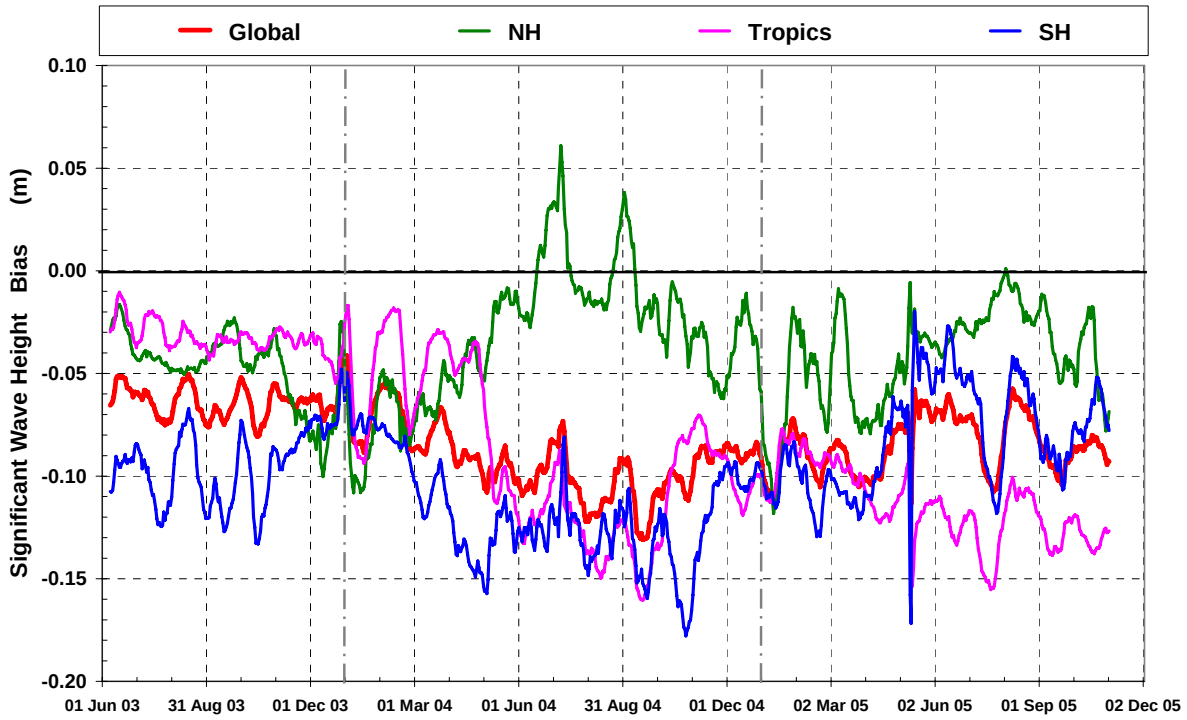

Fig. II.2. Time series of SWH bias between ASAR Level 1b inverted product and WAM.

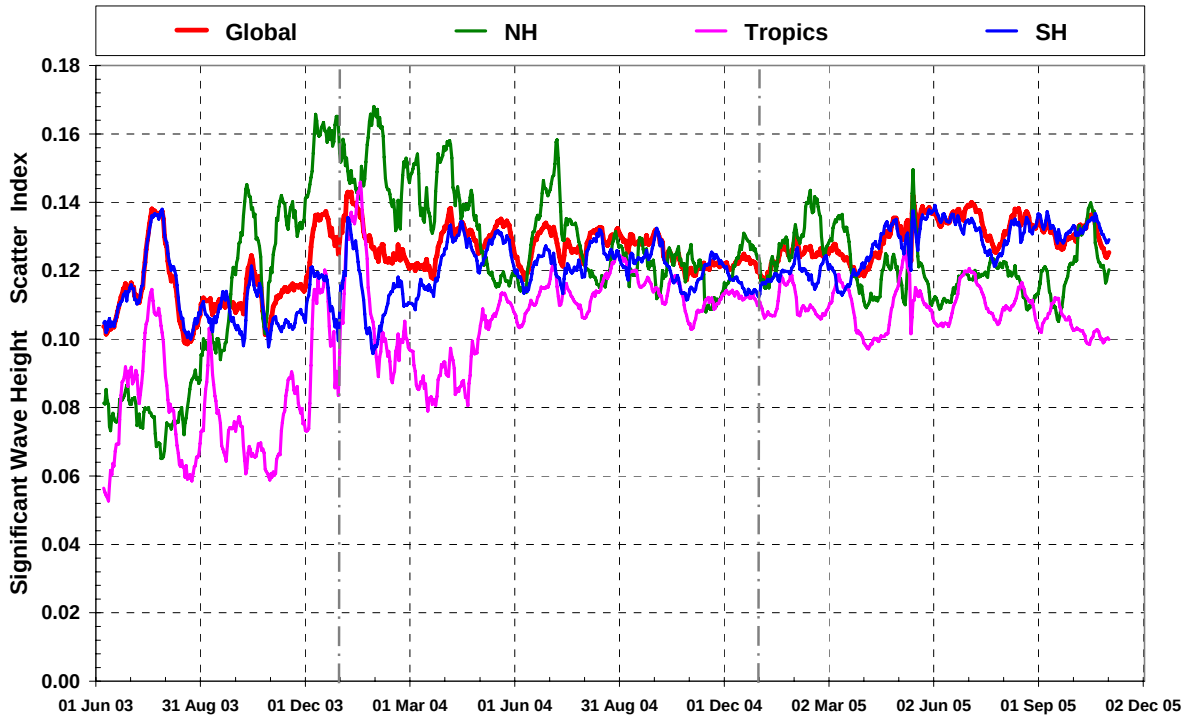

Fig. II.3. Time series of SWH SI between ASAR Level 1b inverted product and WAM.

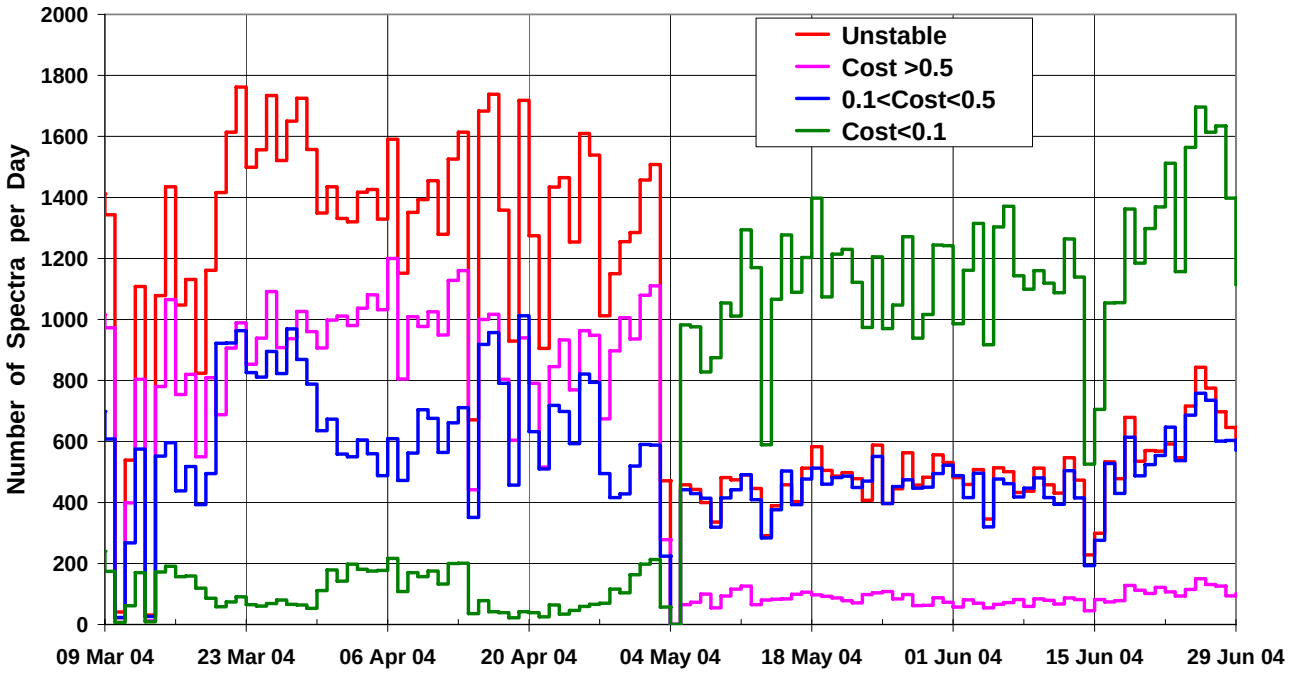

Fig. II.4. Time series of the daily results of the inversion of ASAR Level 1b.

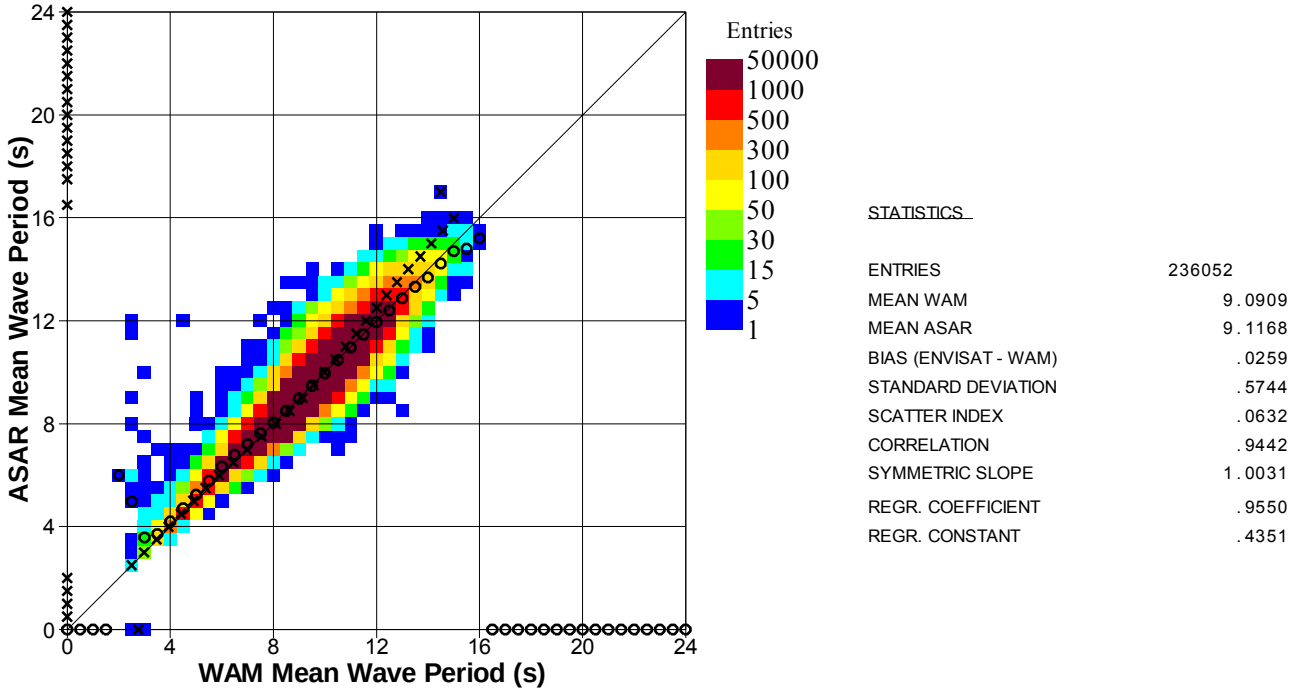

Fig. II.5. Global comparison between inverted ASAR level 1b and ECMWF model MWP during the period from 11 April to 31 August 2005.

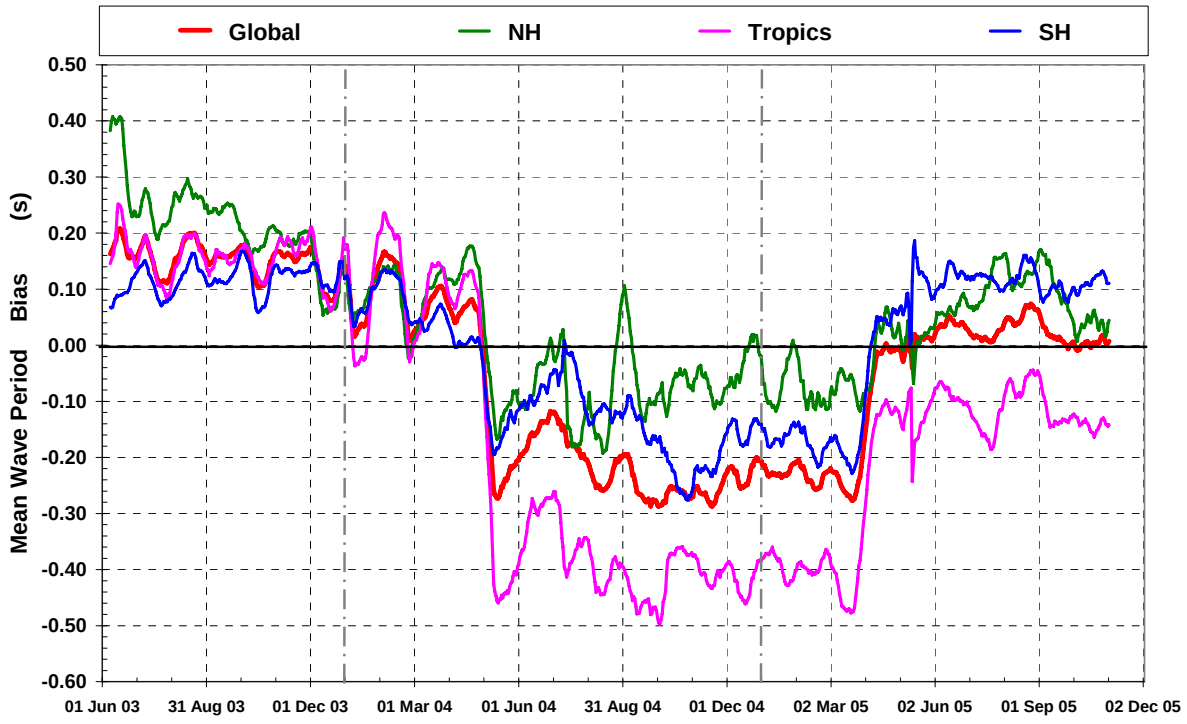

Fig. II.6. Time series of MWP bias between ASAR Level 1b inverted product and WAM.

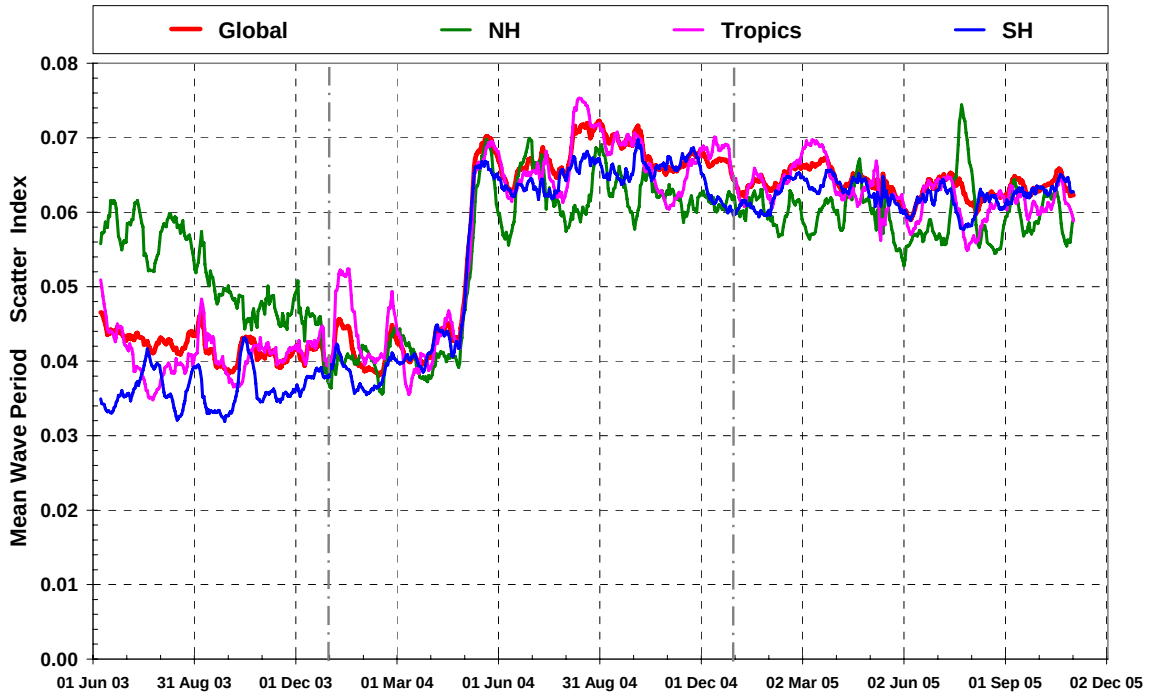

Fig. II.7. Time series of MWP SI between ASAR Level 1b inverted product and WAM.

Globally collocated wave spectral peakedness factor (WPF) pairs of inverted ASAR Wave Mode Level 1B and the analysis WAM wave model for the period from 11 April to 31 August 2005 are plotted as a density scatter plot in Fig. (II.8). There is a good agreement for most of the data, which have WPF values less than ~1.5. However, for larger peakedness factor values the agreement does not hold anymore with a clear split to form two families. The scatter index is rather high (~50%) while the correlation is rather low (~0.49). Table (II.3) lists the WPF bias (inverted ASAR minus model) and SI for the whole globe, the NH, the Tropics and the SH. In general, the bias is less than about 10% of the mean while the SI is about 43% in the Tropics and above 50% in the extra-tropics.

The time series of bias between inverted ASAR Level 1b and WAM model WPF is shown in Fig. (II.9) while the scatter index time series is shown in Fig. (II.10). The impact of the PF-ASAR version 3.07 (4 May 2004) and the model change with new dissipation term (5 April 2005) can be clearly seen especially in the SI time series for the former and the bias time series for the latter. The PF-ASAR Version 3.07 increased the SI similar to the SWH and the MWP cases. One must recall from the discussion above that this is not a real increase of the mismatch between ASAR and the model. On the other hand, the model change has a positive impact on the bias and a negative impact on the SI in the extra-tropics. This latter impact is due to the sensitivity of the new model. The peakedness parameter depends on the square of the spectrum and, therefore, amplifying this model sensitivity.

Similarly, the globally collocated wave directional spread (WDS) pairs of inverted ASAR Wave Model Level 1B and the analysis WAM wave model for the period from 11 April to 31 Au-gust 2005 are plotted as a density scatter plot in Fig. (II.11). The agreement is quite good. There is virtually no bias (bias less than ~1% of the mean) and quite small scatter index value (~9%). Table (II.4) lists the WDS bias (inverted ASAR minus model) and SI for the whole globe, the NH, the Tropics and the SH. In general, the bias is less than 1% of the mean while the SI varies between 7.6% (in the Tropics) and 10.5% in the SH.

	Inverted Level 1b (whole spectral range)			Level 2 (wavelengths ≤ azimuthal cut-off)		
	ASAR mean	Bias	SI (%)	ASAR mean	Bias	SI (%)
Global	1.054	+0.045	50.3	1.936	+0.921	152.3
NH	0.961	+0.089	51.6	2.285	+1.412	218.8
Tropics	0.893	−0.070	43.0	1.942	+0.967	185.7
SH	1.240	+0.122	52.3	1.755	+0.634	78.4

Table II.3: Comparison of ASAR Wave Mode with WAM Wave Model WPF (11 April - 31 August 2005)

	Inverted Level 1b (whole spectral range)			Level 2 (wavelengths ≤ azimuthal cut-off)		
	ASAR mean	Bias	SI (%)	ASAR mean	Bias	SI (%)
Global	0.910	−0.003	8.9	0.633	−0.277	32.6
NH	1.050	−0.009	8.1	0.662	−0.397	30.8
Tropics	0.919	+0.005	7.6	0.667	−0.242	32.2
SH	0.832	−0.006	10.5	0.590	−0.247	32.1

Table II.4: Comparison of ASAR Wave Mode with WAM Wave Model WDS (11 April - 31 August 2005)

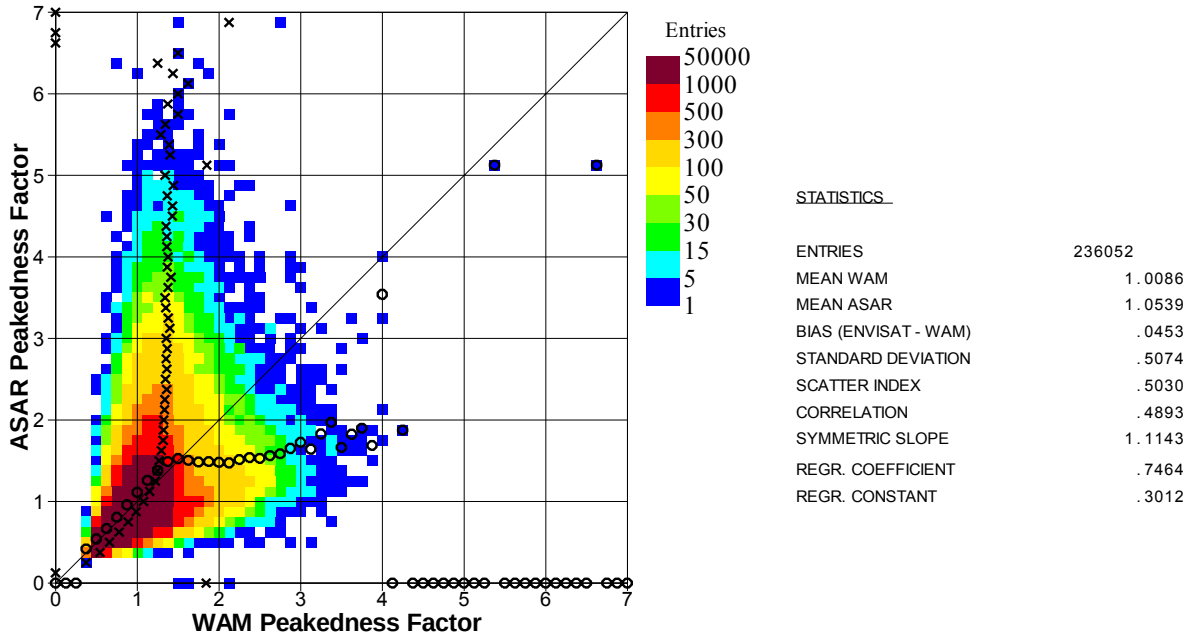

Fig. II.8. Global comparison between inverted ASAR level 1b and ECMWF model WPF during the period from 11 April to 31 August 2005.

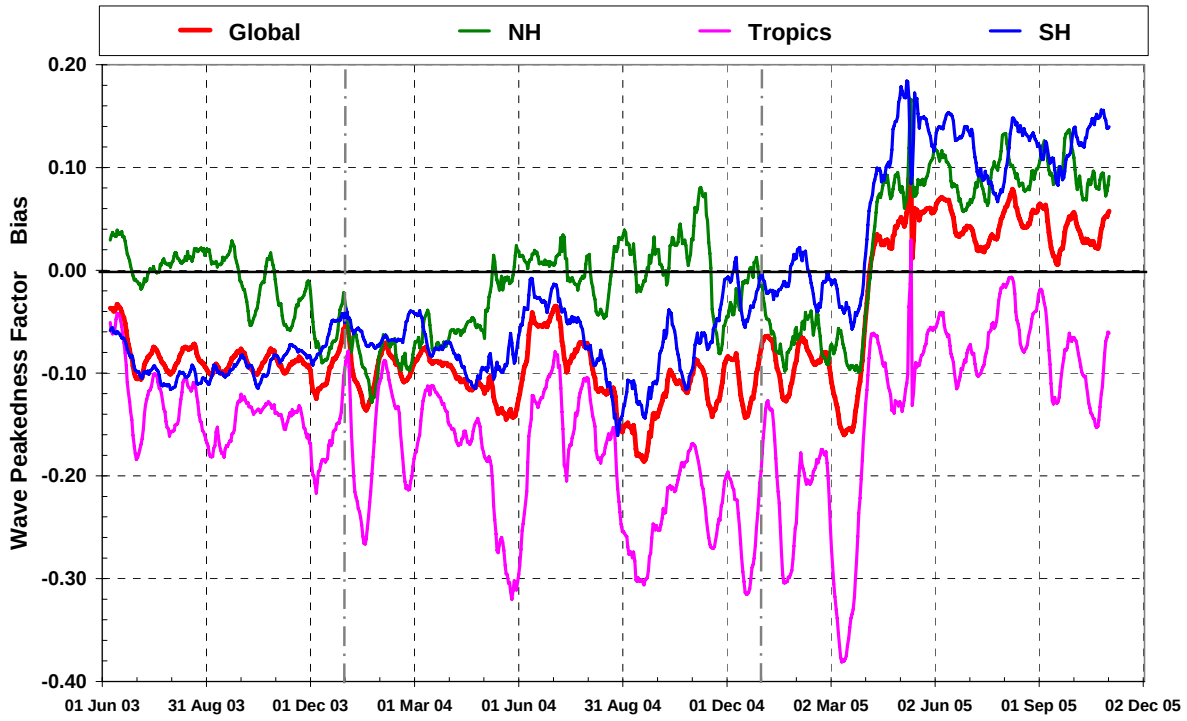

Fig. II.9. Time series of WPF bias between ASAR Level 1b inverted product and WAM.

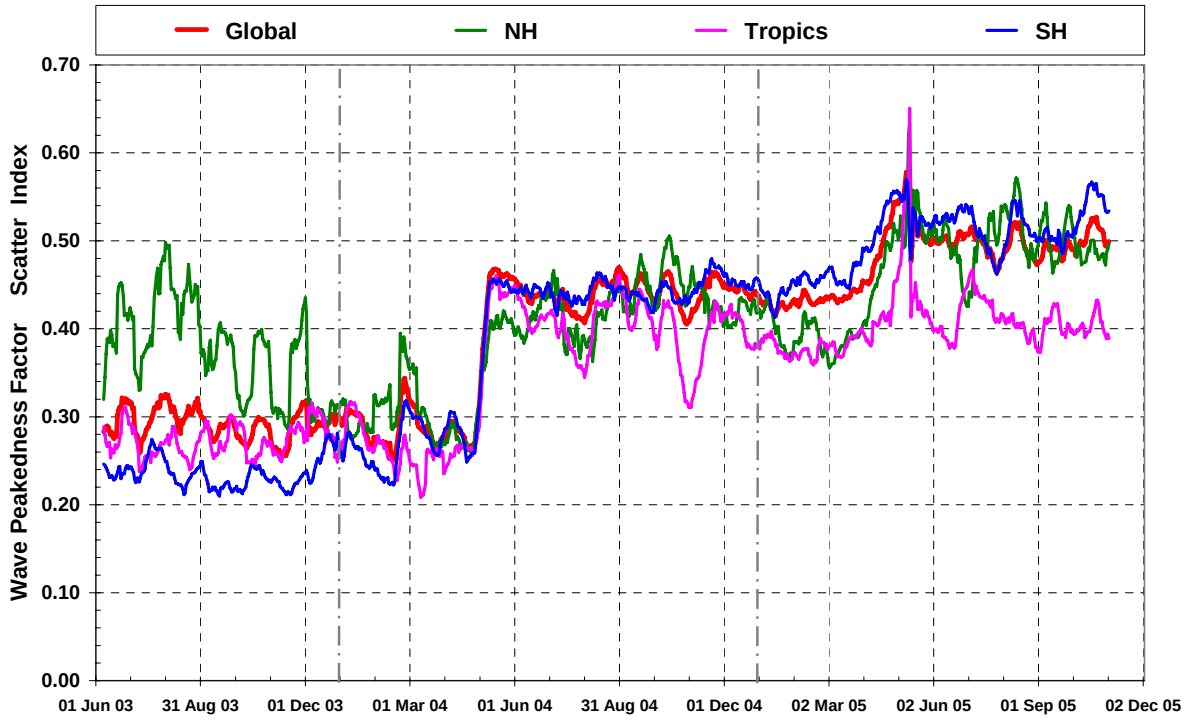

Fig. II.10. Time series of WPF SI between ASAR Level 1b inverted product and WAM.

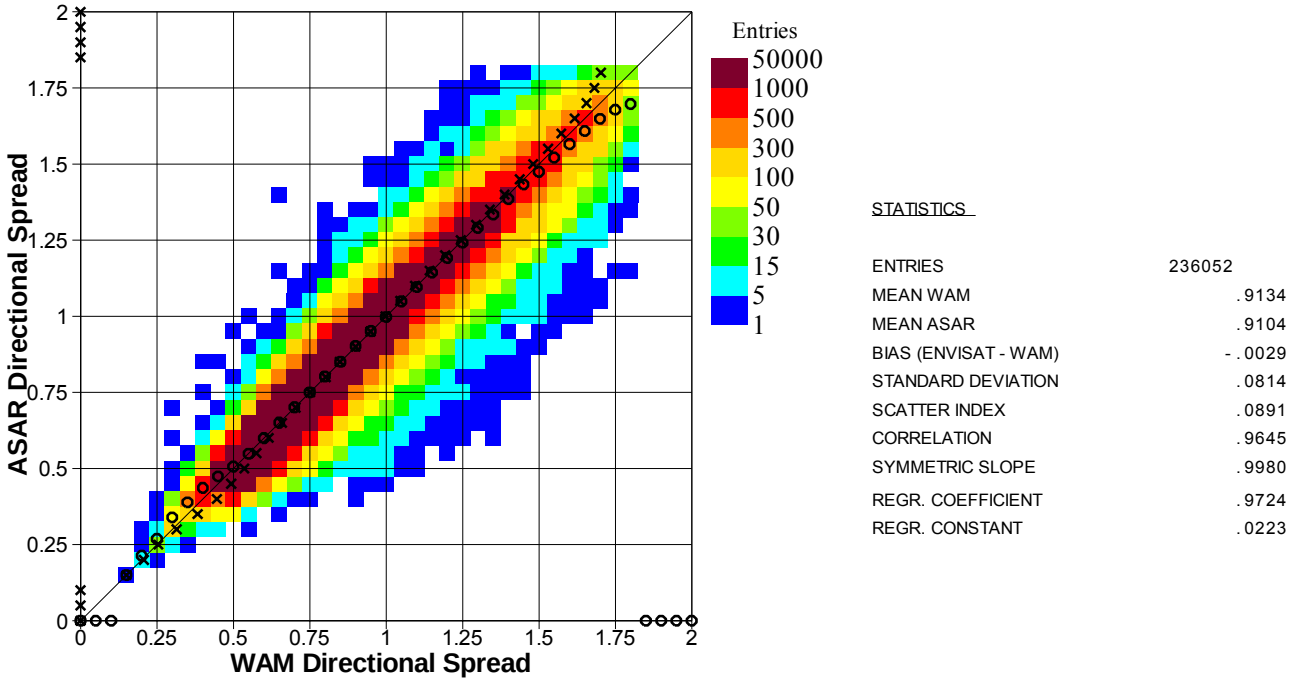

Fig. II.11. Global comparison between inverted ASAR level 1b and ECMWF model WDS during the period from 11 April to 31 August 2005.

The time series of bias between inverted ASAR Level 1b and WAM model WDS is shown in Fig. (II.12) while the scatter index time series is shown in Fig. (II.13). The impact of the PF-ASAR version 3.07 (4 May 2004) can be clearly seen in both figures while the model change with new dissipation term (5 April 2005) can be clearly seen in the bias time series. The PF-ASAR version 3.07 increased the SI similar to the other parameters. One must recall from the discussion above that this is not a real increase of the mismatch between ASAR and the model. On the other hand, the model change has clear positive impact on both the bias and the SI.

Rather detailed comparisons at various spectral wave components in terms of the "2-s wave-period interval equivalent wave heights" ($H_{T1,T2}$), are displayed in Figs. (II.14), (II.15), (II.16) and (II.17) for the whole globe, the NH; the Tropics and the SH, respectively, during the period from 11 April to 31 August 2005. The bias, the standard deviation of difference, the scatter index and the correlation coefficient between the inverted ASAR Wave Mode Level 1b product and the wave model $H_{T1,T2}$ are plotted as functions of wave period. For low wave periods, the agreement is rather high as the ASAR is not able to image those wave components and therefore, they are to a large extent determined by the wave model. The comparisons indicate good overall agreement.

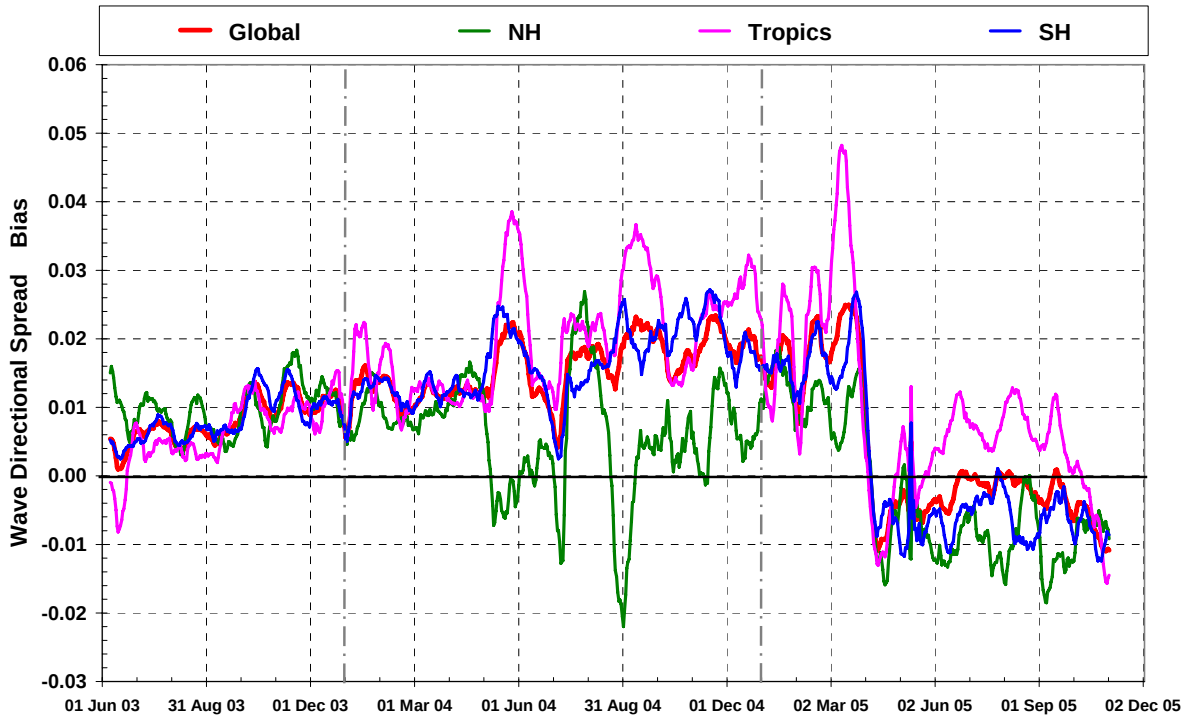

Fig. II.12. Time series of WDS bias between ASAR Level 1b inverted product and WAM.

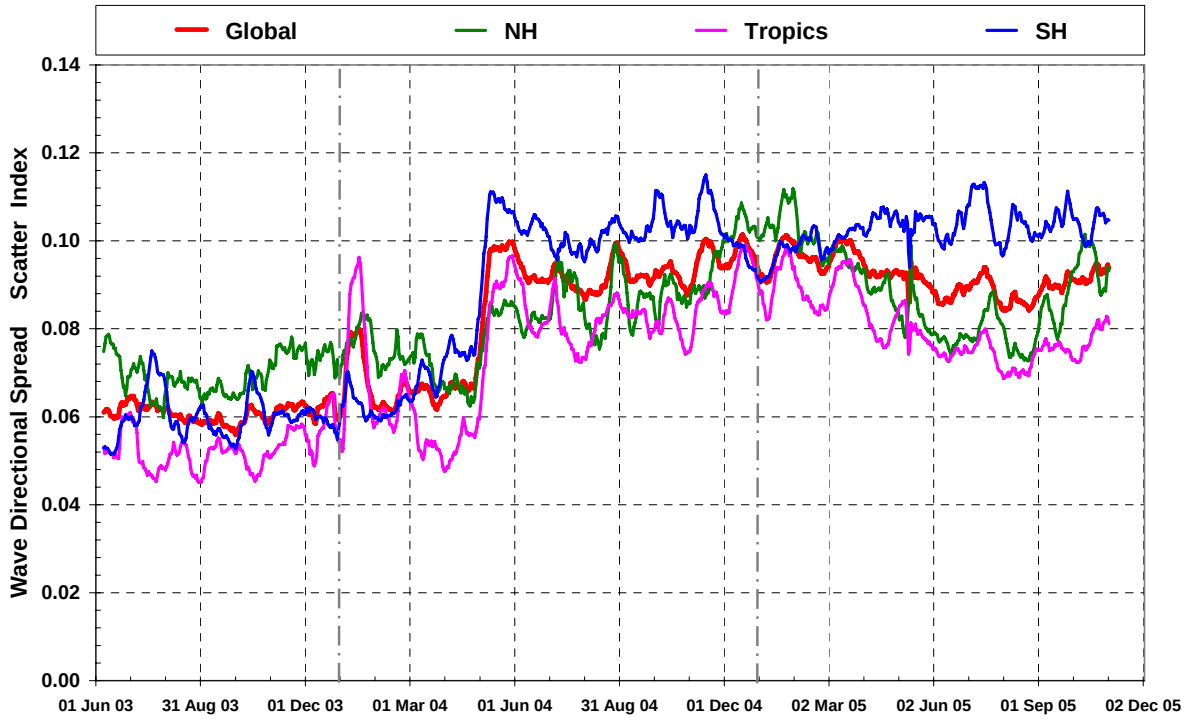

Fig. II.13. Time series of WDS SI between ASAR Level 1b inverted product and WAM.

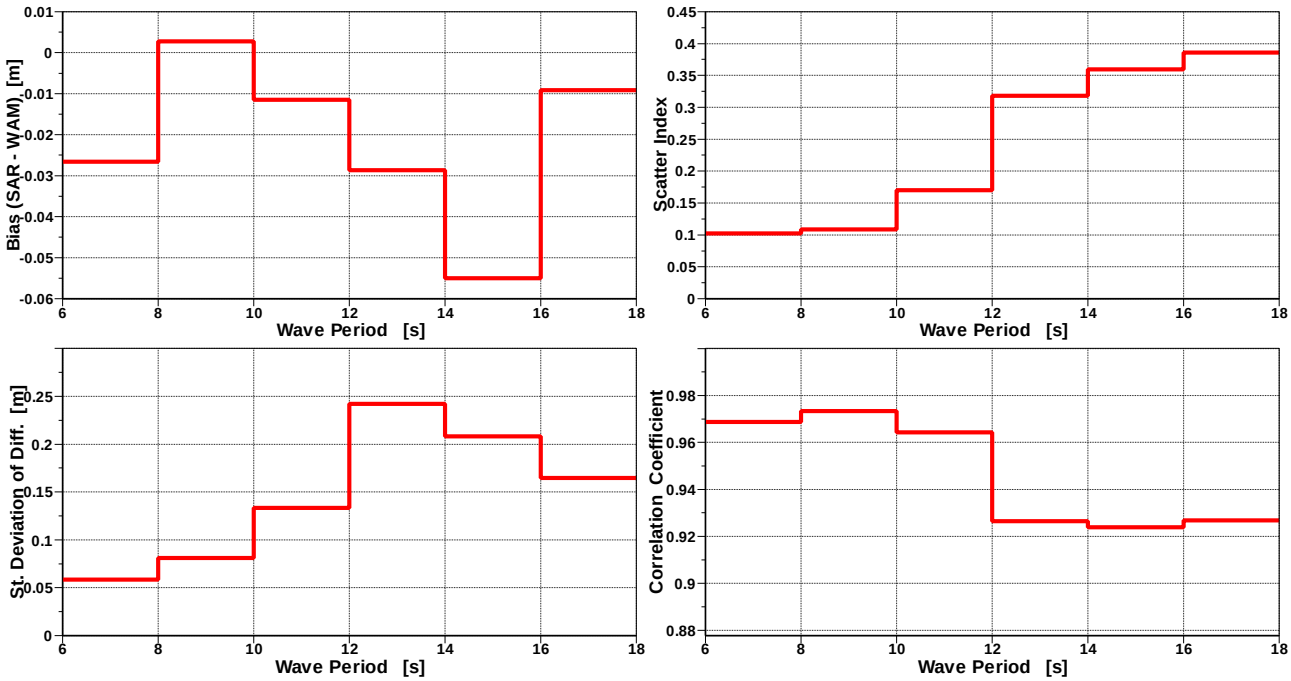

Fig. II.14. Comparison between inverted ASAR level 1b and WAM "2-s wave-period interval equivalent wave heights" for 11 April to 31 August 2005 (Global).

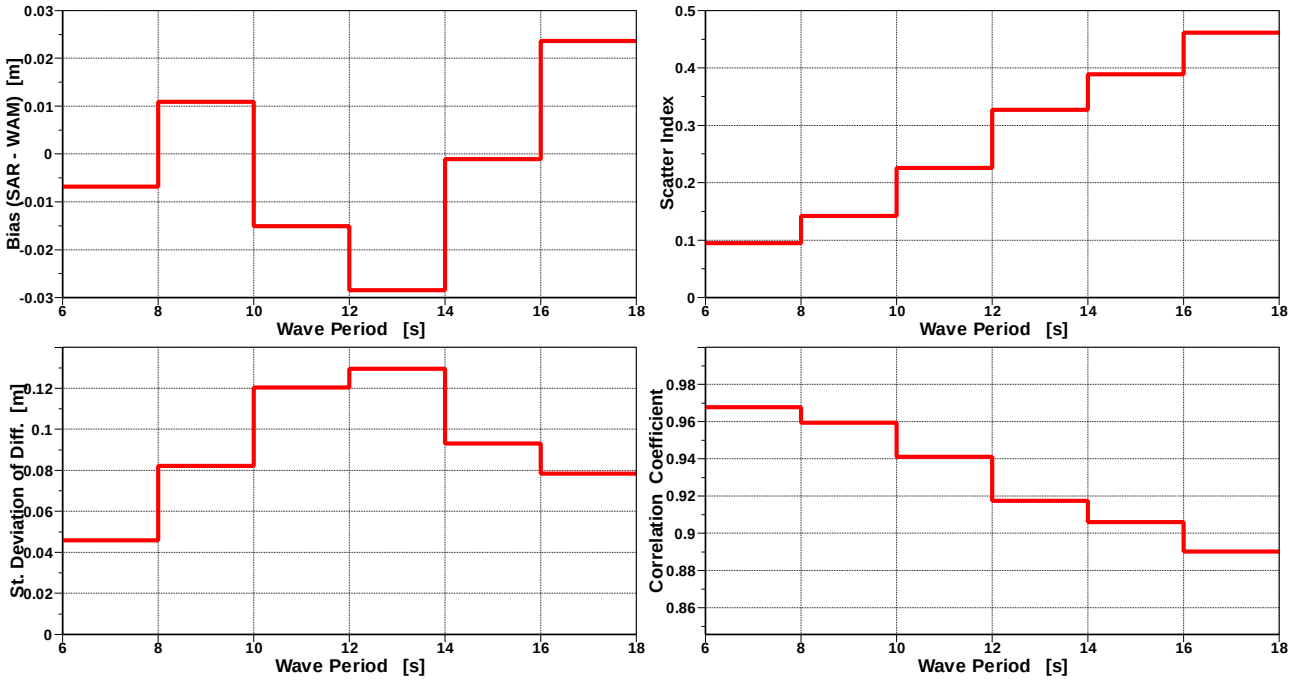

Fig. II.15. Comparison between inverted ASAR level 1b and WAM "2-s wave-period interval equivalent wave heights" for 11 April to 31 August 2005 (NH).

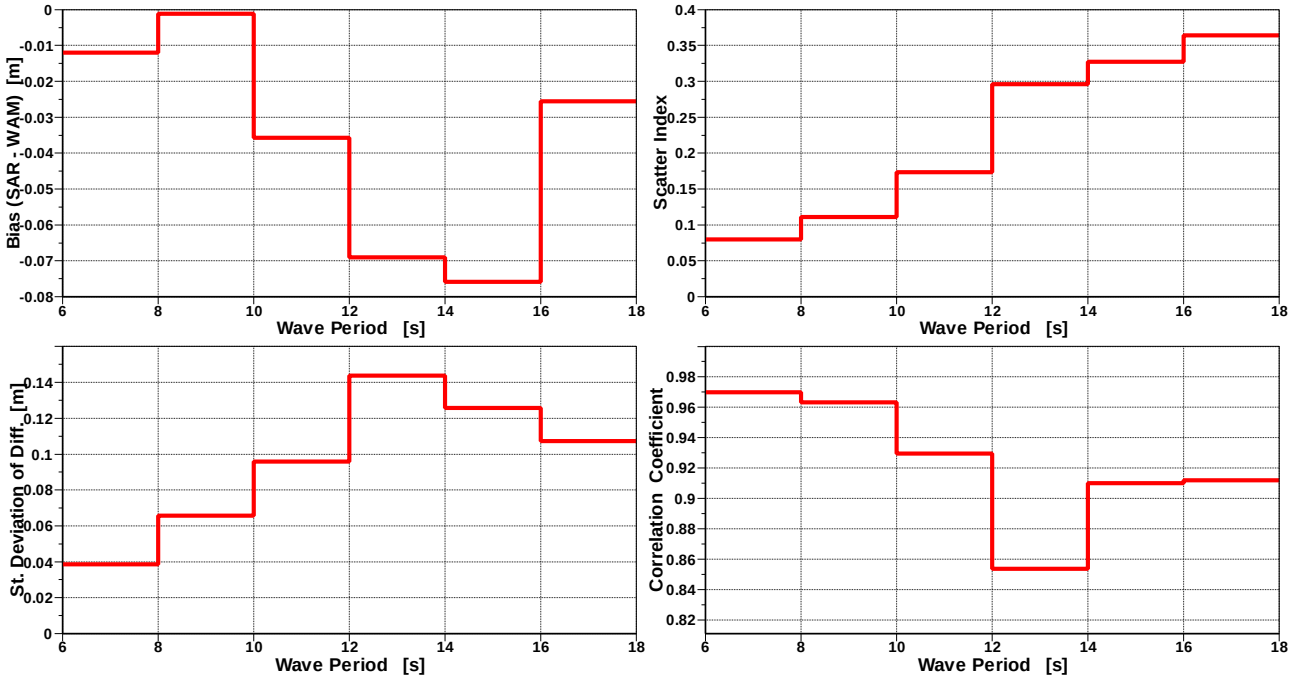

Fig. II.16. Comparison between inverted ASAR level 1b and WAM "2-s wave-period interval equivalent wave heights" for 11 April to 31 August 2005 (Tropics).

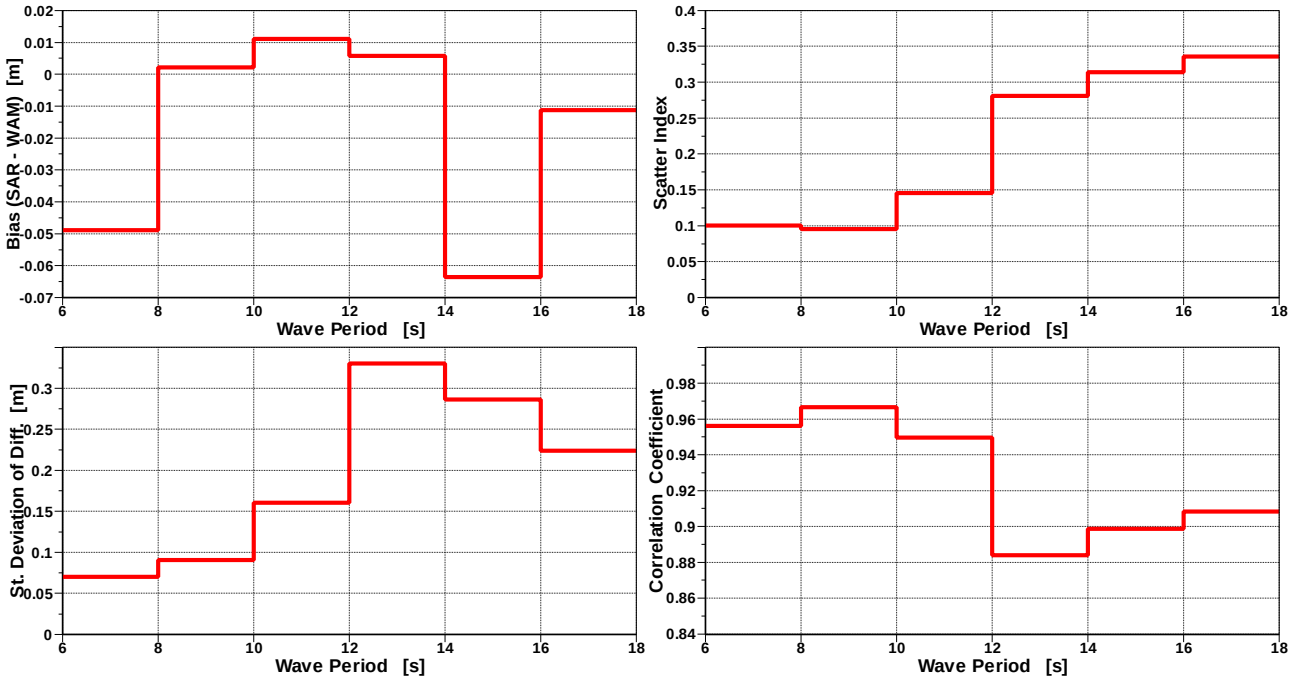

Fig. II.17. Comparison between inverted ASAR level 1b and WAM "2-s wave-period interval equivalent wave heights" for 11 April to 31 August 2005 (SH).

II.4. ASAR level 2 product

It is stressed that the integrated parameters used here for the various comparisons are computed for the part of the spectrum which is resolvable by the ASAR instrument. This means that wave components with wavelengths longer than the azimuthal cut-off wavelength reported in the ASAR Wave Mode Level 2 (ASA_WVW_2P) product are used. The term swell is used for those parameters to reflect this fact (although strictly speaking is not correct).

Fig. (II.18) shows a density scatter plot for globally collocated swell SWH pairs of ASAR Wave Mode Level 2 and the analysis WAM wave model for the period from 11 April to 31 August 2005. The agreement between the ASAR and the model is quite good for the bulk of the data. However, there are quite a number of outliers. The outliers are generally with higher ASAR values in the NH and the Tropics and with lower ASAR values in the SH (not shown). The swell SWH bias (ASAR minus model) and SI for the whole globe, the NH, the Tropics and the SH are listed in Table (II.1). The time series of bias between ASAR Level 2 and WAM model swell SWH is shown in Fig. (II.19) while the scatter index time series is shown in Fig. (II.20). There are clear seasonal variations in both bias and SI time series in the extra-tropics especially in the NH. The bias and SI reach their peaks during June-August in the NH and during December-February in the SH. There is no abrupt or unusual change in SWH statistics at the time of implementation of the PF-ASAR Version 3.07 (4 May 2004) nor at the time of the introduction of the new model dissipation term (5 April 2005). However, there is a clear reduction in SI especially in the Tropics and the SH starting from March 2004 (after the data gap during January-March 2004). This change coincides with a model change that involves a treatment for the impact of the unresolved bathymetry introduced on 9 March 2004. This change seems to be responsible for a reduction in the Tropical bias and at the same time an increase in the extra-tropical bias. Furthermore, there is a clear reduction in the peak of SI in the NH during July/August 2005 compared to the peaks in the previous years which may be related to the model change in April 2005 (to some extent).

Fig. (II.21) shows a density scatter plot for globally collocated swell mean wave period (MWP) pairs of ASAR Wave Mode Level 2 and the analysis WAM wave model for the period from 11 April to 31 August 2005. The agreement between the ASAR and the model MWP is very good for the bulk of the data. For wave periods below ~12 s, the agreement degrades. Table (II.2) lists the swell MWP bias (ASAR minus model) and SI for the whole globe, the NH, the Tropics and the SH. In general, the bias is less than 0.9 s and the SI varies between 2.8% (in the SH) and 8.5% (in the NH). The time series of bias between ASAR Level 2 and WAM model swell MWP is shown in Fig. (II.22) while the scatter index time series is shown in Fig. (II.23). Again, there are clear seasonal variations in both bias and SI time series in the extra-tropics especially in the NH. The bias and SI reach their peaks during June-August in the NH and during December-February in the SH. The impact of the PF-ASAR version 3.07 and the model change with new dissipation term are not reflected in abrupt or unusual jumps. However, the model change with unresolved bathymetry treatment (9 March 2004) may be responsible for the SI reduction in the extra-tropics. The April 2005 model change seems to reduce the SI further in the extra-tropics.

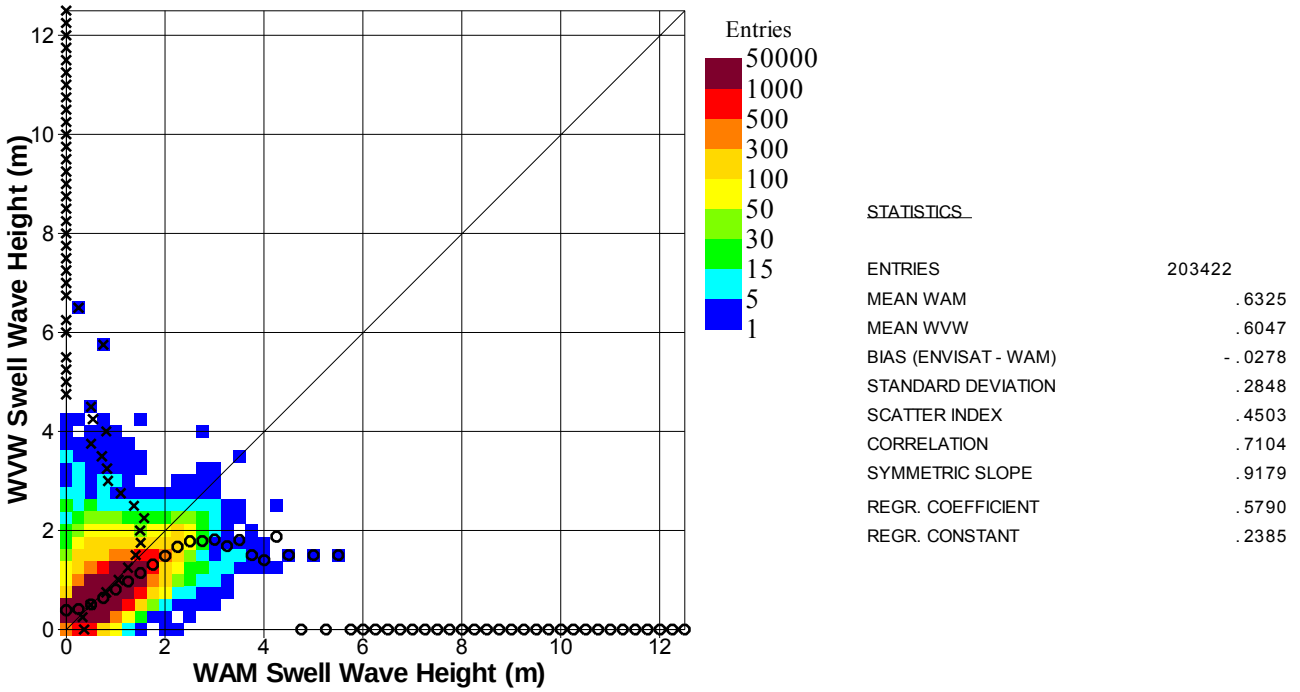

Fig. II.18. Global comparison between ASAR level 2 and ECMWF model swell SWH during the period from 11 April to 31 August 2005.

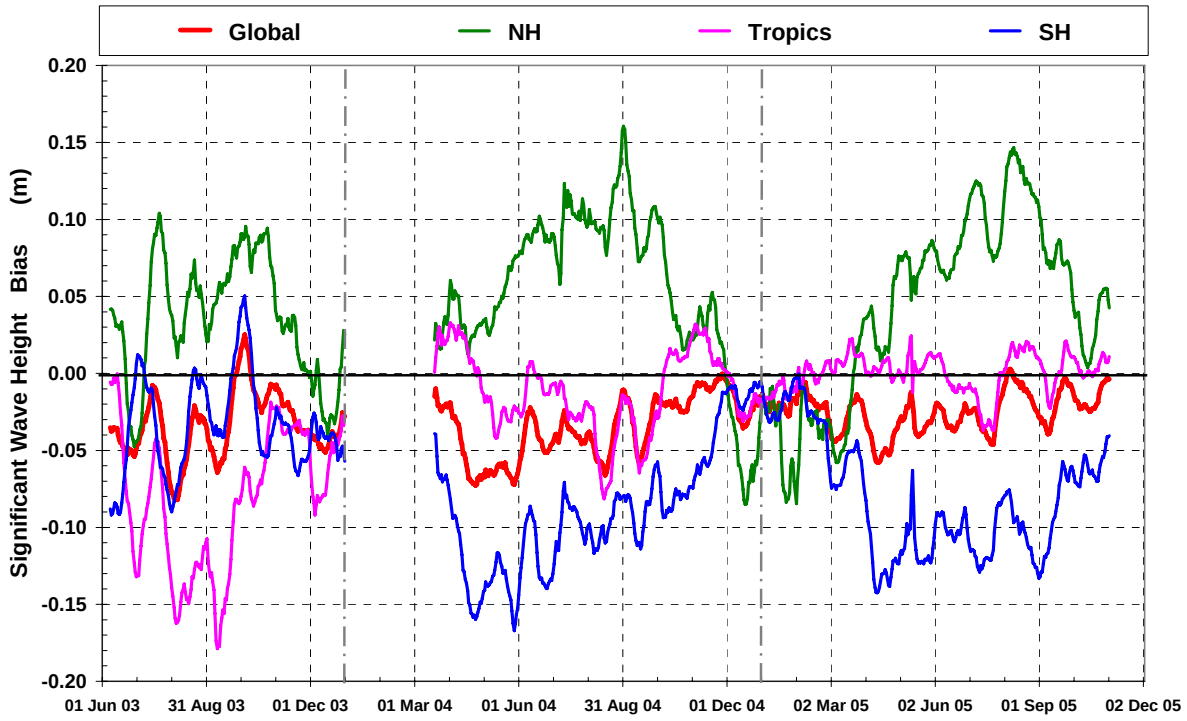

Fig. II.19. Time series of swell SWH bias between ASAR Level 2 product and WAM.

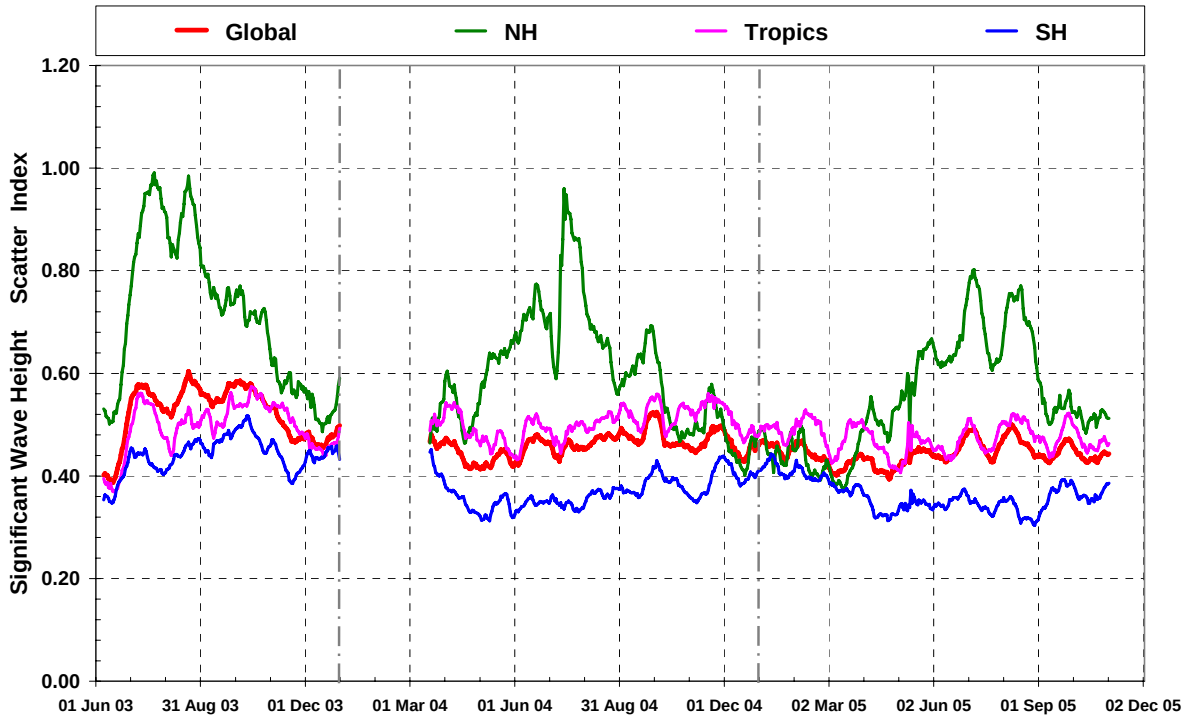

Fig. II.20. Time series of swell SWH SI between ASAR Level 2 product and WAM.

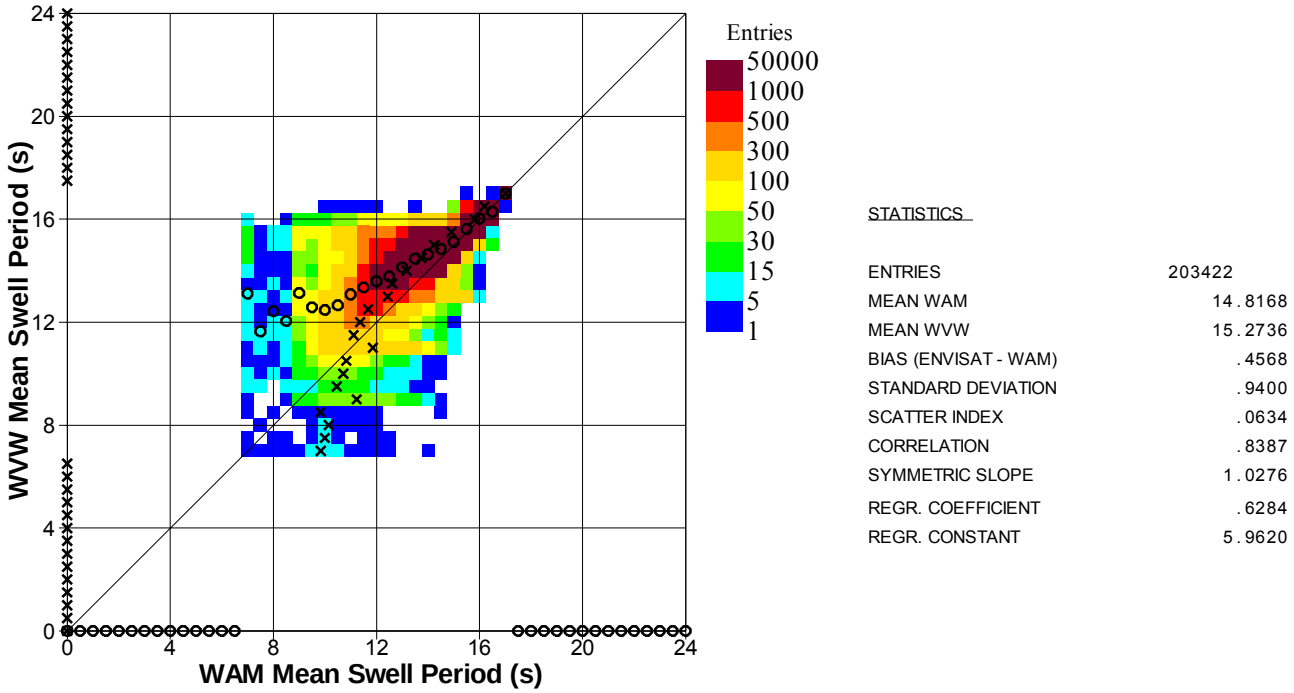

Fig. II.21. Global comparison between ASAR level 2 and ECMWF model swell MWP during the period from 11 April to 31 August 2005.

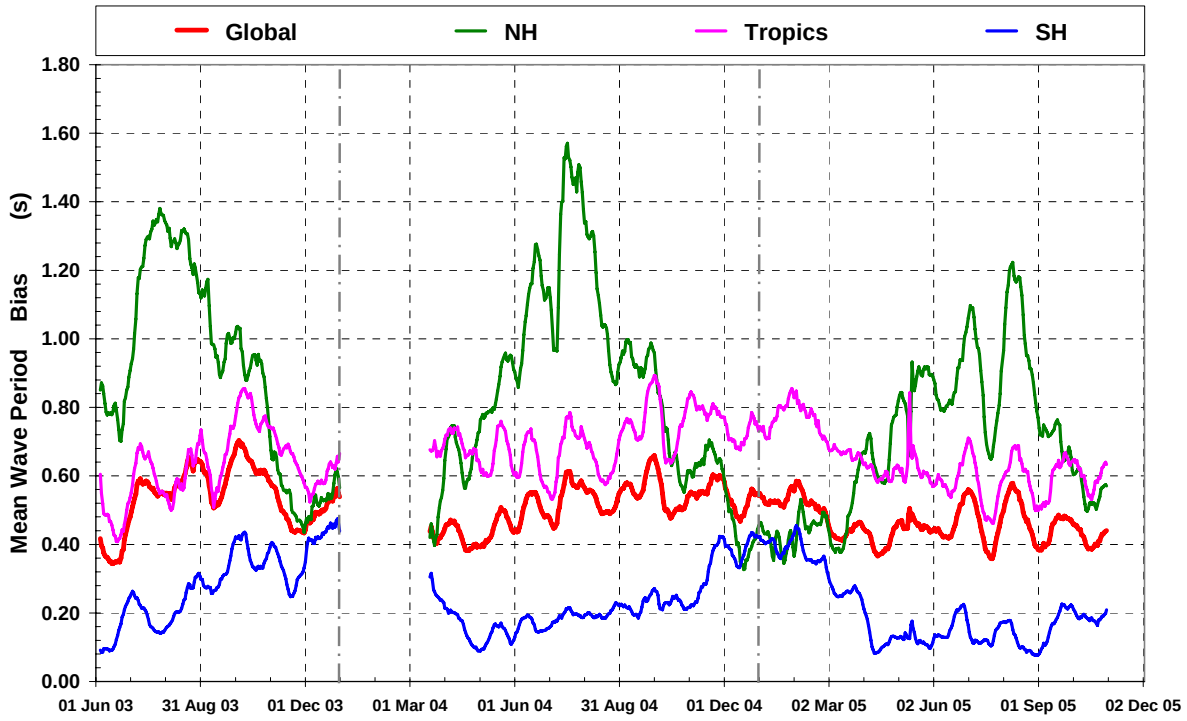

Fig. II.22. Time series of swell MWP bias between ASAR Level 2 product and WAM.

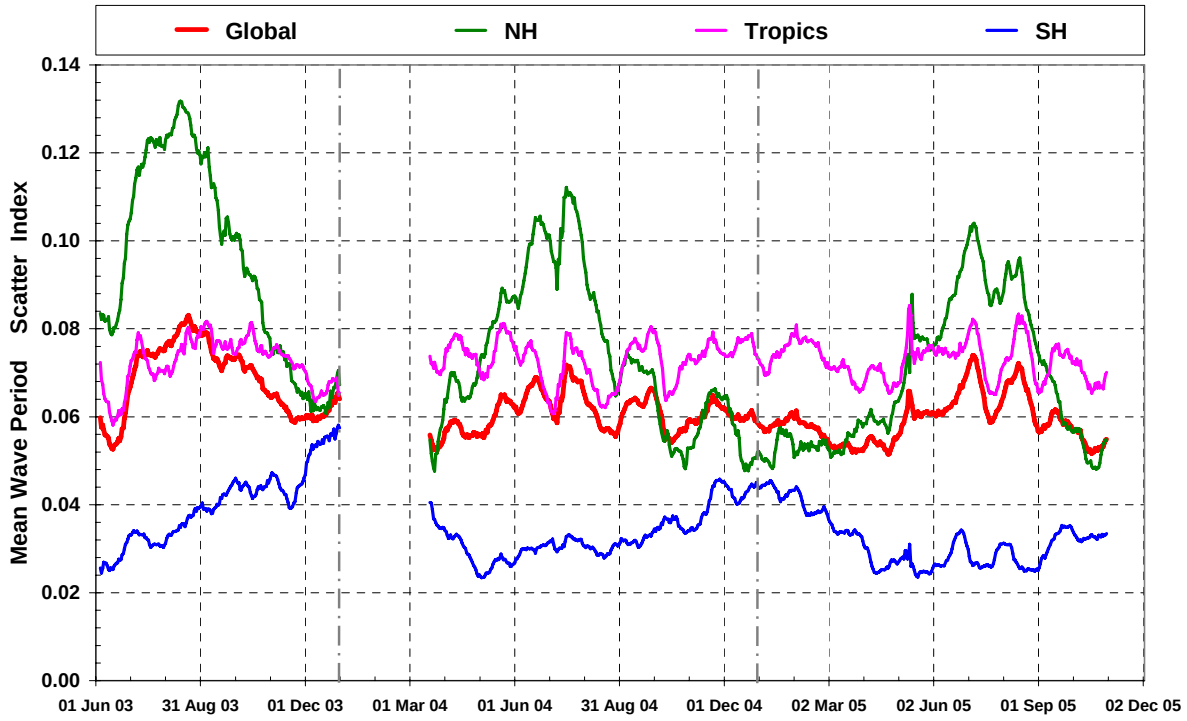

Fig. II.23. Time series of swell MWP SI between ASAR Level 2 product and WAM.

The globally collocated swell wave peakedness factor (WPF) pairs of ASAR Wave Mode Level 2 and the analysis WAM wave model for the period from 11 April to 31 August 2005 are shown in Fig. (II.24). The agreement between the ASAR and the model WPF is rather poor. The ASAR mean value is about twice the model mean value indicating that the ASAR spectra have too narrow peaks compared to the model. Furthermore, the standard deviation of the difference is comparable with the ASAR mean value and larger than the model mean value (scatter index much higher than 100%). More important, there is almost no correlation between both quantities. Table (II.3) lists the swell WPF bias and SI for the various regions. In general, the bias is relatively large compared to the mean value. The same can be said about the SI which reaches about 219% for the NH. However, the SI value in the SH (78%) is rather close to the value of the inverted Level 1b (52%). The correlation between Level 2 product and WAM WPF values is very close to zero everywhere (not shown). The time series of bias between ASAR Level 2 and WAM model swell WPF is shown in Fig. (II.25) while the scatter index time series is shown in Fig. (II.26). There are clear seasonal variations in both bias and SI time series in the extra-tropics especially in the NH similar to those of other parameters. The impact of the PF-ASAR version 3.07 and the model change with new dissipation term are not reflected in abrupt or unusual jumps. However, the model change with unresolved bathymetry treatment (9 March 2004) may be responsible for the SI reduction in the extra-tropics. The April 2005 model change seems to reduce the SI further in the NH.

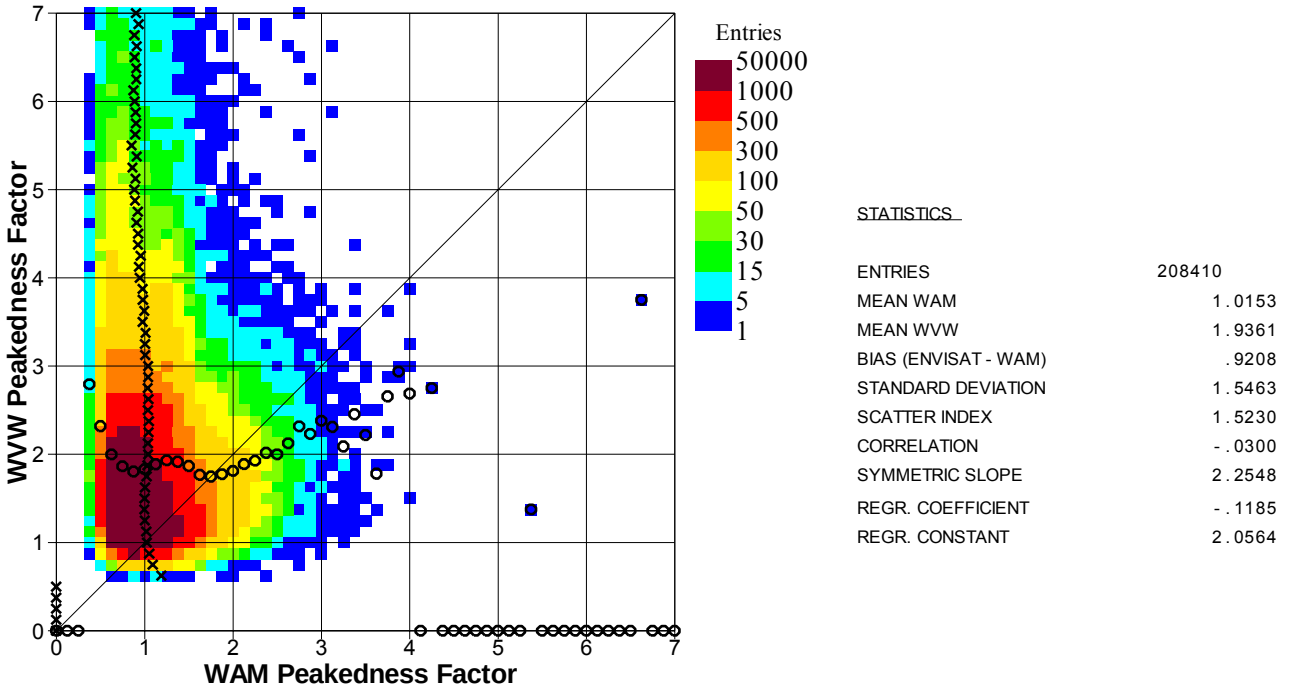

Fig. II.24. Global comparison between ASAR level 2 and ECMWF model swell WPF during the period from 11 April to 31 August 2005.

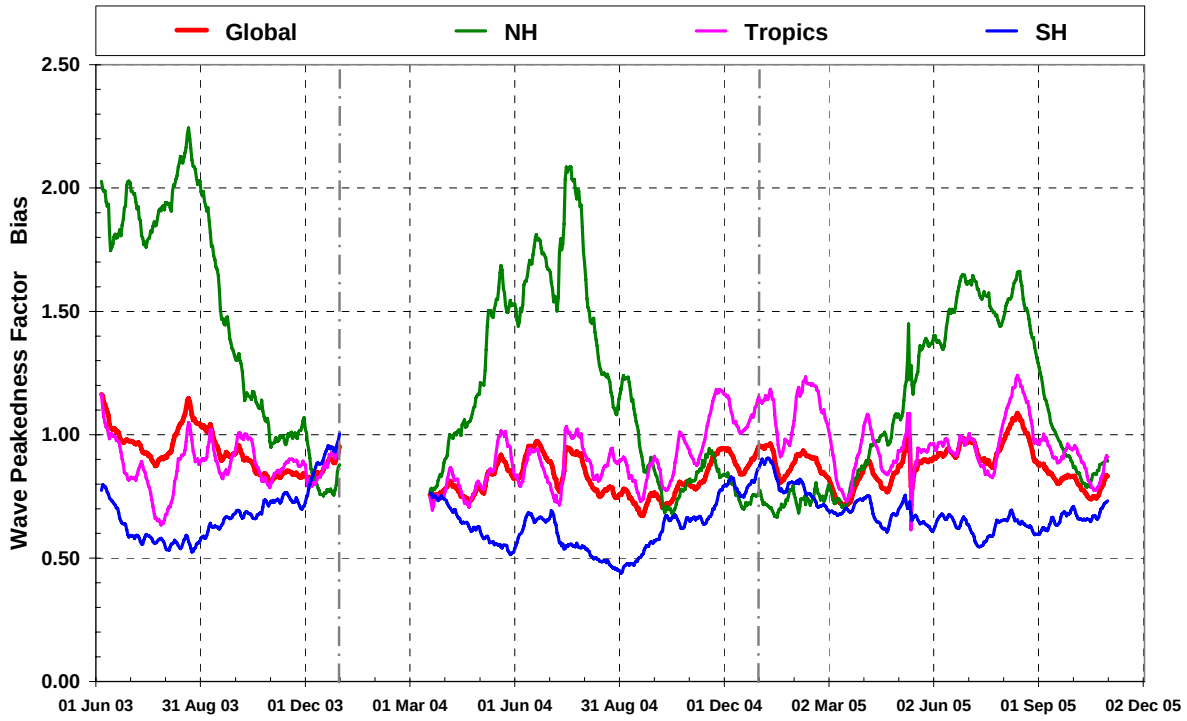

Fig. II.25. Time series of swell WPF bias between ASAR Level 2 product and WAM.

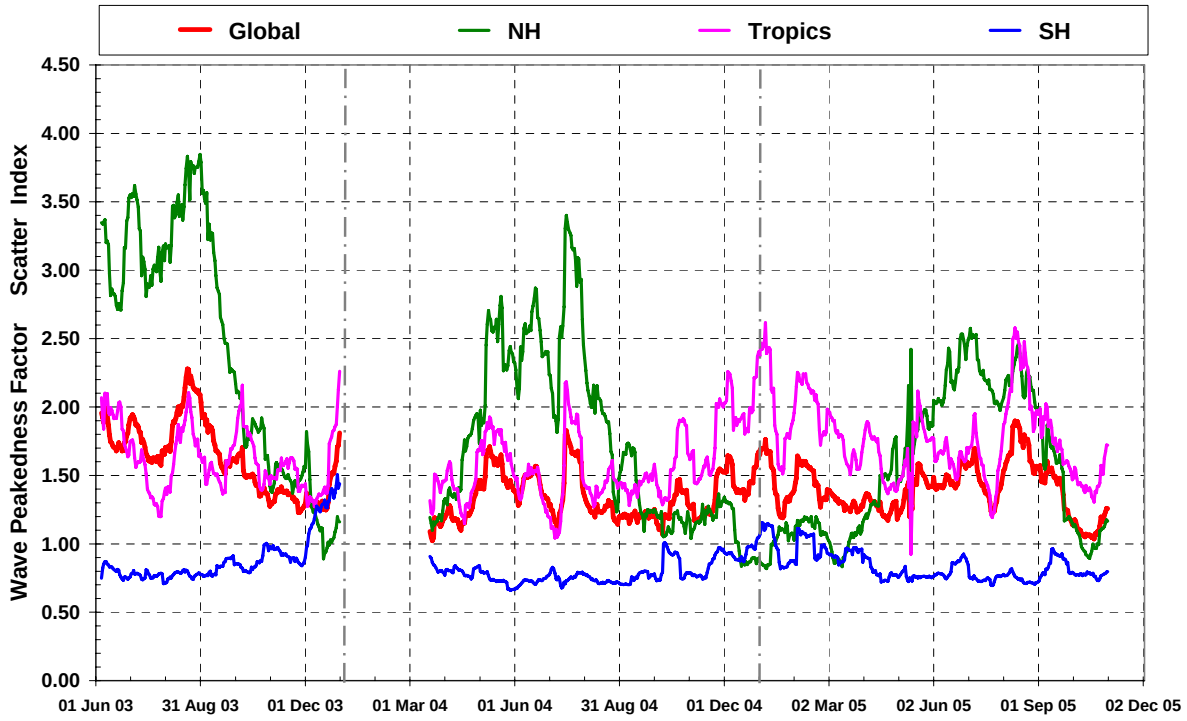

Fig. II.26. Time series of swell WPF SI between ASAR Level 2 product and WAM.

The globally collocated swell wave directional spread (WDS) pairs of ASAR Wave Mode Level 2 and the analysis WAM wave model for the period from 11 April to 31 August 2005 are shown in Fig. (II.27). The agreement between the ASAR and the model WDS is rather poor. The ASAR mean value is about two thirds of the model mean value indicating that the ASAR spectra are too narrow compared to the model. Table (II.4) lists the swell WDS bias and SI for the various regions. In general, the bias is relatively large compared to the mean value. The scatter index values are slightly above 30% and the correlation coefficient can be as low as 0.14 (in the NH; not shown). The time series of bias between ASAR Level 2 and WAM model swell WDS is shown in Fig. (II.28) while the scatter index time series is shown in Fig. (II.29). There are clear seasonal variations in the bias time series in the NH and the Tropics. The bias reaches its peak during December-January in the NH and during August-September in the Tropics. SH statistics do not show clear seasonal variation. There is no clear impact of the PF-ASAR version 3.07 and the model changes except for an apparent change in statistics behaviour after the recovery from the data gap of January-March 2004. If the PF-ASAR Version 3.07 is not responsible for this change (Betlem Rosich, personal communication, 2005), it is highly possible that the model change with the unresolved bathymetry treatment (9 March 2004) is responsible for that change. The April 2005 model change seems to reduce the bias slightly in the NH.

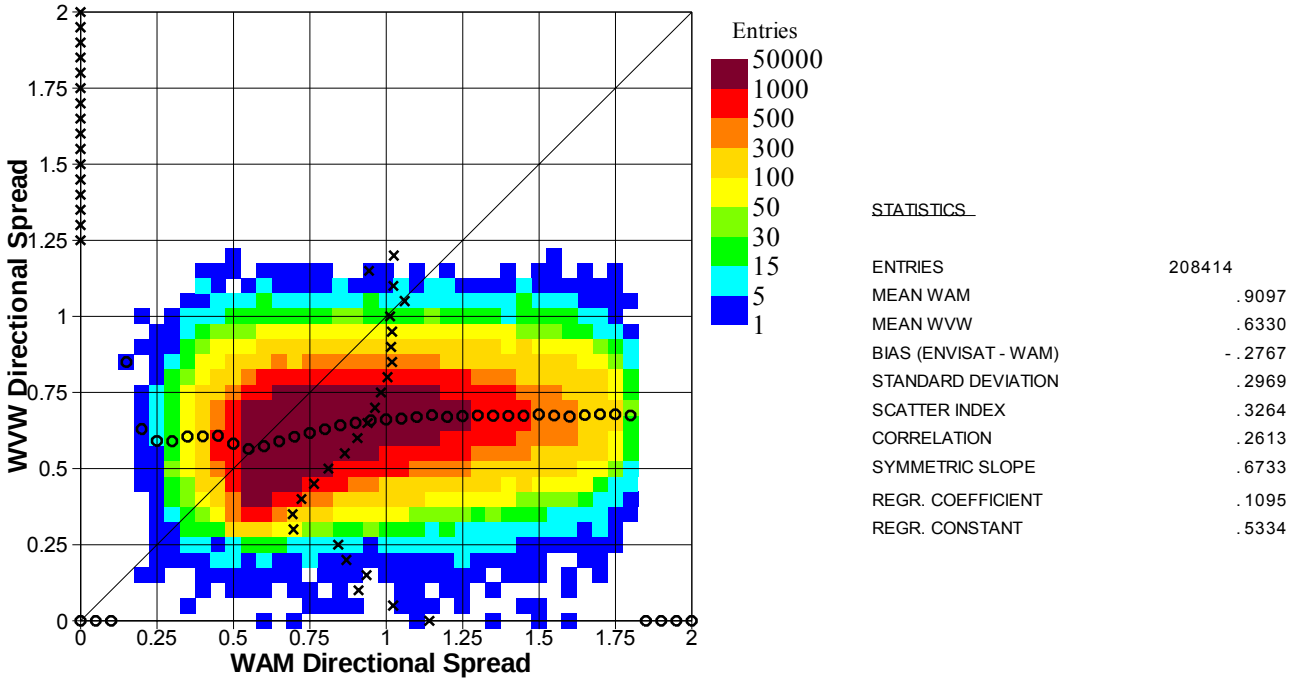

Fig. II.27. Global comparison between ASAR level 2 and ECMWF model swell WDS during the period from 11 April to 31 August 2005.

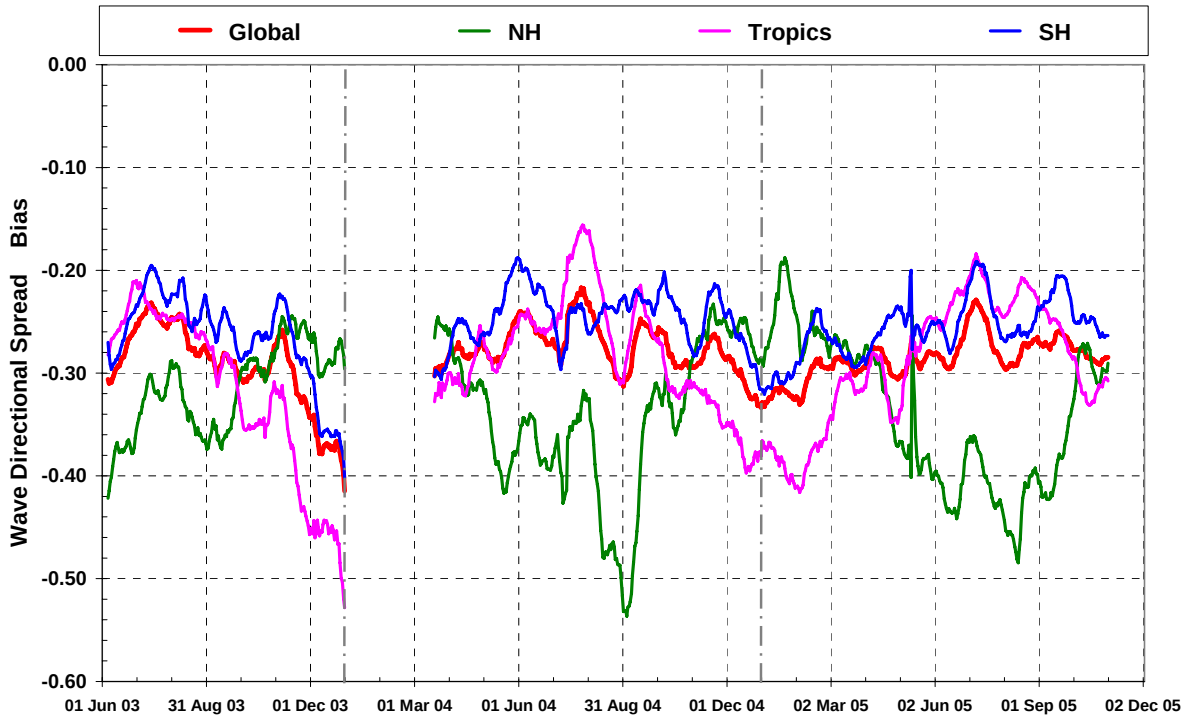

Fig. II.28. Time series of swell WDS bias between ASAR Level 2 product and WAM.

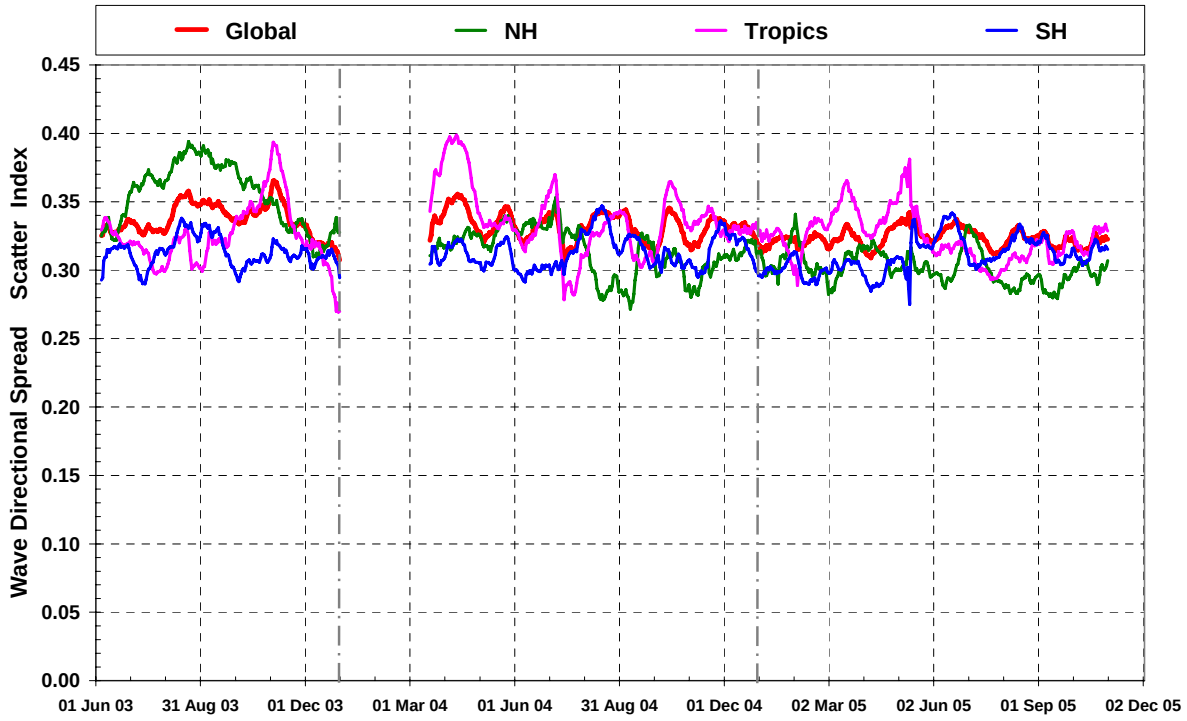

Fig. II.29. Time series of swell WDS SI between ASAR Level 2 product and WAM.

Rather detailed comparisons at various spectral wave components in terms of the "2-s wave-period interval equivalent wave heights" ($H_{T1,T2}$), are displayed in Figs. (II.30) - (II.33) for the whole globe, the NH; the Tropics and the SH, respectively, during the period from 11 April to 31 August 2005. The bias, the standard deviation of difference, the scatter index and the correlation coefficient between the ASAR Wave Mode Level 2 product and the wave model $H_{T1,T2}$ are plotted as functions of wave period. For components with wave periods below 8s, there are few cases and therefore the statistics are not representative. The comparisons between Level 2 and the model indicate acceptable agreement for long wave-period wave components except for the NH.

II.5. Conclusions

Continuous monitoring and validation of the ENVISAT ASAR Wave Mode products are carried out at ECMWF. Data from ECMWF wave model are used for this purpose. Since June 2003, there were there different events that had significant impact on the comparison: a model change to handle the unresolved bathymetry (9 March 2004), an ASAR processing chain PF-ASAR Version 3.07 (4 May 2004) and another model change with a revised dissipation term (5 April 2005). This latter change improves the wave predictions during mild storms in the existence of long swell conditions. Nevertheless, this change resulted in a model which is rather sensitive to wind speed errors.

ASAR Wave Mode Level 1b SAR spectra are inverted using the MPIM scheme. The inverted ocean wave spectra are compared to the wave model in terms of a limited number of integrated parameters. The significant wave height, the mean wave period and the wave directional spread from the inverted products compare very well with the model counterparts. The comparison in terms of the wave spectral peakedness factor, on the other hand, reveals less agreement.

The March 2004 model change does not show significant impact on the statistics of Level 1b possibly due to the problem with the Level 1b product at that time. The PF-ASAR Version 3.07 increased the quality of inverted spectra while reduced the portion of cases with unstable iterations. This reduced the contamination of the inverted spectra with the wave model and thus increased the scatter index of all parameters. The April 2005 model change has positive impact on the bias of all parameters considered and the SI of the mean wave period. However, this model change increased the SI values of the SWH and the WPF. The increased sensitivity of the new model is responsible for this negative impact.

The comparison between ASAR Wave Mode Level 1b and the wave model was done in terms of the same integrated parameters with the exception that the integration is done for the ASAR resolvable wave components (with wavelengths longer than the azimuthal cut-off wavelength). Swell significant wave height and mean wave period from Level 2 product agree well with their wave model counterparts. However, the swell spectral peakedness factor and the directional spread parameters show poor agreement.

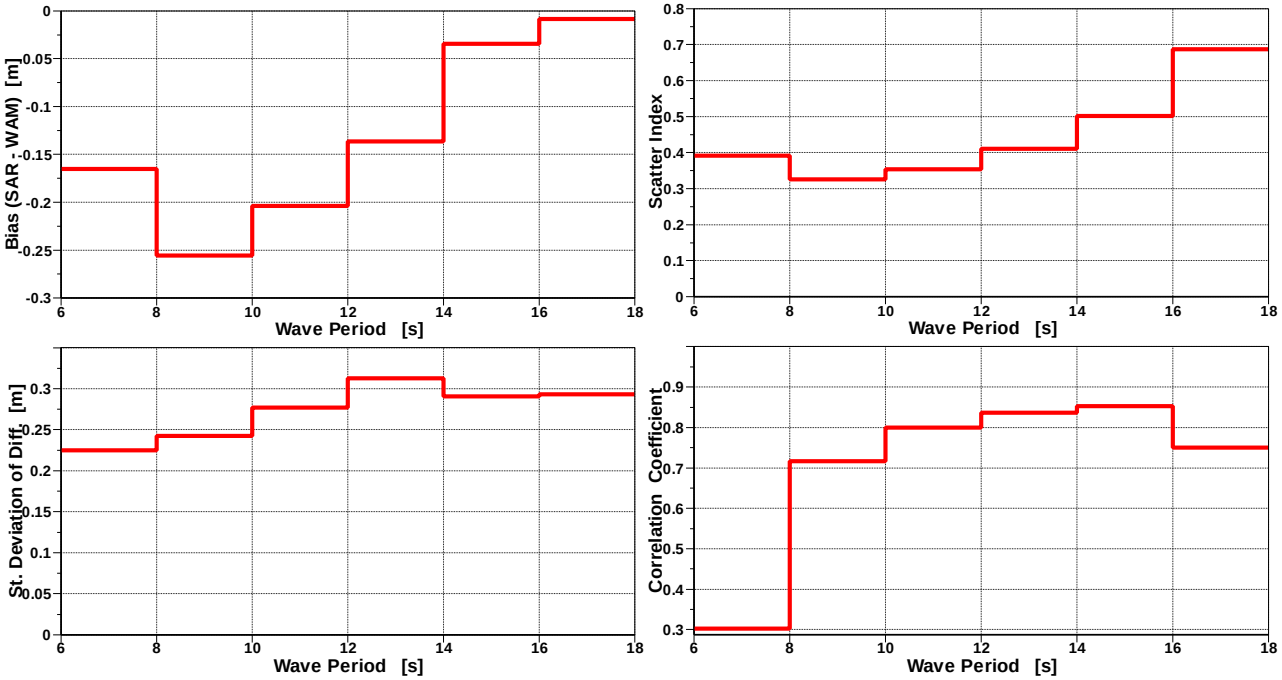

Fig. II.30. Comparison between ASAR level 2 and WAM "2-s wave-period interval equivalent wave heights" for 11 April to 31 August 2005 (Global).

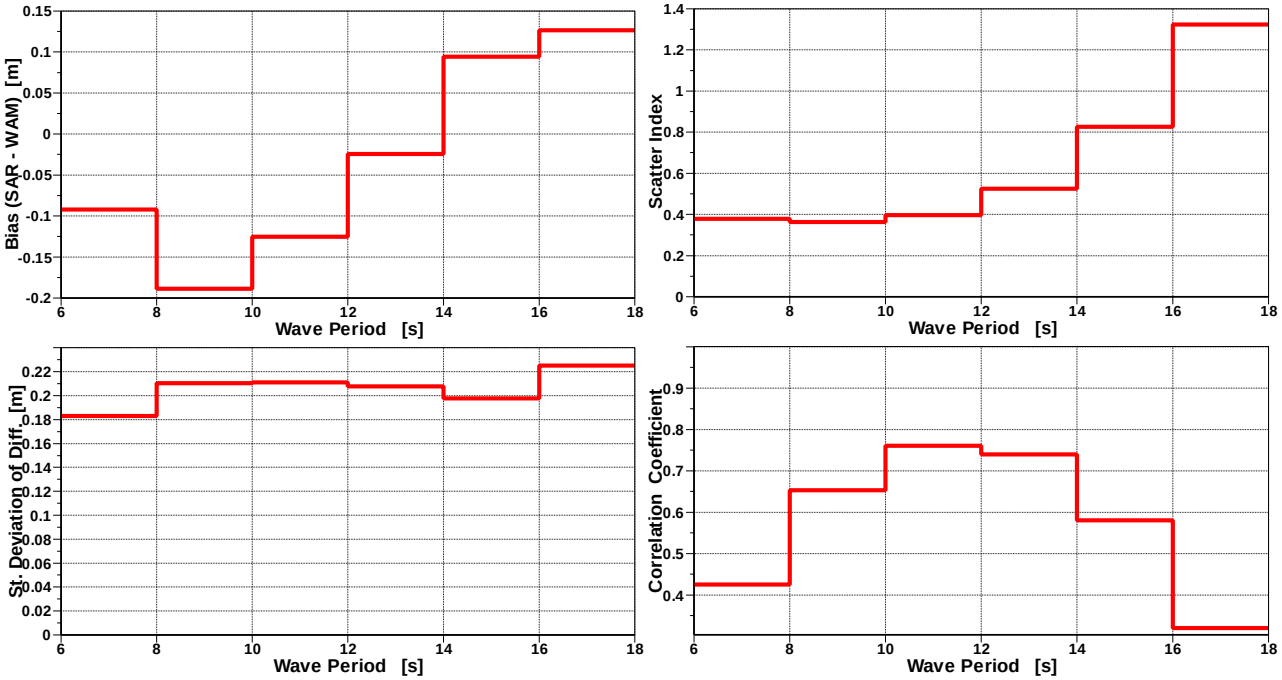

Fig. II.31. Comparison between ASAR level 2 and WAM "2-s wave-period interval equivalent wave heights" for 11 April to 31 August 2005 (NH).

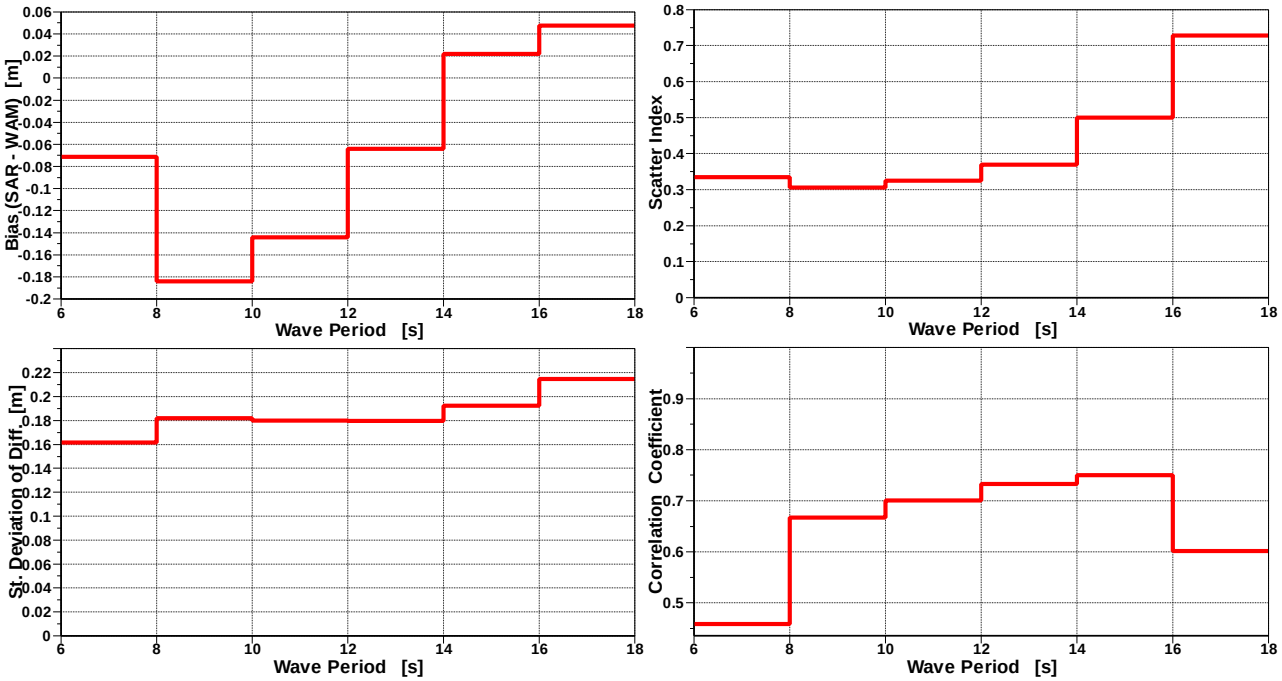

Fig. II.32. Comparison between ASAR level 2 and WAM "2-s wave-period interval equivalent wave heights" for 11 April to 31 August 2005 (Tropics).

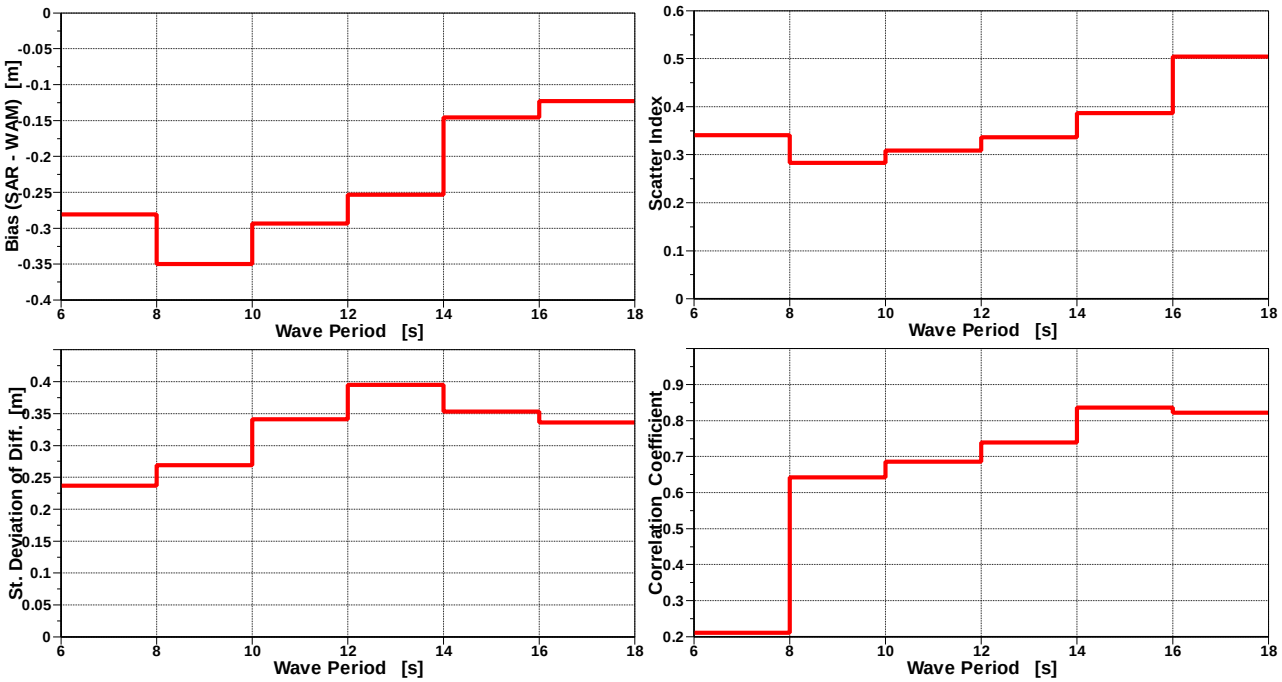

Fig. II.33. Comparison between ASAR level 2 and WAM "2-s wave-period interval equivalent wave heights" for 11 April to 31 August 2005 (SH).

Time series of bias and scatter index of most of the parameters from Level 2 show seasonal variations. Swell wave height, mean period and peakedness bias and SI reach their peaks during June-August in the NH and during December-February in the SH and vice versa for the minima. On the other hand, the swell directional spread shows seasonal variation in the bias time series in the NH and the Tropics. The bias reaches its peak during December-January in the NH and during August-September in the Tropics and vice versa for the minima.

While the PF-ASAR Version 3.07 seems not to have any impact on the statistics of Wave Mode Level 2, the model changes have positive impact. The model change with unresolved bathymetry treatment (9 March 2004) reduced swell SWH bias and SI in the NH and the Tropics. It also reduced the swell MWP and WPF SI in the extra tropics. The April 2005 model change, on the other hand, seems to reduce the SI of all parameters in the NH.

ASAR Wave Mode Level 1b is planned to be assimilated operationally at ECMWF on 1 February 2006.

PART III

MEDIUM RESOLUTION IMAGING SPECTROMETER (MERIS) WATER VAPOUR PRODUCT

III.1. Introduction

MERIS is a 68.5° field-of-view pushbroom imaging spectrometer that measures the solar radiation reflected by the Earth, at a ground spatial resolution of 300m, in 15 spectral bands, programmable in width and position, in the visible and near infra-red. MERIS allows global coverage of the Earth in 3 days. The MERIS product of interest is the Geolocated Cloud Optical Thickness and Water Vapour Content (a low resolution atmosphere Level 2) product (MER_LRC_2P). Specifically, only TCWV is validated here. This is a very dense product with a 1200 km wide swath at a resolution of 4.16 km (across-track) × 4.64 km (along-track) at nadir.

III.2. MERIS data processing

TCWV (or the "atmospheric water vapour content") is one of the products obtained from the MERIS instrument onboard ENVISAT (product MER_LRC_2). This product is validated by com-paring it with the corresponding product produced by the ECMWF atmospheric model (IFS). Due to the scale differences between the MERIS product and the IFS model product, it is required to bring both to the same scale. One way to do this is to average the MERIS product over spatial grid boxes comparable with the model resolution. A procedure for the pre-processing including the averaging and the basic quality control can be summarised as follows (Abdalla, 2005):

1. The stream of MERIS MER_LRC_2 product is split over 6-hour time windows centred at the main synoptic times to coincide with the IFS model output times.
2. All MERIS TCWV observations with missing or zero values are filtered out assuming they are not valid.
3. For each time window, the dense MERIS TCWV data set is averaged over grid boxes of 0.5°×0.5° producing the MERIS super-observations.
4. The super-observation is rejected if the number of its individual observations is less than 10.
5. The super-observation is rejected if it is smaller than 0.1 kg/m^2.
6. The super-observation is rejected if its standard deviation exceeds 35% of its mean.
7. The super-observations that pass the quality control are collocated with the model counter-parts and various statistics are computed.

This procedure may reject more than 40% of MERIS TCWV products. It is important to stress that part of the rejected data may be of good quality and rejected due to their high variability

III.3. MERIS water vapour product

Fig. (III.1) shows a time series of weekly running mean of MERIS TCWV data reception and acceptance per 6-hour time window for the first 10 months of 2005. On average, the data received at a rate exceeding 3 million per 6-hours. Almost 50% of the received data pass the quality control. This is a rather low ratio. It is

not clear if this low ratio is due to the noise/variability in the observations or due to the current quality control procedure which was derived to optimise the data acceptance against the best fit with respect to the model (c.f. Abdalla, 2005).

Collocated TCWV pairs of MERIS super-observation and the ECMWF model AN are plotted as density scatter plot in Fig. (III.2) for the whole globe over the month of October 2005. This is atypical monthly plot during the first 10 months of 2005. The major part of the MERIS observations agrees very well with the model counterpart. However, there are quite a number of outliers as well. MERIS tends to provide a significant number of dry observations especially below ~5 kg/m^2 which are not supported by the model. Globally, MERIS underestimates the TCWV by about 4 kg/m^2 with respect to the ECMWF atmospheric model. This is too high when compared with the bias between the model and the MWR which is around 1 kg/m^2 as can be seen in Figs. (I.23) to (I.25) and in Table (I.4). Furthermore, MERIS tends to have a secondary population of collocations with the model that runs below the main population by ~10 kg/m^2. Although this can be seen in Fig. (III.2), it is more pronounced in the Tropics (not shown).

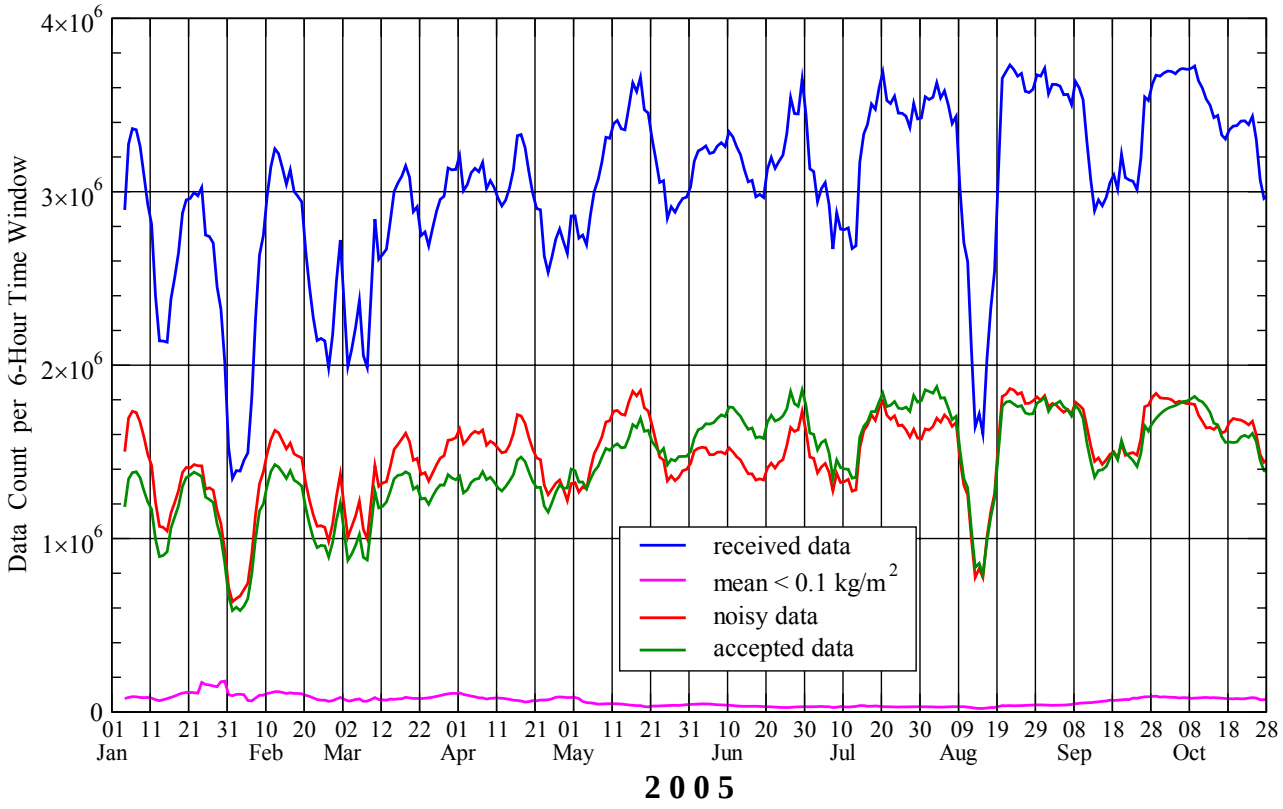

Fig. III.1. Time series of MERIS TCWV data reception and acceptance (weekly running mean).

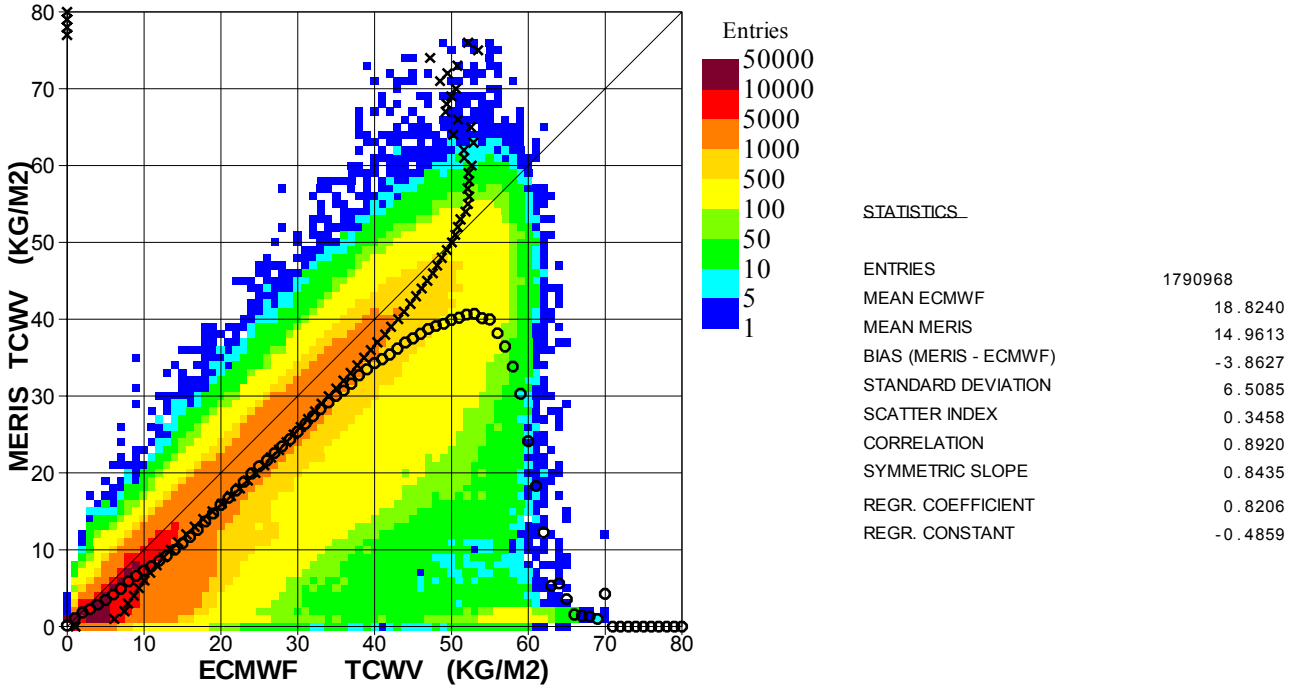

Fig. III.2. Global comparison between MERIS and ECMWF model AN TCWV values during October 2005.

The MERIS TCWV bias (MERIS minus model) and SI for the whole globe, NH, Tropics and SH are listed in Table (III.1). It is clear that MWR underestimates the WTC with respect to the model everywhere by more than 3 kg/m^2. The SI values are relatively high everywhere as well. The results of other months are not much different during the first 10 months of 2005.

	MERIS Mean (kg/m^2)	Bias (kg/m^2)	SI (%)
Global	14.96	−3.86	34.6
NH	12.92	−3.38	34.2
Tropics	30.28	−5.80	24.9
SH	7.41	−3.12	46.1

Table III.1:Comparison of MERIS TCWV with ECMWF Model AN for October 2005

The global distribution of monthly average MERIS TCWV for October 2005 is shown in Fig. (III.3) while the corresponding ECMWF model average is shown in Fig. (III.4). The global distribution of the monthly average difference (bias) between MERIS and the model is shown in Fig. (III.5). It is clear that MERIS is much wetter than the model at various spots especially in the South America and Africa (e.g. the Amazon Delta) while it is much dryer than the model at various parts of the tropical oceans especially in the northern parts of the Indian Ocean and the Gulf of Panama.

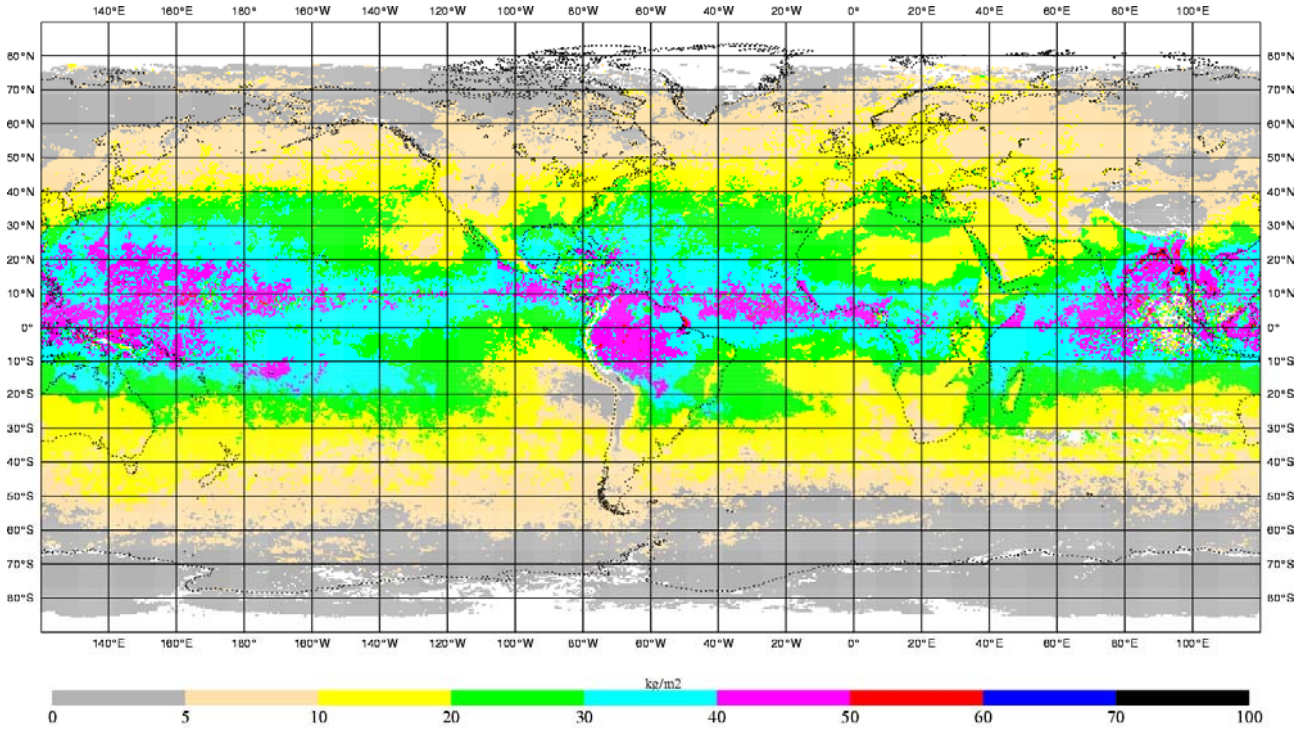

Fig. III.3. Global distribution of monthly average MERIS TCWV for October 2005.

III.4. Conclusions

10 months of validation of MERIS TCWV product shows that there is quite a good value in the product. However, some enhancements are needed for better performance. The product in general is much dryer and much noisier than the model (or even the MWR instruments). There are several spots around the world when MERIS is too dry (e.g. Gulf of Panama) or too wet (e.g. Amazon Delta).

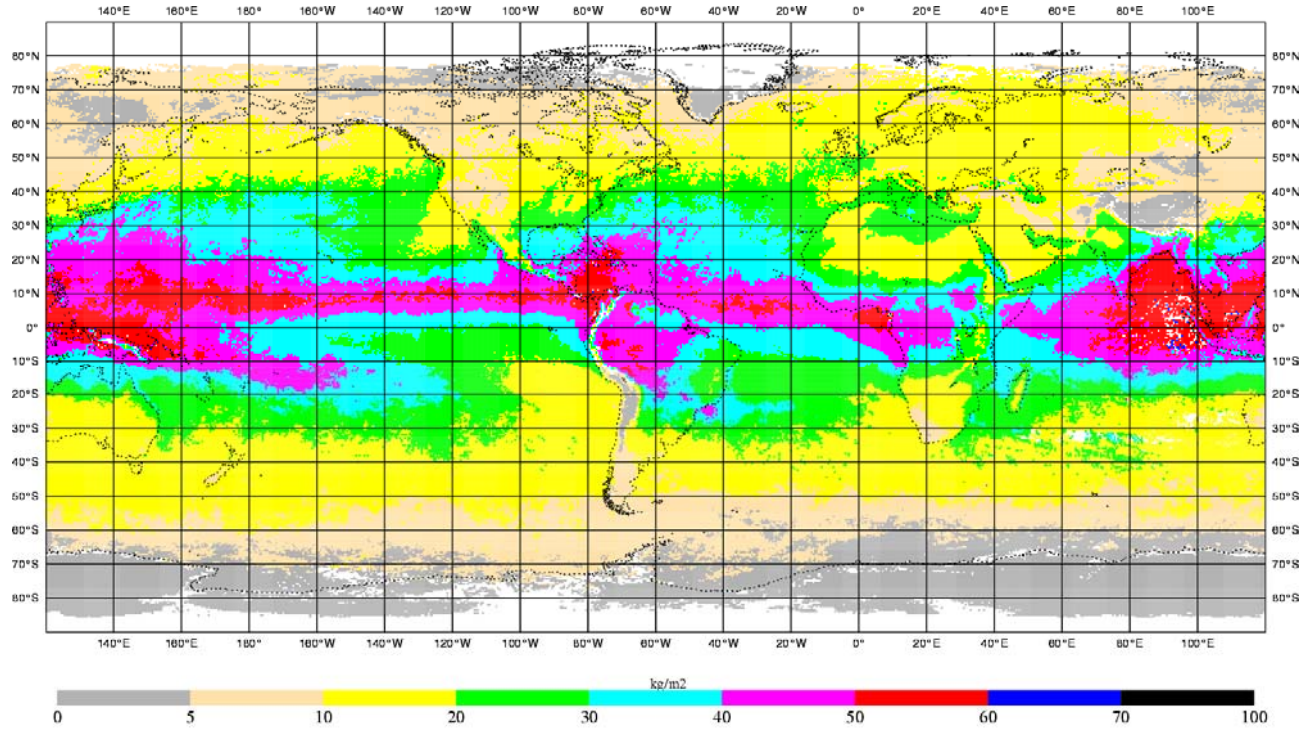

Fig. III.4. Global distribution of monthly average ECMWF model AN TCWV for October 2005.

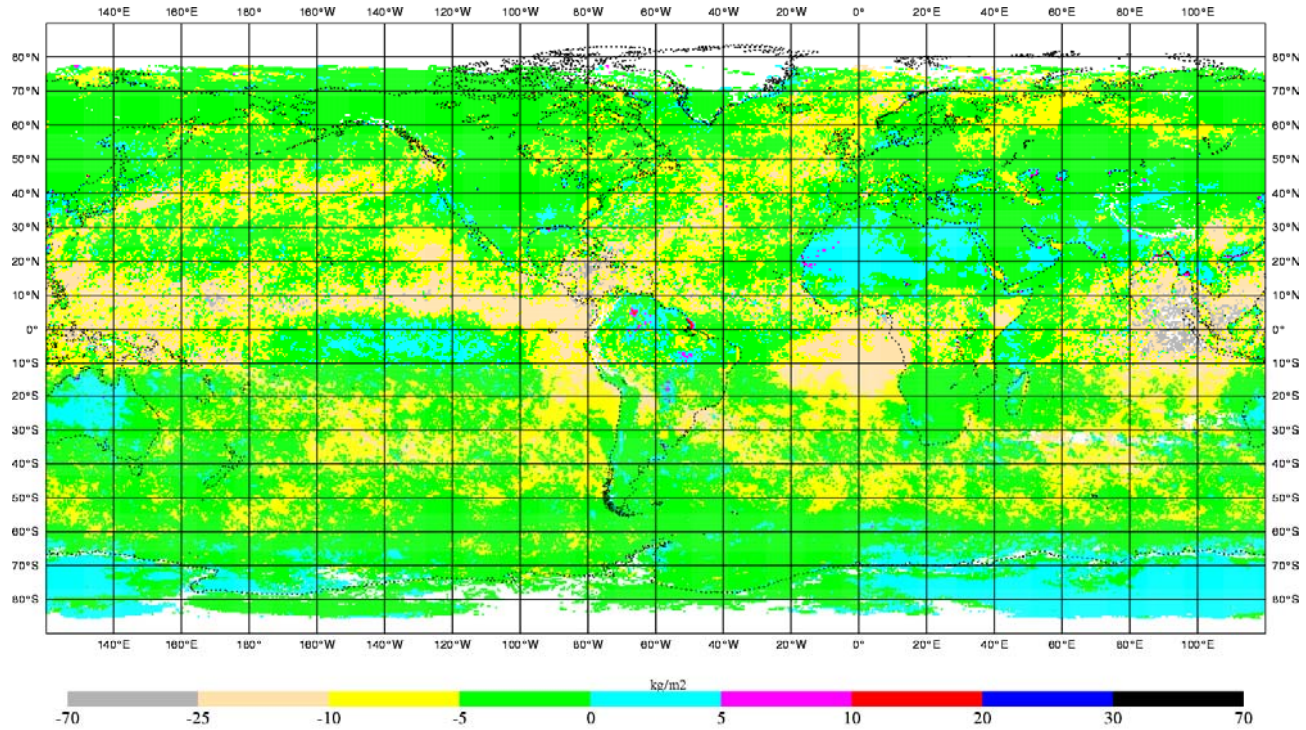

Fig. III.5. Global distribution of monthly average of the difference between MERIS and ECMWF model AN TCWV for October 2005.

APPENDIX: IMPACT OF STRICTER QUALITY CONTROL ON RA-2 S-BAND AND MWR PRODUCTS

Stricter quality control (QC) criteria were used to eliminate S-Band SWH observations during the S-Band anomaly events which appear as outliers in Fig. (I.17). The extra QC criteria include limiting the difference between the S and Ku-Band backscatter coefficients and the standard deviation of S-Band SWH in the super-observations. The resulting global scatter plot between S-Band and ECMWF wave model FG SWH for the year from 1 September 2004 to 31 August 2005 is shown in Fig. (A.1). The reduced number of outliers can not be missed upon comparing Fig. (A.1) with Fig. (I.17). The S-Band SWH bias (RA-2 minus WAM FG) and SI for the whole globe, NH, Tropics and SH are listed in Table (A.1) for stricter QC. As compared to Table (I.3), the bias and the scatter index get lower for stricter QC. However, the qualitative results remain the same.

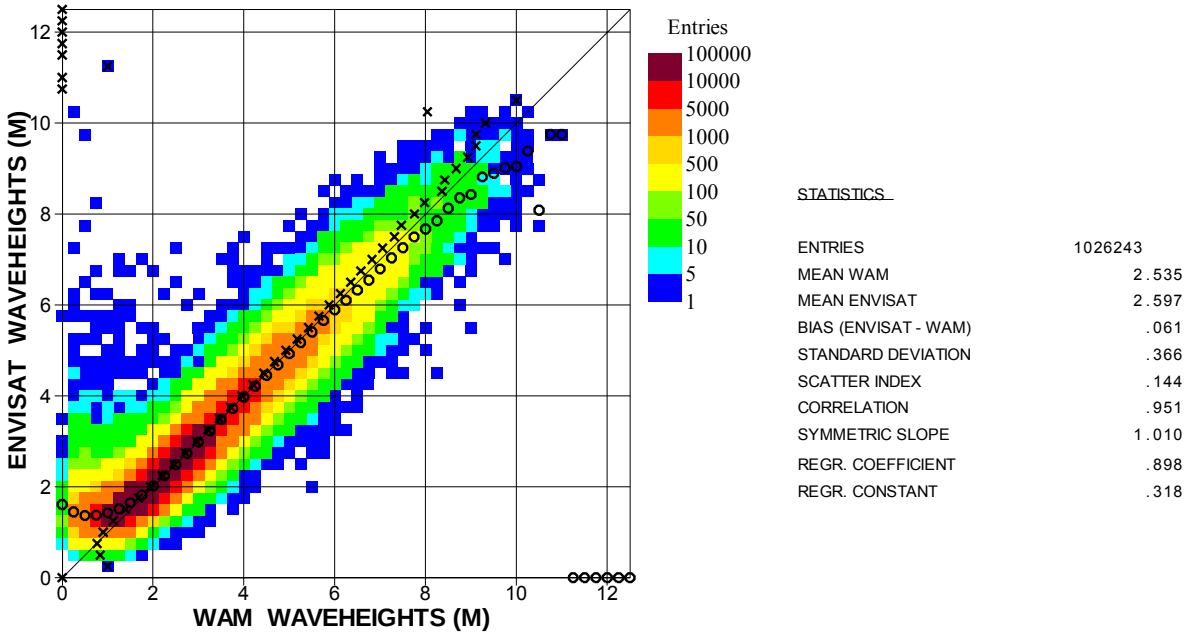

Fig. A.1. Global comparison between RA-2 S-Band and ECMWF wave model FG values during the period from 1 September 2004 to 31 August 2005 after stricter quality control.

	RA-2 Mean (m)	Bias (m)	SI (%)
Global	2.60	+0.06	14.4
NH	2.41	+0.16	17.7
Tropics	2.00	+0.08	17.7
SH	3.13	-0.01	11.1

Table A.1: Comparison of S-Band SWH with stricter quality control against WAM Model FG for Different Regions (1 September 2004 - 31 August 2005)

Similarly, extra QC criteria were used to eliminate the outliers in the scatter plots of the MWR products as can be seen in Figs. (I.23) and (I.27), which are mainly due to possible ice contamination. Tighter standard deviation limits were imposed to accept MWR super-observations. Furthermore, model information about sea ice was also used. The resulting global scatter plots between MWR and ECMWF model for the year from

1 September 2004 to 31 August 2005 are shown in Fig. (A.2) for TCWV and in Fig. (A.3) for WTC. The reduced number of outliers can not be missed upon comparing Fig. (A.1) with Fig. (I.17). The MWR TCWV and WTC bias (MWR minus model) and SI for the whole globe, NH, Tropics and SH are listed in Table (A.2) for stricter QC. As compared to Table (I.4), the scatter index in the case of stricter QC is lower by about 50%. It should be noted, however, that the stricter quality control did no eliminate the hump sagging below the main cloud of TCWV scatter plot between model values of 15 and 20 kg/m^2.

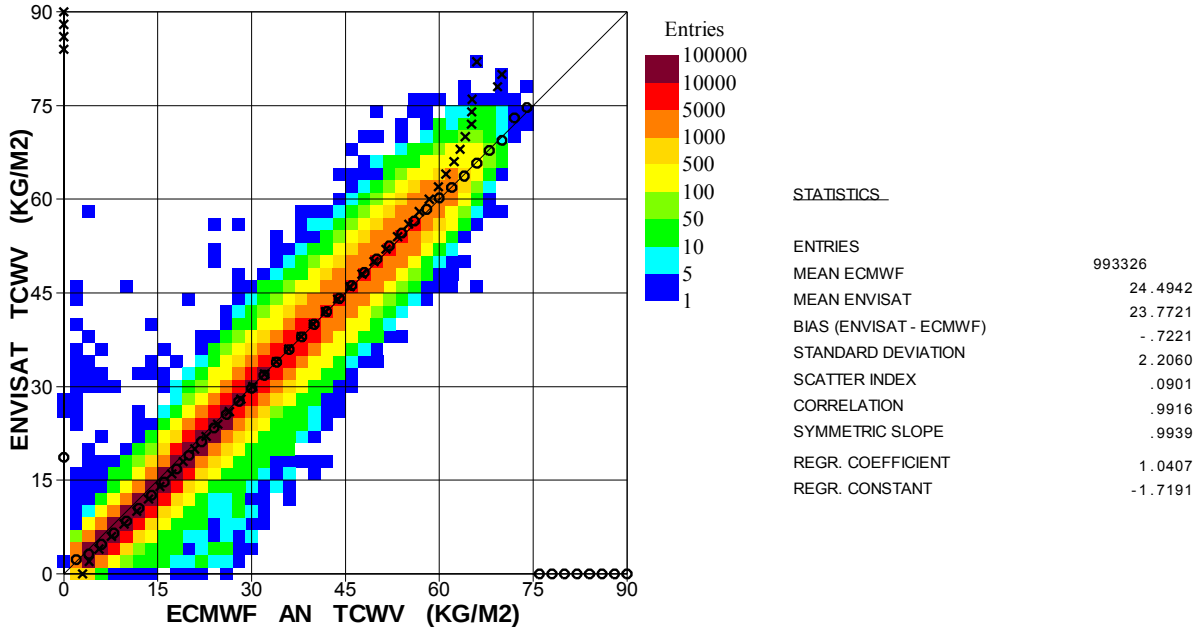

Fig. A.2. Global comparison between MWR and ECMWF model AN TCWV values during the period from 1 September 2004 to 31 August 2005 after stricter quality control.

	TCWV			WTC		
	MWR mean (kg/m^2)	Bias (kg/m^2)	SI (%)	MWR mean (mm)	Bias (mm)	SI (%)
Global	23.77	−0.72	9.0	146	−14	8.6
NH	19.42	−0.95	10.0	120	−14	9.8
Tropics	41.10	+0.47	6.0	249	−12	6.3
SH	14.39	−1.40	11.2	90	−15	11.4

Table A.2: Comparison of MWR Products after stricter quality control against ECMWF Model AN for Different Regions (1 September 2004 - 31 August 2005)

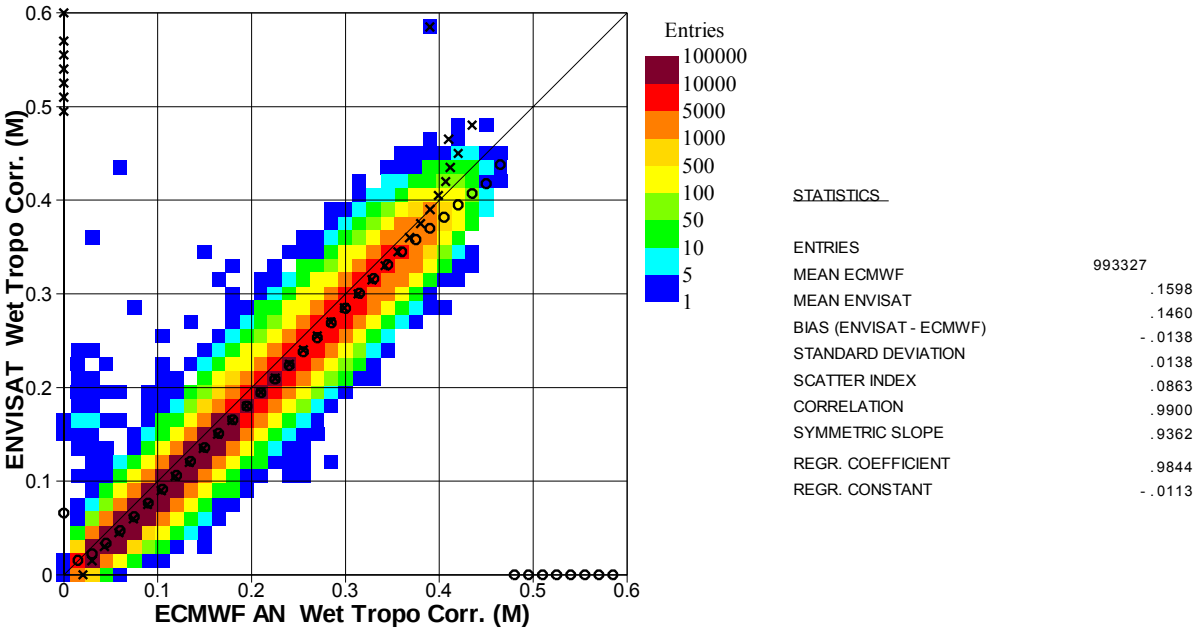

Fig. A.3. Global comparison between MWR and ECMWF model AN WTC values during the period from 1 September 2004 to 31 August 2005 after stricter quality control.

ACKNOWLEDGMENTS

This work was carried out with ESA support through ESA contract No. 17585 (Global Validation of ENVISAT Data Products). Special thanks are due to Peter Janssen and Jean-Raymond Bidlot for support and valuable discussion.

REFERENCES

Abdalla, S. (2005). Note on ENVISAT MERIS MER_LRC_2 TCWV Processing. A special technical memo., available from the author upon request.

Abdalla, S. (2006). A wind retrieval algorithm for satellite radar altimeters. *ECMWF Technical Memorandum*, in preparation.

Abdalla, S. and Hersbach, H. (2004). The technical support for global validation of ERS Wind and Wave Products at ECMWF. *Final Report for ESA c*ontract 15988/02/I-LG,. ECMWF, Reading. Available online at: http://www.ecmwf.int/publications/

Abdalla, S., Bidlot, J. and Janssen, P.A.E.M. (2004). Assimilation of ERS and ENVISAT Wave Data at ECMWF. *Proceedings of the ENVISAT-ERS Symposium*, Salzburg, Austria, 6-10 September 2004.

EOO/EOX - Serco/Datamat (2005). Information to the Users regarding the Envisat RA2/MWR IPF version 5.02 and CMA 7.1. Internet web page visited on 13 Dec. 2005, http://earth.esa.int/pcs/envisat/ra2/articles/RA2_MWR_IPF_5.02.html

ESA (2002). Envisat Tour. Internet web page visited on: 13 Dec. 2005, http://envisat.esa.int/instruments/tour-index/

ESA (2004). ENVISAT Data Products. Issue 1.2e, Dec. 2004, Internet web page visited on: 13 Dec. 2005, http://envisat.esa.int/dataproducts/

Hasselmann, S., Bruning, C., Hasselmann, K. and Heimbach, P. (1996). An Improved Algorithm for the Retrieval of Ocean Wave Spectra from Synthetic Aperture Radar Image Spectra. *J.Geophys.Res*., **101**, 16615-16629.

Janssen, P.A.E.M. (2004). *The Interaction of Ocean Waves and Wind*, Cambridge University Press, Cambridge, U.K., 300+viii pp.

Janssen, P.A.E.M., Abdalla, S. and Hersbach, H. (2003). Error Estimation of Buoy, Satellite and Model Wave Height Data. ECMWF Technical Memorandum No. 402. ECMWF, Reading, UK. Available online at: http://www.ecmwf.int/publications/

Komen, G.J., Cavaleri, L., Donelan, M., Hasselmann, K., Hasselmann, S., and Janssen, P.A.E.M. (1994). *Dynamics and Modelling of Ocean Waves*. Cambridge University Press, 532 p.

Voorrips, A.C., Mastenbroek, C. and Hansen, B. (2001). Validation of two algorithms to retrieve ocean wave spectra from ERS synthetic aperture radar.*J.Geophys.Res.*, **106**, 16825-16840.

Witter, D.L. and Chelton, D.B. (1991). A Geosat Altimeter Wind Speed Algorithm and a Method for Altimeter Wind Speed Algorithm Development. *J.Geophys.Res.*, **96**, 8853-8860.